QUANTITATING THE PERCUTANEOUS ABSORPTION OF MECHANISTICALLY DEFINED CHEMICAL MIXTURES

Jim E. Riviere
Ronald E. Baynes
Charles E. Smith
Nancy A. Monteiro-Riviere

Center for Cutaneous Toxicology and Residue Pharmacology
North Carolina State University
Raleigh, NC 27606

Final Report
AFOSR G F 49620-98-1-0105
January 2001

REPORT DOCUMENTATION PAGE

AFRL-SR-BL-TR-01-

0118

1. REPORT DATE (DD-MM-YYYY)	2. REPORT TYPE	3. DATES COVERED (From - To)
2-2-2001	Final	11-15-97 to 11-14-2000

4. TITLE AND SUBTITLE
Quantitating the Percutaneous Absorption of Mechanistically-Defined Chemical Mixtures

5a. CONTRACT NUMBER

5b. GRANT NUMBER
AFOSR G F49620-98-1-0105

5c. PROGRAM ELEMENT NUMBER

6. AUTHOR(S)
Jim E. Riviere, DVM, PhD

Ronald E. Baynes, DVM, PhD

Charles Smith, PhD Nancy Ann Monteiro-Riviere, PhD

5d. PROJECT NUMBER

5e. TASK NUMBER

7. PERFORMING ORGANIZATION NAME(S) AND ADDRESS(ES)
Center for Cutaneous Toxicology and Residue Pharmacology
College of Veterinary Medicine
4700 Hillsborough Street
North Carolina State University
Raleigh, NC 27606

8. PERFORMING ORGANIZATION REPORT NUMBER

9. SPONSORING / MONITORING AGENCY NAME(S) AND ADDRESS(ES)
AFOSR
801 No. Randolph St., Room 732
Arlington, VA 22203-1977

10. SPONSOR/MONITOR'S ACRONYM(S)

11. SPONSOR/MONITOR'S REPORT NUMBER(S)

12. DISTRIBUTION / AVAILABILITY STATEMENT

AIR FORCE OFFICE OF SCIENTIFIC RESEARCH (AFOSR)
NOTICE OF TRANSMITTAL DTIC. THIS TECHNICAL REPORT
HAS BEEN REVIEWED AND IS APPROVED FOR PUBLIC RELEASE
LAW AFR 190-12. DISTRIBUTION IS UNLIMITED.

13. SUPPLEMENTARY NOTES

14. ABSTRACT

The focus of this research was to assess the percutaneous absorption and cutaneous toxicity of jet fuels (Jet A, JP-8, JP-8 +100). The absorption of jet fuel hydrocarbons (naphthalene, dodecane, hexadecane) was studied as a function of jet fuel type and the presence of individual or all possible combinations of performance additives (DIEGME, 8Q21, Stadis 450). Percutaneous absorption was investigated using *in vitro* flow-through diffusion cells containing inert silastic or dermatomed pig (Sus scrofa) skin and in isolated perfused porcine skin flaps (IPPSFs). Toxicity was assessed in IPPSFs as well as in human and porcine keratinocyte cell cultures as well as *in vivo* pigs. All fuels produced evidence of skin toxicity and resulted in production and release of the cytokines IL-8 and TNFα. Naphthalene absorption was greater than the aliphatic markers, however skin deposition showed the reverse pattern; both of which were affected by the addition of performance additives.

15. SUBJECT TERMS

Jet Fuel, JP-8, Jet A, JP8+100, Percutaneous Absorption, Dermatotoxicity, Skin

16. SECURITY CLASSIFICATION OF:			17. LIMITATION OF ABSTRACT	18. NUMBER OF PAGES	19a. NAME OF RESPONSIBLE PERSON
a. REPORT	b. ABSTRACT	c. THIS PAGE			19b. TELEPHONE NUMBER (include area code)
Unclas	Unclas	Unclas		109	

Standard Form 298 (Rev. 8-98)
Prescribed by ANSI Std. Z39.18

Introduction: The focus of this research has been to assess the percutaneous absorption and cutaneous toxicity of jet fuel hydrocarbons and performance additives that make up Jet-A, JP-8 and JP-8 +100. Hydrocarbon absorption has been assessed using the radiolabelled markers naphthalene and dodecane in three *in vitro* model systems: inert silastic and dermatomed porcine skin diffusion cells and isolated perfused porcine skin flaps (IPPSFs). Cutaneous toxicity of fuels and additives have been evaluated using *in vitro* porcine and human keratinocyte cell cultures as well as *in vivo* pigs. Porcine skin is utilized as the animal model in these studies due to its documented similarity to human skin relative to chemical and drug absorption. A number of the studies supported by this grant have been published (see below) and the attached manuscripts should be consulted for full details. These studies will only be overviewed in this report.

The underlying hypothesis of this research is that the chemical components of a mixture (e.g. jet fuel performance additives) may modulate the percutaneous absorption of other components (e.g. hydrocarbons in jet fuel). If these modulated components are the agents responsible for toxicity, then an additive that alters their absorption, but in itself is not toxic, could potentiate the toxicity of a mixture in which the additive is present. If skin deposition is favored, this mixture might be expected to induce dermal toxicity; while in contrast if percutaneous absorption is facilitated then systemic toxicity may be potentiated. If the toxicity of the additive were assessed singly, this potential to enhance the toxicity of a mixture of which it is a component, would not be detected. If the component were in addition directly toxic, the toxicity of the resultant mixture might even be exaggerated. *The fundamental scientific concept being investigated then is the ability to extrapolate the toxicity and disposition of a single chemical to more complex mixtures, and a simple mixture to a complex mixture.* This work has involved developing both the experimental models capable of detecting interactions that would modulate dermal absorption or toxicity, as well as efficient statistical approaches to graphically identify significant interactions.

Compass Plots: The complexity of interactions seen in these mixture studies makes comparisons across experiments difficult and confusing. To facilitate the identification of statistically significant changes, as well as comparing interactions across markers and model systems, a graphical technique based on an analysis of means was developed (Budsaba et al., 2000). A compass plot (Figure One) for both treatment effects and interactions is a radial plot with the magnitude of each treatment mean determining the length of the ray. Simultaneous confidence intervals are added to produce inner and outer polygons, resulting in doughnut shaped plots. All treatment combinations are then plotted which allow for a direct comparison of significant treatment effects by assessing which treatment means fall inside (decreased) or outside (increased) the doughnut. These plots are employed to illustrate the significant interactions detected in all of the experiments.

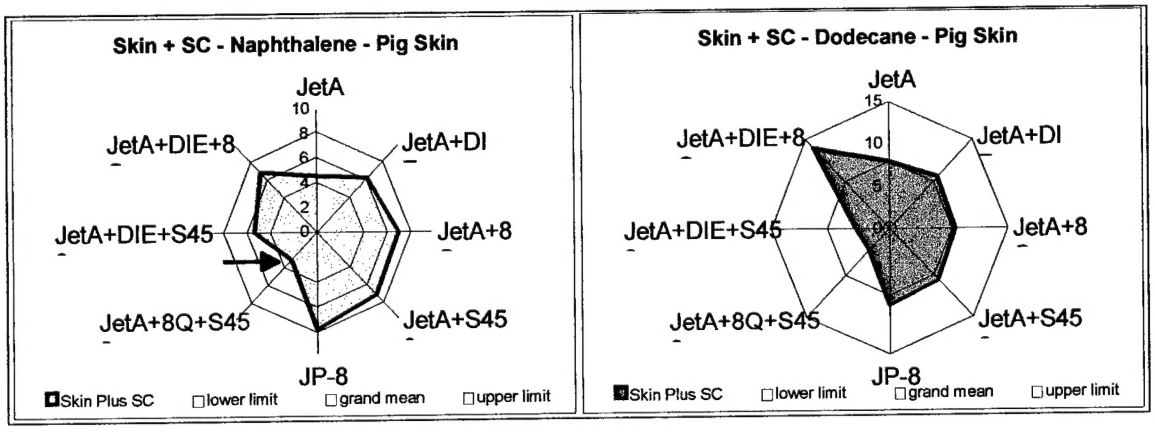

Figure One: Compass plot of three-component chemical interaction. This plot demonstrates the mean and confidence intervals for all treatment means. Points outside or inside of this polygon (→) are significantly different.

Dermal Absorption Studies: The effects of JP-8 additives (DIEGME, 8Q21, Stadis 450) singly and in all combinations (single, 2x2, 3x3 =JP-8), on the percutaneous absorption and dermal deposition of radiolabelled dodecane and naphthalene, was compared to the base fuel Jet-A using the above three *in vitro* systems. Use of three systems of increasing biological complexity allows mechanisms of observed interactions to be inferred.

The primary model system used to assess these effects is the IPPSF (Figure Two) *(Riviere et al. Fundamental and Applied Toxicology 7: 444-453, 1986)*. A two-stage surgical procedure is employed which results in a single pedicle axial pattern tubed skin flap supplied by a cannulated artery that is then perfused in an isolated organ perfusion chamber (Figure Three). Test substances are placed on the surface of the flap and percutaneous absorption is tracked by assaying chemical flux in the venous effluent. Absorption of compounds in the IPPSF has been shown to be predictive of *in vivo* human absorption (*Wester et al. Toxicology and Applied Pharmacology 151: 159-165, 1998).* At the end of an experiment, the skin is biopsied for histopathology and assessment of cutaneous deposition of the applied drug. Venous effluent may simultaneously be assayed for pro-inflammatory cytokines release due to skin irritation from the applied chemicals.

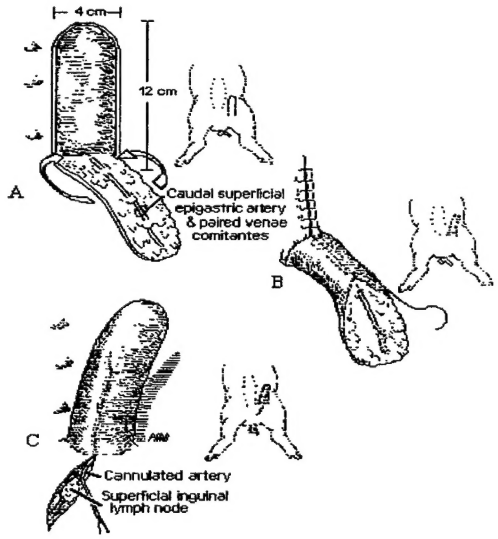

Figure Two: Two-stage IPPSF surgery

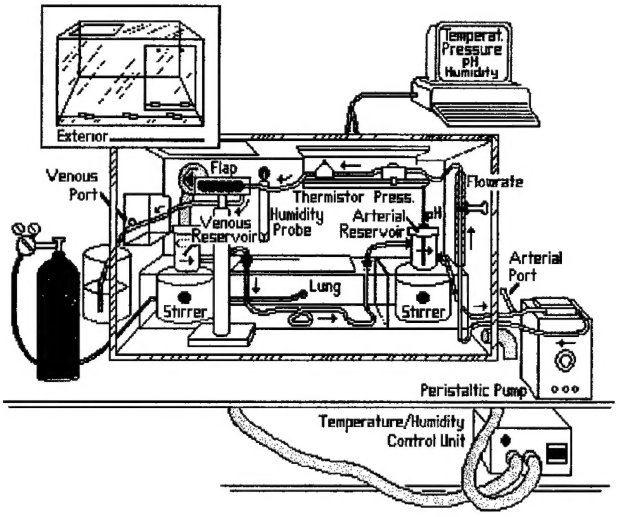

Figure Three: IPPSF perfusion chamber

Naphthalene absorption in the IPPSF (0.76-2.39%) was greater than dodecane absorption (0.1-0.84%) across all mixtures (Riviere et al., 1999). When absorption of these markers plus hexadecane absorption was assessed from JP-8, the pattern was naphthalene > dodecane > hexadecane (Figure Four). This pattern was reversed (hexadecane > dodecane > naphthalene) for skin deposition (Figure Five). Note in most of the interaction studies

conducted, changes in percutaneous absorption (*reflective of potential systemic exposure*) often diverged from skin deposition (*reflective of potential dermal toxicity*).

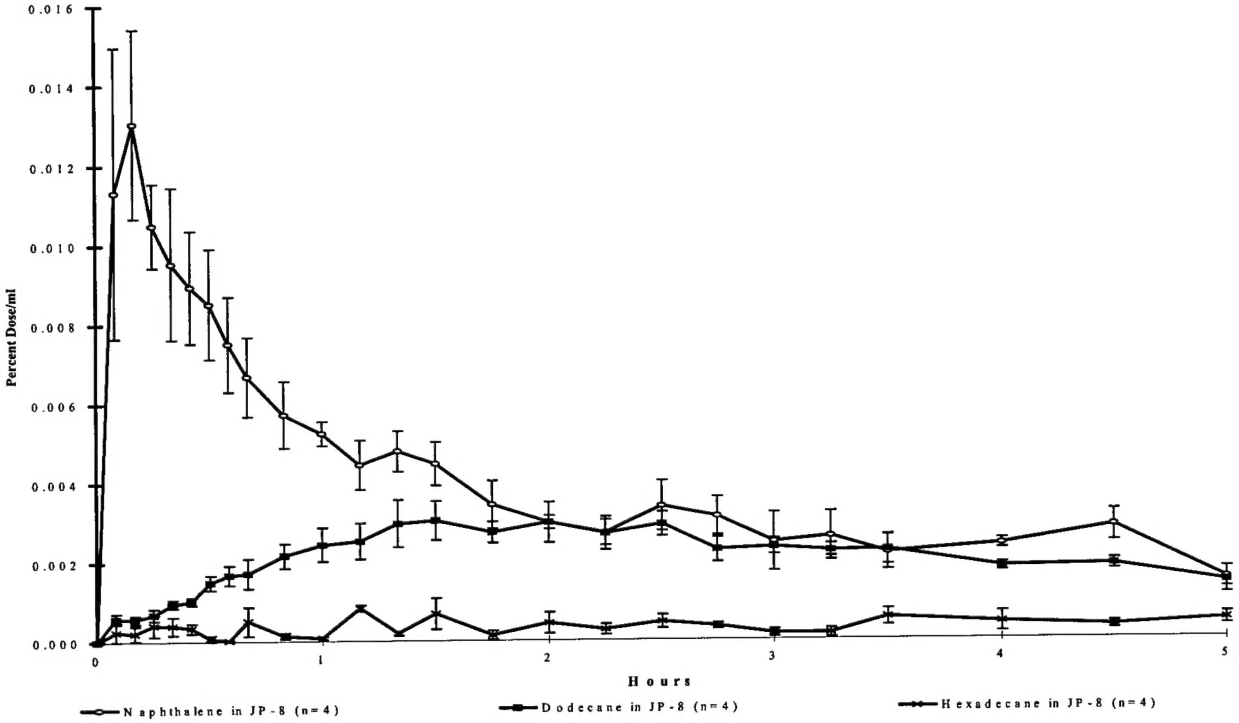

Figure Four. Naphthalene, Dodecane and Hexadecane IPPSF Absorption Profiles from JP-8

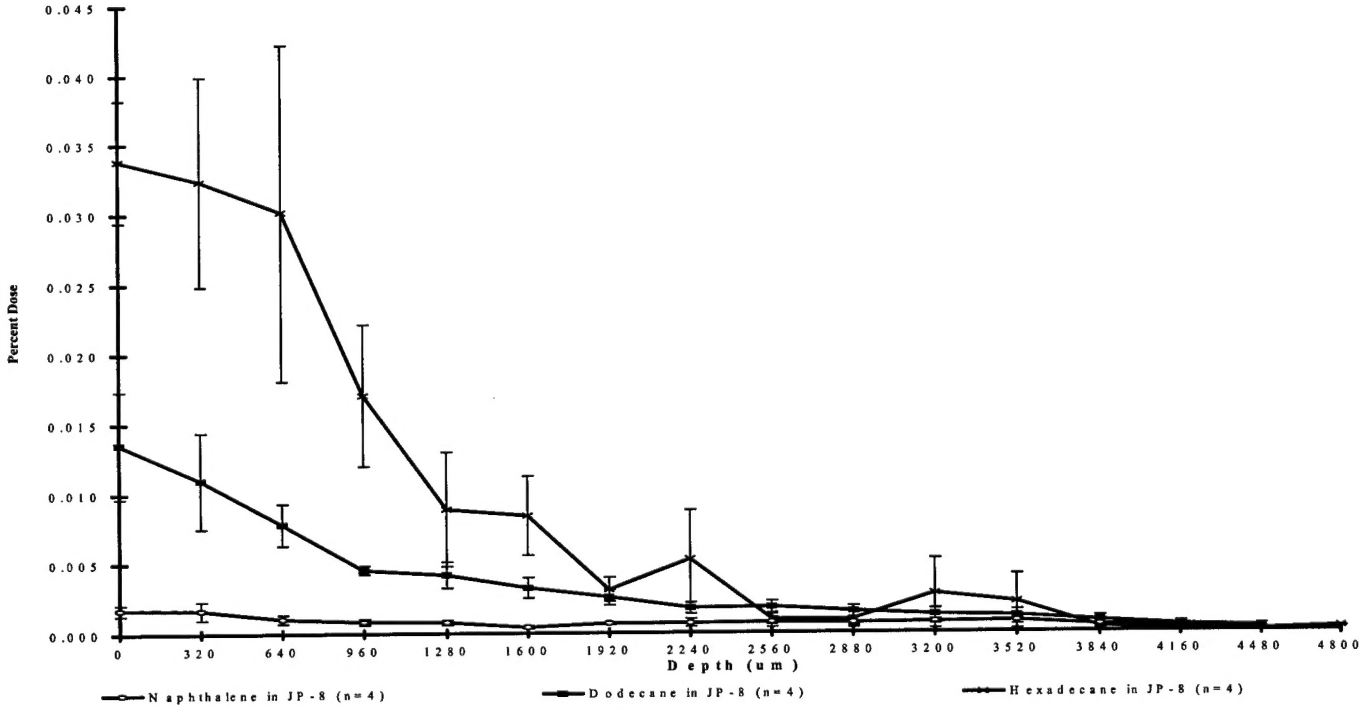

Figure Five: Naphthalene, dodecane and hexadecane skin deposition in the IPPSF using serial sections from JP-8 (Note x-axis is now depth of penetration into skin)

Marker absorption was also compared across all fuel types. Naphthalene absorption into perfusate was similar across all fuel types, however, total penetration into and through skin was highest with JP-8(100). Dodecane absorption and total penetration was greatest from JP-8. *Aged* (evaporated) JP-8 was created to more closely mimic field exposure to spilled fuels. The most pronounced effect seen was an enhanced skin/perfusate deposition ratio for dodecane from the aged or weathered JP-8 "puddle" suggesting that absorption from this jet fuel vehicle tended to promote skin deposition of this marker.

Absorption of naphthalene and dodecane were also studied using 5-hr *in vitro* flow-through diffusion cells with inert silastic or dermatomed porcine skin (Baynes et al., 2001). In both membrane systems and across all jet fuels tested, naphthalene absorption (1.29-1.84% dose) was significantly greater than dodecane absorption (0.14 – 0.28% dose). Significantly more dodecane than naphthalene was observed in the stratum corneum (SC; 4.23 – 7.23% dose *vs.* 1.88 – 4.08% dose) and silastic membranes (59.2 – 81.7% dose *vs.* 30.5 – 36.7% dose). In porcine skin, weathered JP-8 significantly increased dodecane absorption, permeability and diffusivity, as well as naphthalene deposition in the stratum corneum compared to other fuels (Figure Six). The effect of weathered JP-8 on dodecane diffusivity is clearly seen in this Compass Plot. In contrast to the IPPSF, there were no differences among the three fuels in terms of their ability to influence naphthalene or dodecane disposition in skin, and generally no significant differences among the four jet fuel mixtures were observed in silastic membranes. This is not surprising since dermatomed skin lacks the normal vasculature and intact physiology that is present in intact animals and the IPPSF.

These findings prompted further investigations into the effect of specific JP-8 additives (DIEGME, 8Q21, Stadis 450), singly and in all combinations on the percutaneous absorption and cutaneous deposition of naphthalene and dodecane in all model systems. A number of 2x2 and 3x3 interactions were detected for both markers. Interactions seen in the silastic model system were different than those seen in the skin diffusion cell and IPPSF experiments. Curiously, additives

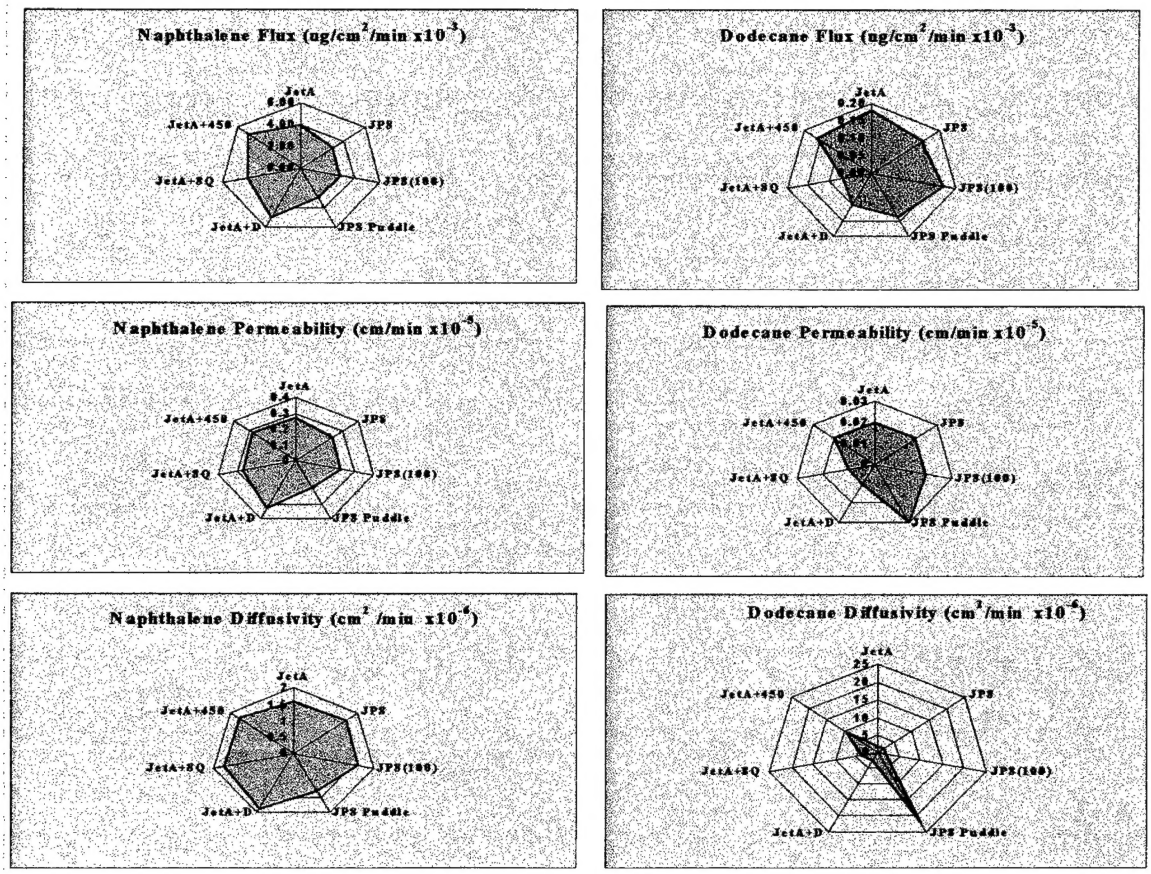

Figure Six: Compass plots of naphthalene and dodecane transport in jet fuels.

occurring singly had a smaller effect on marker absorption than when present in combination. DIEGME and Stadis 450 combinations tended to alter stratum corneum and skin deposition of both markers, while 8Q21 and Stadis 450 altered the absorptive flux. These complex patterns of interactions suggest that models with different levels of biological complexity demonstrate different interactions, and that knowledge of 2x2 interactions do not predict the behavior of a three component additive package. A manuscript describing these observations (Baynes et al., 2001) has been submitted for publication.

In Vivo Toxicity: A number of toxicological investigations have also been conducted using intact pigs. The primary data has been submitted for publication (Monteiro-Riviere et al., 2001) while a manuscript describing the histochemical analysis of these studies has been accepted for publication (Rhyne et al., 2001) and should be consulted for full details. We evaluated the ability of topical jet fuel exposure to cause skin irritation by exposing Yorkshire pigs to single doses of Jet-A, JP-8, and JP-8(100) under occluded (Hill Top Chamber or cotton fabric) and nonoccluded conditions for 5hr, 24hr and repeated dosing for 4 days observed at 5 days. All jet fuels produced dermal

irritation characterized grossly by erythema, edema, and increased transepidermal water loss (TEWL); and histologically by a thickened epidermis, increased epidermal cell layers and depth of rete pegs in the four day fabric treated sites. Epidermal thickness tended to increase after 24 hr exposure. Enzyme histochemistry demonstrated significant increases in alkaline phosphatase (ALP) staining in the stratum basale layer of the epidermis and nonspecific esterase (NSE) activity in the stratum granulosum after jet fuel exposure. In most endpoints studied in these *in vivo* toxicology trials, JP-8(100) produced the most severe fuel effect. These findings are tabulated in Table 1 and illustrated in Figure Seven. These studies clearly illustrate that in vivo exposure to jet fuels results in statistically significant dermal irritation marked by significant epidermal thickening (Table 1). These were most obvious in the occluded fabric treated sites which were the highest doses studied. A complete dose-response relationship needs to be defined. It is clear that all fuels are capable of inducing dermal irritation, however JP-8(100) seems to be the most severe. The finding of irritation with all fuels suggests that it is a hydrocarbon component responsible for the irritation, and that severity may be modulated by additive components.

TABLE 1: Erythema score, edema score, and epidermal thickness in the in vivo 5 hr, 24 hr, and 5 D fabric occluded sites exposed to jet fuels.

Treatments	Mean (±SEM)		
	Erythema Score	**Edema Score**	**Epidermal Thickness (μm)**
5 hr Control	0.0 ± 0.0^{a}	0.0 ± 0.0	48.9 ± 2.5^{H}
5 hr Jet-A	$1.0 \pm 0.0^{b,g}$	0.0 ± 0.0^{o}	54.0 ± 2.5^{I}
5 hr JP-8	$1.0 \pm 0.0^{b,i}$	0.0 ± 0.0^{q}	48.4 ± 1.8^{K}
5 hr JP-8 (100)	$1.0 \pm 0.0^{b,k}$	0.0 ± 0.0^{s}	49.8 ± 1.9^{M}
24 hr Control	0.0 ± 0.0^{c}	0.0 ± 0.0	$44.9 \pm 2.5^{A,H}$
24 hr Jet-A	$0.8 \pm 0.2^{d,g}$	0.0 ± 0.0^{o}	66.7 ± 6.0^{B}
24 hr JP-8	$0.6 \pm 0.2^{d,i}$	0.0 ± 0.0^{q}	$62.8 \pm 4.1^{B,L}$
24 hr JP-8 (100)	$0.8 \pm 0.1^{d,k}$	0.0 ± 0.0^{s}	$71.7 \pm 8.1^{B,N}$
5 day Control	0.0 ± 0.0^{e}	0.5 ± 0.3^{m}	$32.4 \pm 1.4^{C,G}$
5 day Jet-A	$2.8 \pm 0.5^{f,h}$	$2.0 \pm 0.4^{n,p}$	$70.2 \pm 5.1^{D,E,J}$
5 day JP-8	$3.0 \pm 0.4^{f,j}$	1.8 ± 0.5^{r}	$75.8 \pm 6.7^{D,L}$
5 day JP-8 (100)	$2.8 \pm 0.6^{f,l}$	$2.3 \pm 0.5^{n,t}$	$86.6 \pm 6.1^{D,F,N}$

(^{a} and ^{b}), (^{c} and ^{d}), (^{e} and ^{f}), (^{g} and ^{h}), (^{i} and ^{j}), (^{k} and ^{l}) are significantly different ($p<0.05$).
(^{m} and ^{n}), (^{o} and ^{p}), (^{q} and ^{r}), (^{s} and ^{t}) are significantly different ($p<0.05$).
(^{A} and ^{B}), (^{C} and ^{D}), (^{E} and ^{F}), (^{G} and ^{H}), (^{I} and ^{J}), (^{K} and ^{L}), (^{M} and ^{N}) are significantly different ($p<0.05$).

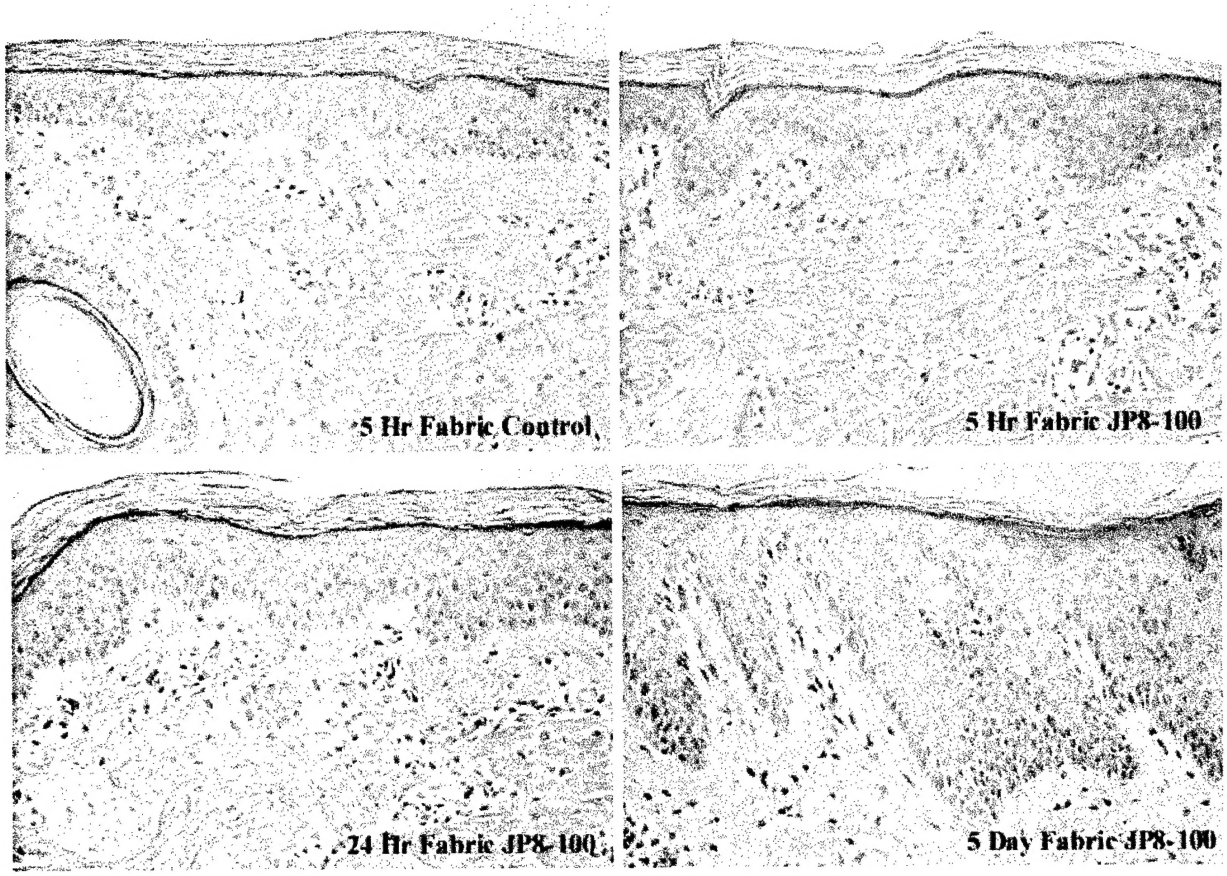

Figure Seven: Significantly Thickened Epidermis and Rete Pegs in Skin Exposed to JP-8 (100) Compared to Controls.

Keratinocyte Cell Culture Studies: The effects of fuels and hydrocarbons on release of pro-inflammatory cytokines IL-8 and TNFα were evaluated, both by enzyme-linked immunoassay of product as well as mRNA signal induction through quantitative RT-PCR. Normal human epidermal keratinocyte (NHEK) cultures suggested that all jet fuels resulted in production and release of IL-8 and TNFα (Figures Eight and Nine) (Allen et al., 2000). All fuels demonstrated a similar level of cytokine release, the only difference being a slightly lower release of TNFα at one hour with JP-8(100). This suggests that there is no inherent difference in jet fuel toxicity to epidermal keratinocytes, and supports our hypothesis that any differences in dermal toxicity seen between fuel types may be related to additive effects on modulating skin deposition of hydrocarbon components.

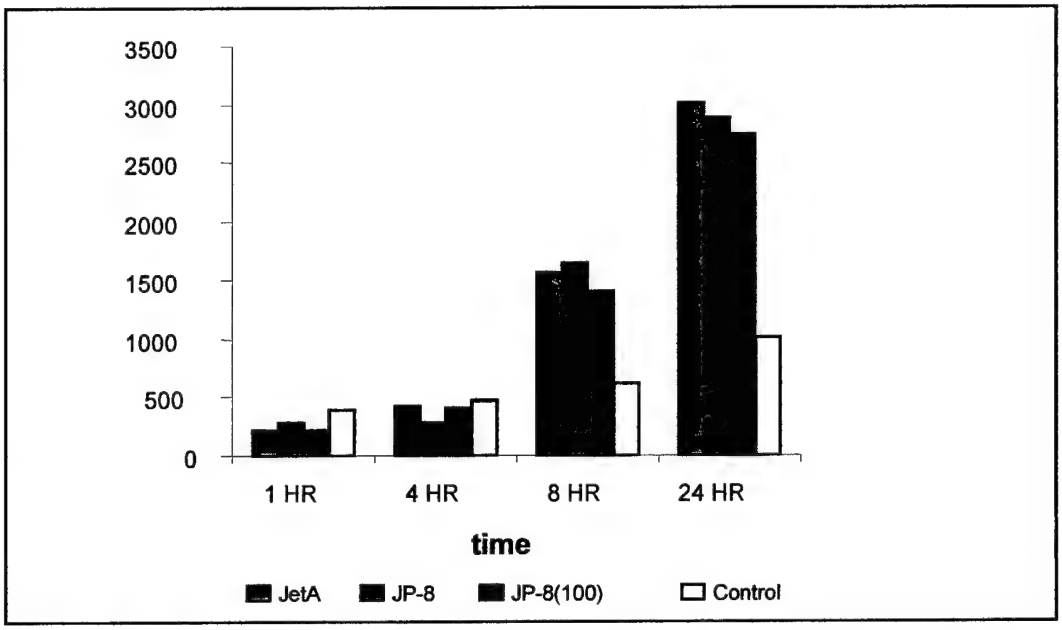

Figure Eight: Release of IL-8 (pg/ml) in Human Keratinocytes Secondary to Jet Fuel Exposure

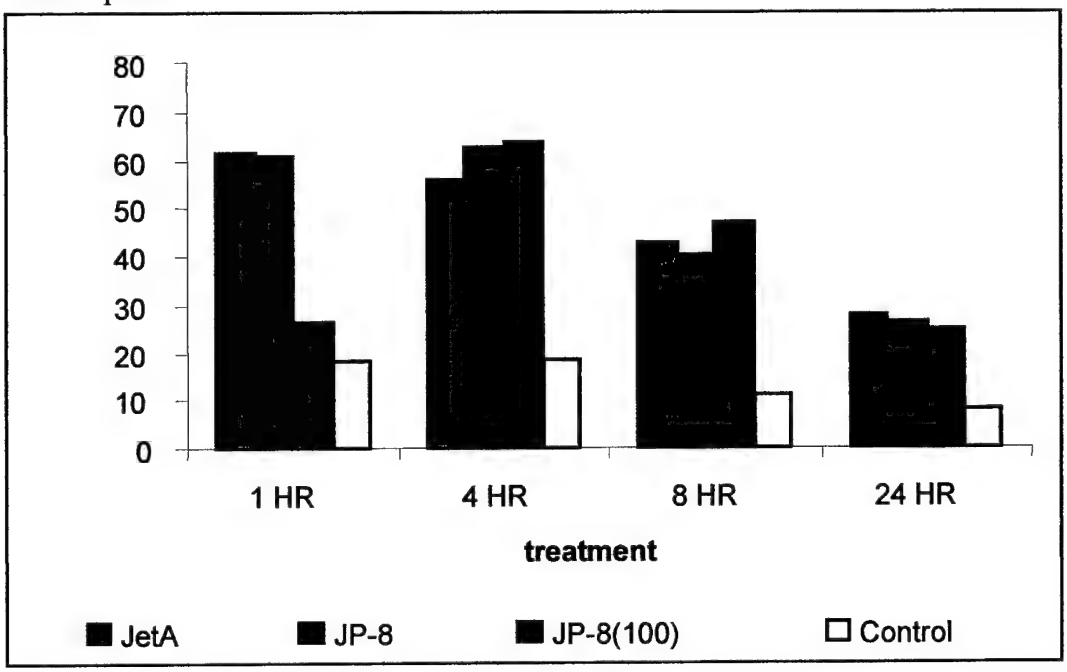

Figure Nine: Release of TNFα (pg/ml) in Human Keratinocytes Secondary to Jet Fuel Exposure

Studies in primary porcine keratinocytes (PKC) showed some similarities to NHEK responses, supporting the use of the pig as an animal model for these studies. However, studies in an immortalized porcine keratinocyte cell line (MSK3877) differed from both NHEK and PKC in that IL-8 protein release was inhibited, rather than increased after jet fuel exposure (Allen et al., 2001). These data reaffirm that model selection is critical in the *in vitro* assessment of jet fuel toxicity.

A complete factorial study of Jet-A plus all combinations of performance additives was then conducted to assess whether individual additives modulated keratinocyte response to Jet-A. No additive effect was detected. These data also suggest that at least for keratinocytes, hydrocarbon components of fuel were responsible for pro-inflammatory cytokine release. Studies were then conducted to assess which hydrocarbons were responsible for cytokine release compared to controls. At this point in the conduct of these studies, both aliphatic and aromatic constituents are capable of eliciting this response.

Discussion: These studies demonstrate that individual jet fuel additives modulate the percutaneous absorption and skin deposition of hydrocarbon components of fuels. The effects are dependent upon the specific additives present, as well as what level of *in vitro* system is used to assess the absorption. The inert silastic membrane studies were the least consistent with the other systems. Dodecane seemed to be the most susceptible hydrocarbon studied to modulation by fuel type and/or JP-8 additives, with dermal disposition primarily affected. The response of exposure to single additives could not be used to predict response to pairs of additives or the complete additive package. Significant effects on dodecane skin deposition in all model systems were seen with the occupationally relevant *weathered* or *aged* JP-8, with diffusivity through skin being an especially sensitive, and experimentally accessible endpoint in the simpler *in vitro* systems. Changes in diffusivity may reflect modulation of the pathway of dodecane transit through skin that could result in the observed formation of depots in the IPPSF; as well as alter exposure to cellular targets of toxicity. Percutaneous absorption (and thus systemic exposure) of naphthalene appears to be greatest from JP-8(100), although the mechanism of this effect was not elucidated since JP-8 (100) additives were not studied in the present proposal.

In contrast to these disposition studies, *in vivo* exposure resulted in cutaneous irritation for all jet fuels. There was a tendency for JP-8(100) to result in a slightly greater

in vivo response. Similarly, all jet fuels resulted in cytokine release from keratinocyte cell cultures, independent upon which additives are present. It is the hydrocarbon component that appears responsible for this toxicity. Differences in dermal toxicity seen between fuels may be due to modulation of hydrocarbon component absorption secondary to the additives. These studies indicate that a skin irritation component of topical exposure to jet fuels is present and may result in immuno-modulation by virtue of altered cytokine release. Similarly, changes in enzyme function reflected by the histochemical analysis suggests that skin functions related to enzyme activity (e.g. dermal metabolism of applied chemicals) may likewise be altered. Longer term exposures to fuel are required to see if this difference in fuel effects is occupationally significant.

Transition / Technology Transfers: Our knowledge gained in studying the absorption of jet fuels in the IPPSF and assessing their toxicity in keratinocyte cell culture systems was directly applied to study the effects of chemical mixtures in a U.S. Army supported Gulf War Illness research project (DAMD-17-99C-9047). In fact, the effect of co-exposure of skin to topical permethrin and DEET was also studied after JP-8 exposure, a treatment combination which further enhanced permethrin absorption. This research would not have occurred in the absence of the present AFOSR grant. The pharmacokinetic modeling approach developed in this proposal was also used to compare the percutaneous absorption of methyl salicylate as a simulant for the chemical warfare agent sulfur mustard (DAAD-13-98D-0014), a study accepted for publication in Journal of Applied Toxicology. The Compass Plots developed under the auspices of the present grant (see attached manuscript by Budsaba et al. in Toxicology Methods) are being extensively used in other research projects being conducted on complex chemical mixtures within the NCSU Center for Cutaneous Toxicology and Residue Pharmacology.

Publications

Copies of these manuscripts are attached to this report in the following chronological order.

Riviere JE, Monteiro-Riviere NA, Brooks JD, Budsaba K, Smith CE: Dermal absorption and distribution of topically dosed jet fuels Jet A, JP-8, and JP-8(100). Toxicology and Applied Pharmacology 160: 60-75, 1999.

Allen DG, Riviere JE, Monteiro-Riviere NA: Induction of early biomarkers of inflammation produced by keratinocytes exposed to jet fuels Jet-A, JP-8 and JP-8(100). Journal of Biochemical and Molecular Toxicology 14: 231-237, 2000.

Budsaba K, Smith CE, Riviere JE: Compass Plots: A combination of star plot and analysis of means (ANOM) to visualize significant interactions in complex toxicology studies. Toxicology Methods 10: 313-332, 2000.

Riviere JE, Brooks JD, Qiao, GL: Methods for assessing the percutaneous absorption of volatile chemicals in isolated perfused skin: Studies with chloropentafluorobenzene and dichlorobenzene. Toxicology Methods 10: 265-281, 2000.

Baynes RE, Brooks JD, Riviere JE: Membrane transport of naphthalene and dodecane in jet fuel mixtures. Toxicology and Industrial Health (2001). *In Press*

Allen DG, Riviere JE, Monteiro-Riviere NA: Cytokine induction as a measure of cutaneous toxicity in primary and immortalized porcine keratinocytes exposed to jet fuels and their relation to normal human keratinocytes. Toxicology Letters (2001). *In Press*

Rhyne BN, Pirone JR, Riviere JE, Monteiro-Riviere NA: The use of enzyme histochemistry in detecting cutaneous toxicity of three topically applied jet fuel mixtures. Toxicology Methods (2001). *In Press*

In addition the following manuscripts have been submitted for publication but are not included with this report:

Baynes RE, Brooks JD, Budsaba K, Smith C, Riviere JE: Influence of JP-8 additives on the dermal disposition of jet fuel components.

Monteiro-Riviere NA, Inman A, Riviere JE: The effects of short term high dose and low dose dermal exposure to Jet A, JP-8, and JP-8 +100 jet fuels.

Allen DG, Riviere JE, Monteiro-Riviere NA: Aliphatic hydrocarbons induce the release of interleukin-8 from normal human epidermal keratinocytes: Delivery of hydrocarbons to cells in culture via complexation with α-cyclodextrin.

Abstracts

Allen DG, Monteiro-Riviere NA, Riviere JE: Cytokine release from keratinocytes exposed to Jet A, JP8, JP8-100 jet fuels. Toxicological Sciences. 54: 151, 2000.

Basak SC, Gute BD, Grunwald G, Mills D, Riviere JE, Opitz D: Clustering of JP-8 chemicals using structure spaces and property spaces. A computational approach.

Proceedings International. Conference on Medicinal Chemistry and Biostatistics, New Delhi, India, 1999.

Basak SC, Gute BD, Grunwald G, Mills D, Riviere JE: Clustering of JP-8 chemicals using structure spaces and property spaces. A computational approach. AFOSR JP-8 Jet Fuel Toxicology Workshop. Tucson, AZ, 2000.

Baynes, RE, Brooks, JD, Abdullahi, AR, Wilkes, R, and Riviere, JE: Influence of jet fuel mixtures on dermal absorption of aromatic and aliphatic components. Toxicological Sciences 54: 155, 2000.

Monteiro-Riviere NA, Inman AO, Rhyne BN, Riviere JE: Cutaneous irritation of topically applied jet fuels in the pig. Toxicological Sciences. 54: 151, 2000.

Rhyne BN, Riviere JE, Monteiro-Riviere NA: Cutaneous enzyme histochemistry of topically applied jet fuels in the pig. Toxicological Sciences. 54: 151, 2000.

Riviere JE, Monteiro-Riviere NA, Brooks JD, Budsaba K, Smith C. Dermal absorption and toxicity of jet fuels. Toxicological Sciences 48(1S): 71, 1999.

Riviere JE, Monteiro-Riviere NA, Brooks JD, Budsaba K, Smith C: Dermal absorption, distribution and toxicity of topically dosed jet fuels Jet A, JP-8 and JP-8(100). AFOSR JP-8 Jet Fuel Toxicology Workshop, Tucson, AZ, 1998.

Riviere JE, Baynes RE, Allen DG, Monteiro-Riviere NA: Percutaneous absorption and cutaneous toxicity of topically applied Jet A, JP-8, and JP-8 (100). AFOSR JP-8 Jet Fuel Toxicology Workshop. Tucson, AZ, 2000.

Riviere JE, Baynes RE, Allen DA, Budsaba K, Smith CE, Monteiro-Riviere NA: Dermal absorption and toxicity of topically applied jet fuels: *In vitro* and *in vivo* studies. AFOSR JP-8 Jet Fuel Toxicology Workshop. Tucson, AZ, 2001.

Toxicology and Applied Pharmacology 160, 60–75 (1999)
Article ID taap.1999.8744, available online at http://www.idealibrary.com on IDEAL®

Dermal Absorption and Distribution of Topically Dosed Jet Fuels Jet-A, JP-8, and JP-8(100)

Jim E. Riviere,*[,1] James D. Brooks,* Nancy A. Monteiro-Riviere,* Kamon Budsaba,† and Charles E. Smith†

*Center for Cutaneous Toxicology and Residue Pharmacology, College of Veterinary Medicine, and †Department of Statistics, College of Agricultural and Life Sciences, North Carolina State University, Raleigh, North Carolina 27606

Received March 15, 1999; accepted July 2, 1999

Dermal Absorption and Distribution of Topically Dosed Jet Fuels JET-A, JP-8, and JP-8(100). Riviere, J. E., Brooks, J. D., Monteiro-Riviere, N. A., Budsaba, K., and Smith, C. E. (1999). *Toxicol. Appl. Pharmacol.* **160**, 60–75.

Dermal exposure to jet fuels has received increased attention with the recent release of newer fuels with novel performance additives. The purpose of these studies was to assess the percutaneous absorption and cutaneous disposition of topically applied (25 μl/5 cm^2) neat Jet-A, JP-8, and JP-8(100) jet fuels by monitoring the absorptive flux of the marker components ^{14}C naphthalene and ^{3}H dodecane simultaneously applied nonoccluded to isolated perfused porcine skin flaps (IPPSF) (n = 4). Absorption of ^{14}C hexadecane was estimated from JP-8 fuel. Absorption and disposition of naphthalene and dodecane were also monitored using a nonvolatile JP-8 fraction reflecting exposure to residual fuel that might occur 24 h after a jet fuel spill. In all studies, perfusate, stratum corneum, and skin concentrations were measured over 5 h. Naphthalene absorption had a clear peak absorptive flux at less than 1 h, while dodecane and hexadecane had prolonged, albeit significantly lower, absorption flux profiles. Within JP-8, the rank order of absorption for all marker components was (mean ± SEM % dose) naphthalene (1.17 ± 0.07) > dodecane (0.63 ± 0.04) > hexadecane (0.18 ± 0.08). In contrast, deposition within dosed skin showed the reverse pattern. Naphthalene absorption into perfusate was similar across all fuel types, however total penetration into and through skin was highest with JP-8(100). Dodecane absorption and total penetration was greatest from JP-8. Absorption of both markers from aged JP-8 was lower than other fuels, yet the ratio of skin deposition to absorption was greatest for this treatment group. In most exposure scenarios, absorption into perfusate did not directly correlate to residual skin concentrations. These studies demonstrated different absorption profiles for the three marker compounds, differential effects of jet fuel types on naphthalene and dodecane absorption, and uncoupling of perfusate absorption from skin disposition.

Key Words: jet fuel; naphthalene; dodecane; hexadecane; percutaneous/dermal absorption; skin.

Jet fuels used in commercial and military aircraft are a complex multicomponent mixture of aromatic and aliphatic hydrocarbons. Due to their natural petroleum base, their chemical composition is not defined and the fuels are classified according to broad performance criteria such as boiling and flash points. Military fuels are designated as members of the JP (jet propellant) series with JP-4 and JP-7 being the primary fuels used in earlier years. Recently, the military has fielded two new fuels [JP-8 and JP-8(100)] containing several performance additives, which result in fuels with higher flash points and improved heat sink characteristics.

The primary military jet fuel is JP-8 which is essentially a kerosene-cut commercial jet fuel base, Jet-A, to which additives are added to make up <2% of the formulation [a corrosion inhibitor DC1-4A, an antistatic compound Stats 450, and an icing inhibitor diethylene glycol monomethyl ether (DIEGME)]. In the base fuel, 13 components, present at greater than 1% v/v concentrations, comprise 29% of the formulation (see Table 1). JP-8(100) is JP-8 with an additional additive package consisting of antioxidant, chelator, detergent, and dispersant components. Because of the chemical complexity of these fuels, one cannot assess the absorption of the entire fuel, but must instead monitor absorption of individual so-called marker components.

Although there is a relatively large reviewed database on the toxicology and absorption after inhalational exposure to early jet fuels (Jet-A, JP-4, and JP-7) (ATSDR, 1995), and more recently to JP-8 (ATSDR, 1996; Pfaff *et al.*, 1995; Harris *et al.*, 1997), there is no information on the percutaneous absorption after topical exposure to any jet fuels (ATSDR, 1995, 1996). Skin sensitization assays have demonstrated some level of irritation after exposure to the older fuels that may lead to chemical burns (Clark *et al.*, 1988; ATSDR, 1995, 1996), providing indirect evidence of dermal penetration. In reality, the potential for percutaneous absorption leading to dermal and systemic tissue exposure to components of jet fuels has not been systematically investigated.

To quantitate the dermal absorption and cutaneous distribution of these fuels, we utilized a radiolabeled aromatic (^{14}C-naphthalene) and an aliphatic (^{3}H-dodecane) marker from

[1] To whom correspondence and reprint requests should be addressed: Center for Cutaneous Toxicology and Residue Pharmacology, College of Veterinary Medicine, 4700 Hillsborough Street, North Carolina State University, Raleigh, NC 27606. E-mail: Jim_Riviere@NCSU.EDU.

0041-008X/99 $30.00

TABLE 1
Major Components of JetA

Class	Component	Percent of total	No. of carbons	No. of hydrogens	Mol. wt.
Alkane	Dodecane*	4.7%	12	26	170
Alkane	Tridecane	4.4%	13	28	184
Alkane	Undecane	4.1%	11	24	156
Alkane	Tetradecane	3.0%	14	30	198
Alkane	2,6-Dimethylundecane	2.1%	13	28	184
Alkane	Pentadecane	1.6%	15	32	212
Alkane	2-Methylundecane	1.2%	12	26	170
Alkane	Heptylcyclohexane	1.0%	13	26	182
Aromatic	1-methylnaphthalene	1.8%	11	10	142
Aromatic	2-methylnaphthalene	1.5%	11	10	142
Aromatic	2,6-Dimethylnapthalene	1.3%	12	12	156
Aromatic	Naphthalene*	1.1%	10	8	128
Aromatic	1,2,3,4-Tetramethylbenzene	1.1%	10	14	134
	Total	28.9%			

Note. Jet fuel is composed of some 228 components and these 13 only represent 28.9% of the total fuel. The marker compounds studied represent only 5.8% of total.

* Chosen as a marker compound in this study.

among the most prevalent components of JP-8 listed in Table 1. To determine a constituent effect, we studied the absorption, penetration, and cutaneous distribution of these marker compounds in the *in vitro* isolated perfused porcine skin flap (IPPSF) when dosed from Jet-A, JP-8, and JP-8(100). This model system has been successfully utilized to model the mechanism of percutaneous chemical absorption (Riviere and Monteiro-Riviere, 1991; Riviere *et al.*, 1995b; Qiao *et al.*, 1996) and to extrapolate these results to humans (Riviere *et al.*, 1992; Wester *et al.*, 1998; Williams *et al.*, 1990). We also assessed the absorption of naphthalene and dodecane from a fraction of a so-called aged JP-8 "puddle" which was produced by allowing JP-8 to evaporate from an open glass petri dish left in a fume hood for 24 h. After the more volatile components evaporated, the remaining mixture should resemble residual jet fuel remaining 24 h after a jet fuel spill. Finally, to further probe the absorption characteristics of the primary fuel JP-8, we also studied the absorption of a longer chain aliphatic hydrocarbon, ^{14}C-hexadecane after exposure in JP-8.

MATERIALS AND METHODS

Chemicals. Radiolabeled ^{14}C-naphthalene (specific activity = 8.1 mCi/mmol) and ^{3}H-dodecane (specific activity = 10,000 mCi/mmol) in methylene chloride were custom labeled by the NCI Chemical Carcinogen Reference Standard Repository (Chemsyn Science Laboratories, Lenexa, KS). The ^{14}C-hexadecane (specific activity = 4.1 mCi/mmol) was obtained from Sigma Chemical (St. Louis, MO). Radiochemical purity of both compounds ranged from 98 to 100%.

All jet fuels, Jet-A, JP-8, and JP-8(100), were kindly supplied by Major T. Miller from Wright Patterson Air Force Base. To produce an aged JP-8 (puddle), JP-8 was allowed to evaporate in an open glass petri dish within a fume hood for 24 h (n = 2). The decline in mass was recorded using an analytical balance over the course of the 24-h period. The shape of the two evaporation curves was similar with no discernible "plateau" evident. As expected, there was a first-order decay to approximately 30% of the initial mass. This remnant solution was then spiked with the radiotracer markers and used for all exposures.

IPPSF studies. The IPPSF procedure has been previously documented (Riviere *et al.*, 1986; Riviere and Monteiro-Riviere, 1991; Riviere *et al.*, 1995b). In these studies, jet fuel mixtures were applied nonoccluded to mimic field exposure conditions, and experiments were conducted for a total of 5 h in IPPSFs with 4 replicates per treatment condition. A 1 × 5 cm dosing area was drawn on the surface of the skin flap with a surgery marker. A dose, containing 25 μl of the specified jet fuel containing approximately 2 μCi of ^{14}C-naphthalene plus 10 μCi of ^{3}H-dodecane, was applied directly to the surface of the skin flap. The specific activities of the marker compounds were sufficient that the added radiolabeled compounds had little effect on the final concentration of naphthalene (1.21% instead of 1.1%) and dodecane (4.701% instead of 4.7%). Single label studies were initially conducted and compared to the dual-label results to test whether using this dual-label experimental design had any effect on marker absorption. No effect was detected.

Perfusate samples (3 ml) were collected every 5 min for the first 40 min, then every 10 min until 1.5 h, and then every 15 min until termination at 5 h. At termination, several samples were taken for mass balance of the marker compounds. The surface of the dose area was swabbed twice with a 1% soap solution and gauze, and then 12 stratum corneum tape strips were collected using cellophane tape (3M Corporation, Minneapolis, MN). The entire dose area was removed. A 1 × 1 cm core of the dose area was removed and frozen for subsequent depth of penetration studies. This consisted of laying the core sample epidermal side down in an aluminum foil boat and embedding in Tissue-Tek OCT compound (Miles, Inc., Elkhart, IN), snap freezing in liquid nitrogen, followed by sectioning (40 μm) on a Reichart-Jung Model 1800 Cryocut (Warner Lambert, Buffalo, NY). The remaining dosed area as well as the surrounding skin was separated from the fat and held for analysis. All samples (including swabs, tape strips, core sections, skin, fat, mass balance samples, etc.) were dissolved separately in Soluene. A representative volume of each sample was oxidized completely via a Packard Model 307 Tissue Oxidizer. The ^{3}H and ^{14}C samples were counted separately on a Packard Model 1900TR TriCarb Scintillation Counter.

Data analysis. Data was entered into a custom IPPSF database and the resulting analysis reported. Since all experiments were conducted using the

identical marker doses across all fuels, and the absolute concentrations of these marker compounds were similar, these results are expressed as percentage applied dose to give a representative assessment of the absorption and cutaneous penetration of a complex mixture such as jet fuel. This is appropriate since the absolute concentrations of jet fuel hydrocarbons is not fixed across all fuels due to differences that arise from the natural source of the petroleum and different refining processes. Area under the curve (AUC) in the perfusate was calculated using the trapezoidal method. Peak flux was the maximum flux (% dose/min) observed at any one time point.

Figure 1 depicts the experimental compartments which were analyzed in these studies where the following definitions apply. (1) Surface is the residue removed by washing the surface of the IPPSF at termination of the experiment plus the residues remaining in the dosing template. (2) Stratum corneum is the residue extracted from the outermost stratum corneum via 12 tape strips at the termination of the experiment. (3) Dosed skin is the residue that remained in the dosed skin plus the depth of penetration core taken at termination. (4) Absorption is the cumulative amount of the marker compound collected in the effluent over the course of the 5-h experiment. (5) Fat is the residue remaining in the fat when it was separated from the dermis at the end of the experiment. (6) Penetration is the summation of the label in the effluent plus skin plus fat, but not stratum corneum nor surface. (7) Evaporative loss is that label which was lost to evaporation. Our previous studies in the IPPSF indicated that the penetration estimate is the best empirical correlate to predict eventual *in vivo* absorption in humans (Wester *et al.*, 1998).

Statistical significance of absorption and penetration parameters were determined using ANOVA or by a priori-defined orthogonal contrasts where appropriate (SAS 6.12 for Windows; SAS Institute, Cary, NC) at the 0.05 level of significance. A least significance difference (LSD) procedure was used for multiple comparisons on overall tissue disposition.

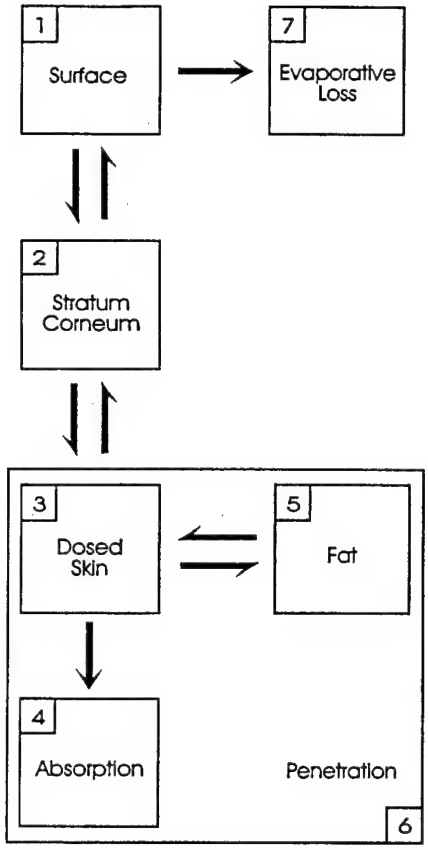

FIG. 1. Schematic depicting sampling sites for which absorption and disposition data are collected. (1) Surface is the residue removed by washing the surface of the IPPSF at termination of the experiment plus the residues remaining in the dosing template. (2) Stratum corneum is the residue extracted from the stratum corneum via 12 tape strips at the termination of the experiment. (3) Dosed skin is the residue that remained in the dosed skin plus the depth of penetration core taken at termination. (4) Absorption is the cumulative amount of the marker compound collected in the effluent over the course of the 5-h experiment. (5) Fat is the residue remaining in the fat when it was separated from the dermis at the end of the experiment. (6) Penetration is the summation of the label in the effluent plus skin plus fat, but not stratum corneum nor surface. (7) Evaporative loss is the unaccounted label.

RESULTS

There are two primary comparisons that are of interest in this study. The first is the relative absorption of the individual marker compounds from jet fuel, and the second is the effect of a specific jet fuel's composition on the absorption of a specific marker.

Absorption of Marker Compounds

Figure 2 compares the absorption flux profiles for naphthalene and dodecane across all fuels, while Fig. 3 depicts all three markers in JP-8. Naphthalene absorption peaks at less than 1 h while the aliphatic compounds are characterized by an absorption plateau at later time points. The primary effect seen in these data is this differential absorption of the individual chemical entities, an effect which overshadows any differences seen as a result of individual fuel composition effects. Table 2 summarizes the absorption parameters of naphthalene, dodecane, and hexadecane from JP-8. It is clear from these data that the rank order of marker absorption (% dose mean ± SEM) is naphthalene (1.17 ± 0.07) > dodecane (0.63 ± 0.04) > hexadecane (0.18 ± 0.08) ($p < 0.05$). Similarly, AUC and peak flux are both significantly different among all three markers.

However, a different perspective is achieved when the cutaneous deposition of these markers after dosing in JP-8 is compared. There are differences in the depth of penetration profiles evident (Fig. 4), with the rank order of compounds now reversed at the outermost layers of skin: hexadecane > dodecane > naphthalene. This is especially evident with the hexadecane data. A similar pattern is seen when the disposition of the markers in all skin compartments are examined (Fig. 5). Naphthalene absorption is highest in the perfusate but paradoxically is lowest on the surface and in the stratum corneum and dosed skin. Naphthalene total penetration, which in the IPPSF should correlate to overall absorption *in vivo* in humans, is still marginally greater than the other markers, primarily due to a significantly greater ($p < 0.05$) partitioning into the fat compartment (0.22 vs 0.08 and 0.12 for naphthalene, dodecane, and hexadecane, respectively). These data highlight the importance of the experimental perspective. If an estimate of systemic exposure is desired, then naphthalene has the greatest potential of the three markers studied. If local cutaneous toxicity is the desired endpoint, then the reverse is true since higher amounts of the aliphatic markers remain deposited in the skin at the termination

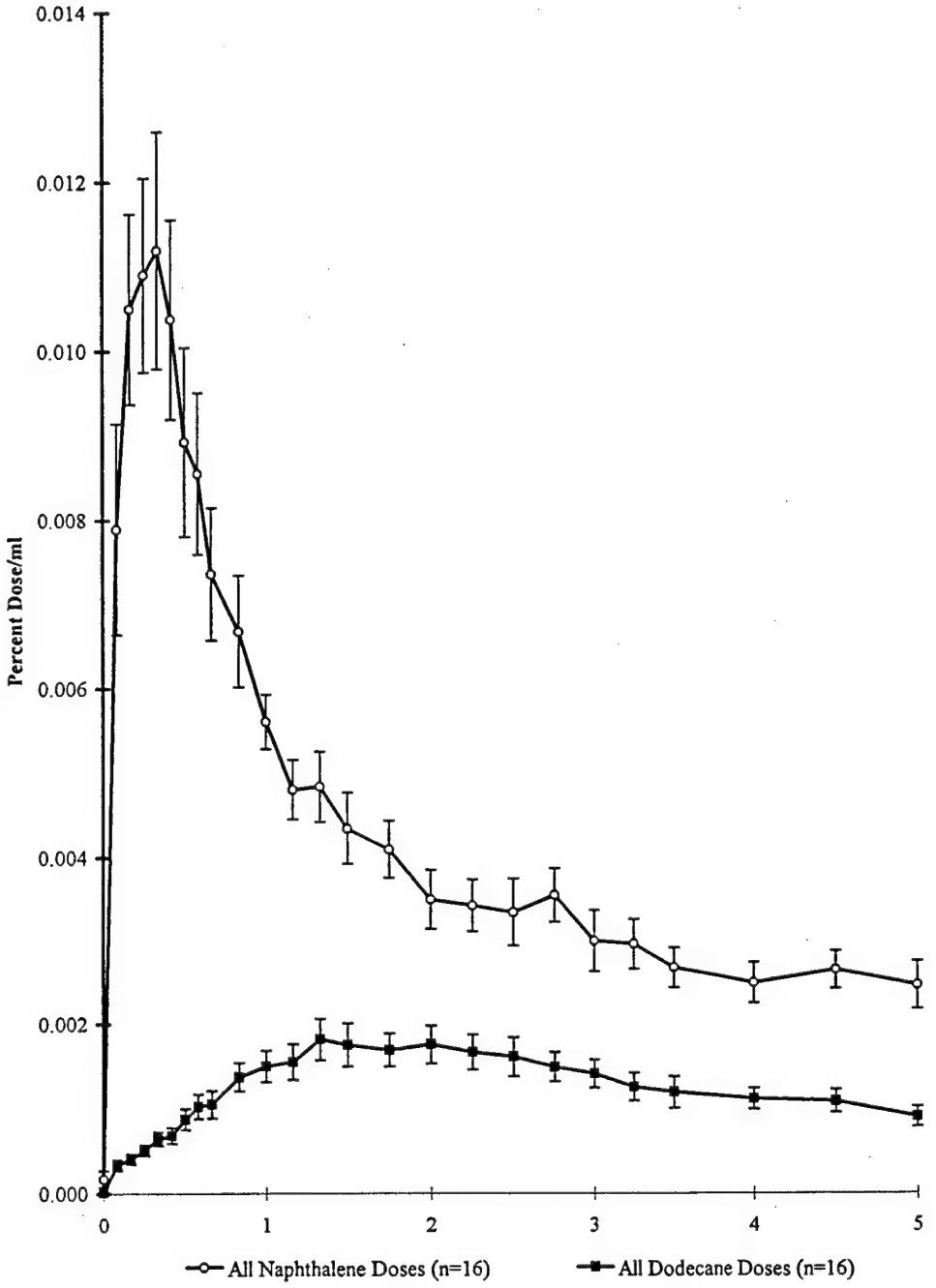

FIG. 2. Perfusate absorption profiles of naphthalene and dodecane (mean % dose/ml ± SEM) pooled from dosing in all jet fuel types.

of an experiment. However, it should be noted that if the compound present in the outermost stratum corneum, recovered in these studies by 12 tape strips, were totally available, then the rank order of penetration would be hexadecane (9.84% dose) > dodecane (6.24% dose) > naphthalene (2.12% dose).

Effect of Fuel Composition

The second phenomenon studied was the effect of the specific fuel formulation on absorption and deposition of the markers naphthalene and dodecane. The rank order of naphthalene perfusate absorption based on AUC, % dose absorbed, and peak flux was JP-8(100) > Jet-A > JP-8 > JP-8 (puddle) for naphthalene and JP-8 > JP-8(100) > Jet-A > JP-8 (puddle) for dodecane (Table 3). Figure 6 depicts the comparative perfusate absorption profiles, and Figure 7 illustrates overall tissue deposition. A dichotomy similar to that discussed above is seen when absorption parameters are compared to skin deposition. Naphthalene and dodecane disposition in skin com-

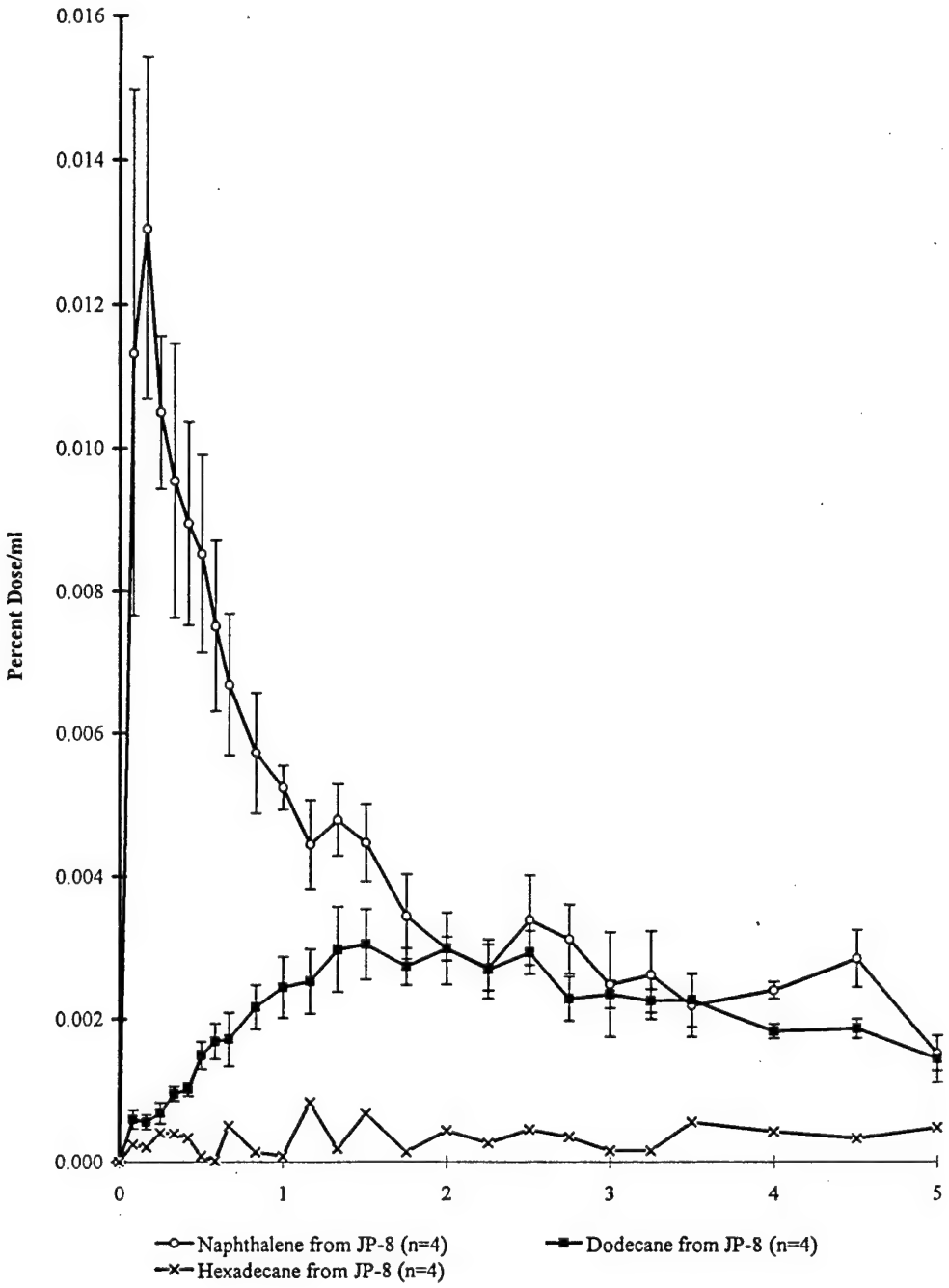

FIG. 3. Comparison of naphthalene, dodecane, and hexadecane absorption into perfusate (mean % dose/ml ± SEM) after dosing in JP-8 jet fuel.

partments did not exactly parallel that seen in perfusate. However, despite these differences in local skin disposition, overall penetration still tracks the pattern in the perfusate with naphthalene from JP-8(100) statistically greater ($p < 0.05$) than JP-8 or JP-8 (puddle). For dodecane, absorption from JP-8 is greater ($p < 0.05$) than the other fuels.

This apparent dichotomy between skin deposition and absorption is further explored in Fig. 8 which presents histograms of the dosed skin/absorption and absorption/dosed skin ratios for naphthalene and dodecane in Jet-A, JP-8, JP-8 (puddle), and JP-8 (100). The major effect seen with this analysis is the significantly different ratios for dodecane disposition from JP-8 (puddle), and again the differences between the naphthalene and dodecane markers.

Statistical Comparisons

Table 4 provides an alternative perspective and statistical summary of the role of naphthalene and of dodecane seen in

TABLE 2
Comparison of Three Marker Compounds from JP-8
Mean (SEM) of Each Parameter

^{14}C-Naphthalene	(n = 4)
AUC (%D-h/ml)	0.0199 (0.0020)[A]
Absorbed (%D)	1.17 (0.07)[A]
Peak flux (%D/min)	0.015 (0.003)[A]
^{3}H-Dodecane	(n = 4)
AUC (%D-h/ml)	0.0107 (0.0009)[B]
Absorbed (%D)	0.63 (0.04)[B]
Peak flux (%D/min)	0.0036 (0.0004)[B]
^{14}C-Hexadecane	(n = 4)
AUC (%D-h/ml)	0.0017 (0.0003)[C]
Absorbed (%D)	0.18 (0.08)[C]
Peak flux (%D/min)	0.0011 (0.0002)[B]

Note. Means with the same letter are not significantly different.

Fig. 7, A and B, respectively, and in Table 3. Two orthogonal contrasts on the four fuel treatments [Jet-A, JP-8, JP-8 (puddle), JP-8(100)] are used to examine two questions. (1) Is the mean response to Jet-A different from the average of the three JP-8 treatments, namely contrast 1 [3, −1, −1, −1]? (2) Is the mean response of JP-8 different from the mean of JP-8(100), namely contrast 2 [0, 1, 0, −1]? For answering these specific a priori questions based on the structure of the fuel treatments, orthogonal contrasts are statistically preferable to multiple comparison techniques such as LSD (Swallow, 1984; Hsu, 1996). While the LSD procedure allowed pairwise comparisons among the fuels, for question 1, Jet-A (a commercial fuel) is compared to the average of the three military fuels. For question 2, a specific pairwise comparison examines the role of additives in the JP-8 fuel series. The overall p value from the F statistic in ANOVA for the four jet fuels is also presented and denoted as ALL. Note that the overall F may fail to detect some differences that do exist, and that are indicated by the orthogonal contrasts.

In Table 4, the tissue disposition of naphthalene is analyzed using the two contrasts in columns 2 and 3. The only significant differences seen are for contrast 2 in fat and penetration. Surface indicates some difference ($p > 0.10$). For an overall effect (column 4), penetration and surface also have a $p < 0.10$. The use of log responses give a similar result. Note that the p value for surface and contrast 1 now becomes more significant at $p = 0.036$ as the variance is stabilized by the log transformation. In a similar manner, the last two rows (AUC and peak flux) are compared with Table 3. While the overall p value indicates a difference in AUC means, it is not primarily due to the two contrasts examined. For peak flux there is a bigger spread in the SEM and the overall p value becomes more significant after a log transformation, but again this is not due to the two contrasts of interest.

The last three columns in Table 4 examine the tissue disposition of dodecane in a similar manner. For contrast 1, all skin layers, AUC, and peak flux are significant with the exception of fat. For contrast 2, stratum corneum, absorption, penetration, AUC, and peak flux are significant. The overall p values are significant at all the places that contrast 2 is, but also indicate mean differences in dosed skin and evaporative loss. Similar results are found by the log responses. Note that the LSD approach in Fig. 7 and contrast 2 in Table 4 agree in indicating significant differences between JP-8 and JP8(100). However the LSD results from Fig. 7 are pairwise and cannot easily give the comparable results between Jet-A and the JP-8 fuels (contrast 1).

DISCUSSION

These studies highlight the complexities inherent in studying the percutaneous absorption of complex mixtures such as jet fuel. This complexity arises both from the heterogeneity of the chemicals comprising fuel as well as from the different interpretations obtained if systemic absorption vs local cutaneous disposition are the endpoints of concern.

Based on analyses of the fuel stock used in these studies, dodecane is a primary component present at 4.7% (v/v). Naphthalene is a primary aromatic constituent of jet fuel at 1.1%. In contrast, hexadecane is a minor component being present at less than 1%. There are a total of 228 characterized major nonadditive hydrocarbon constituents of these fuels. It is impossible to characterize the absorption of even a fraction of these constituents at the level of detail presented in this investigation. Being relatively nonvolatile, the long-chain hydrocarbons typified by dodecane and hexadecane make up a large percentage of this mixture. As seen in these studies, they have the greatest surface concentrations at the end of an experiment (Fig. 5) and tend to have a larger fraction of dose deposited in the skin. However, they have a decreased systemic absorption as characterized by perfusate fluxes and total penetration. Because the fractional absorption is almost an order of magnitude greater for naphthalene than for dodecane, absolute naphthalene mass absorbed (% dose × concentration in fuel) is still two-fold greater than dodecane even if the latter compound is present at close to 5 times the concentration. A similar ordering of naphthalene and dodecane was reported in preliminary *in vitro* rat absorption studies of JP-8 components (McDougal and Miller, 1998). The magnitude of the differences in total absorption between naphthalene and dodecane overshadow any effect that fuel composition has on marker absorption as can be appreciated by examining the composite absorption profiles in Fig. 2.

A limitation of any short duration study of this design is that steady-state conditions are impossible to achieve due to biological limitations of the model coupled with the volatility of

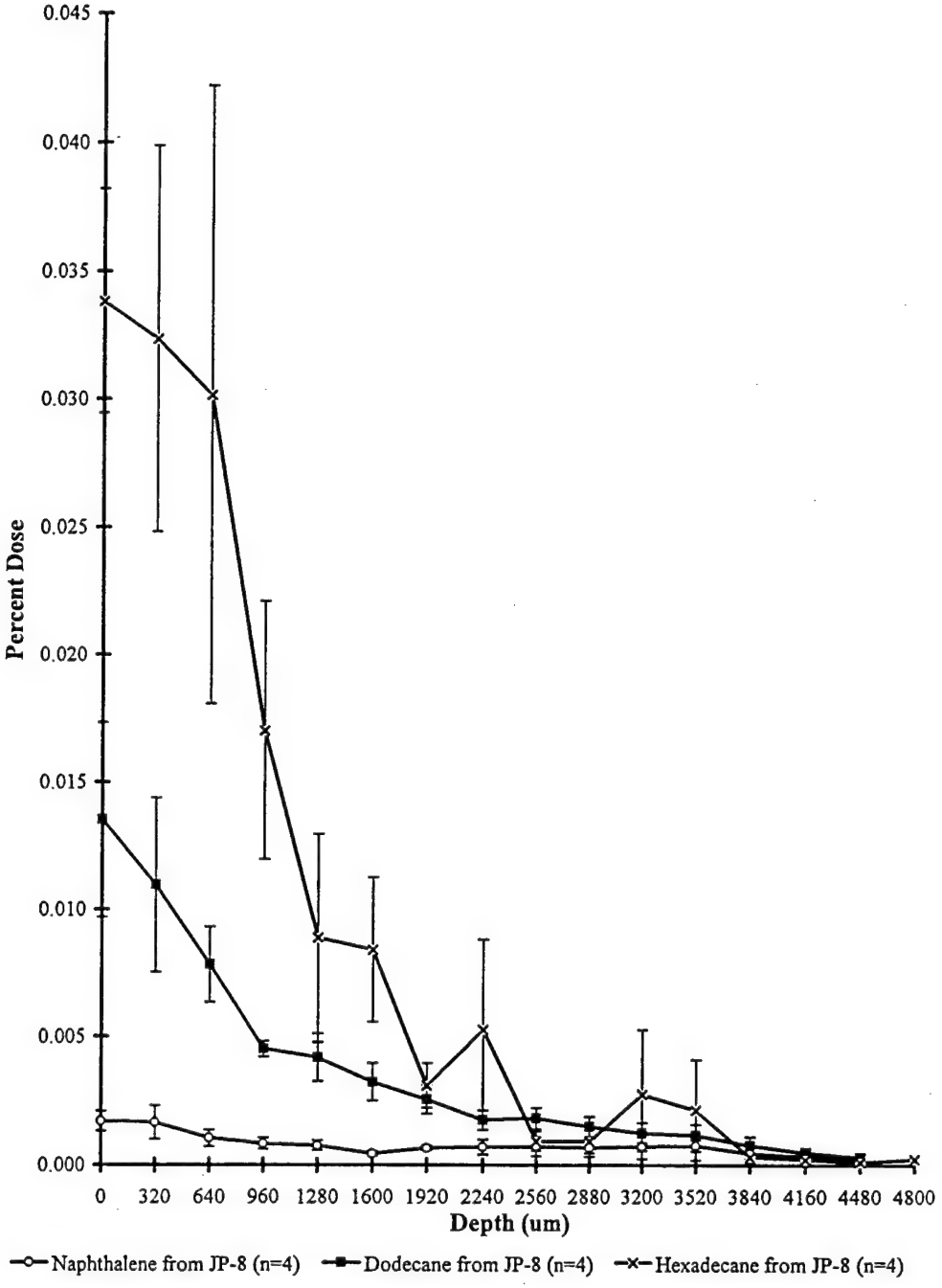

FIG. 4. Depth of penetration of naphthalene, dodecane, and hexadecane into skin (mean % dose ± SEM) after dosing in JP-8.

the hydrocarbons being investigated. This is especially evident when interpreting tissue concentrations at a single 5 h time point at the termination of a study. Previous IPPSF studies have taught that an accurate estimate of potential *in vivo* absorption is obtained by combining skin and fat residues with absorbed perfusate flux (Wester *et al.*, 1998; Williams *et al.*, 1990). This is the penetration parameter reported in this work. Furthermore, skin concentrations at any single time point must be interpreted in the context of a continuum (Williams and Riviere, 1995; Manitz *et al.*, 1998). Finally, it is expected that some fraction of dose in skin will remain nonabsorbed since a concentration gradient may no longer exist to deliver the compound if the compound preferentially partitions in the skin and forms a depot. These residual skin concentrations could have toxicological significance for a bioactive molecule. The full prediction and description of skin concentrations is obviously more complex. Various pharmacokinetic models are being developed to assess such phenomenon (Manitz *et al.*, 1998;

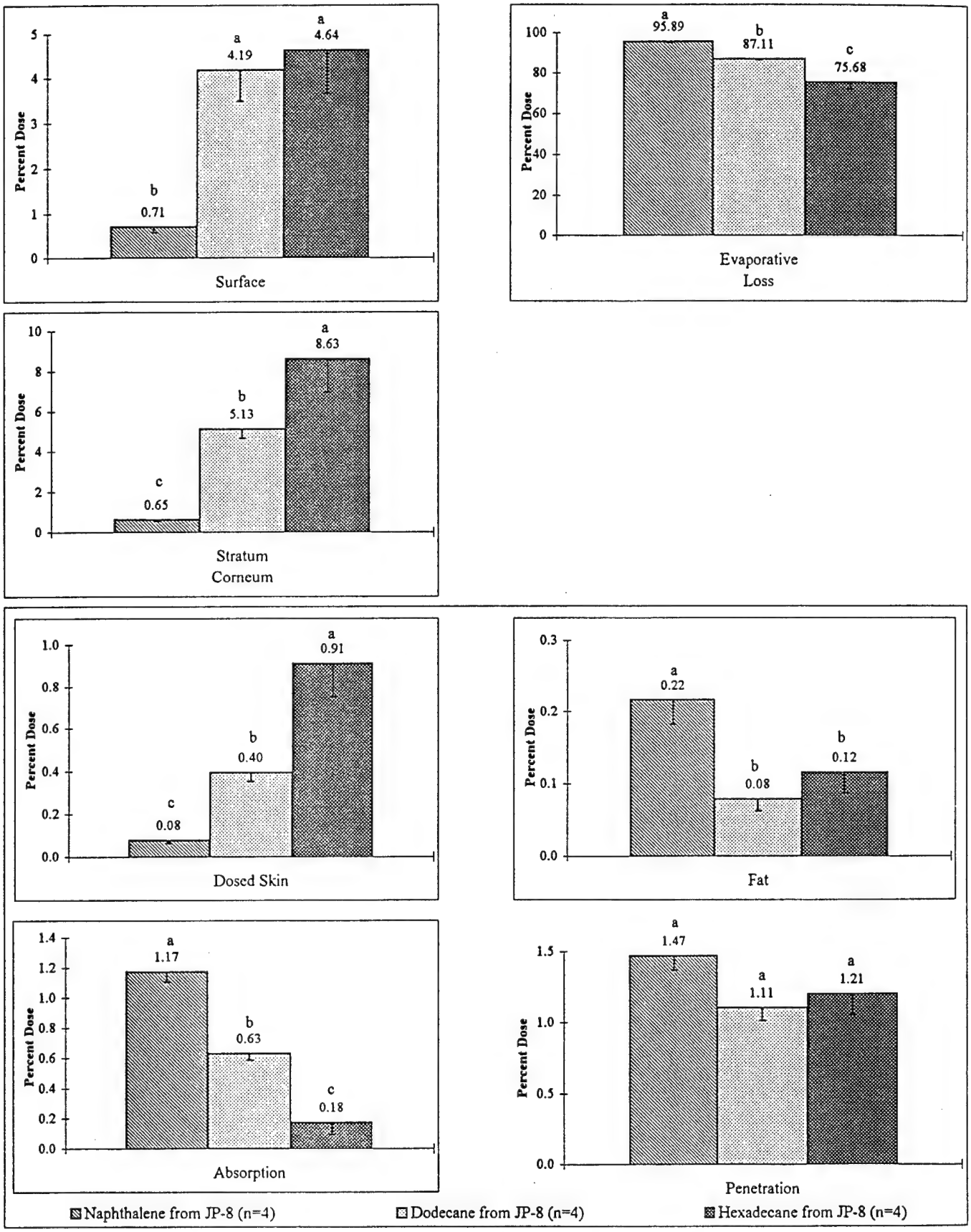

FIG. 5. Pattern of tissue deposition and absorption of naphthalene, dodecane, and hexadecane dosed in JP-8 fuel. All values are expressed as mean % dose ± SEM. Values with different letters are significantly different ($p < 0.05$).

TABLE 3
Jet Fuel Comparison Mean (SEM) of Each Parameter

	Jet-A (n = 4)	JP-8 (n = 4)	JP-8(Puddle) (n = 4)	JP-8(100) (n = 4)	All 16 Doses (n = 16)
^{14}C-Naphthalene					
AUC (%D-h/ml)	0.025 (0.002)^{a}	0.020 (0.002)^{ab}	0.015 (0.003)^{b}	0.026 (0.003)^{a}	0.021 (0.002)^{A}
Absorbed (%D)	1.49 (0.18)^{a}	1.17 (0.07)^{a}	1.11 (0.16)^{a}	1.63 (0.29)^{a}	1.35 (0.10)^{A}
Peak flux (%D/min)	0.015 (0.001)^{ab}	0.015 (0.003)^{ab}	0.008 (0.001)^{b}	0.016 (0.003)^{a}	0.013 (0.001)^{A}
^{3}H-Dodecane					
AUC (%D-h/ml)	0.0048 (0.0005)^{bc}	0.0107 (0.0009)^{a}	0.0039 (0.0004)^{c}	0.0061 (0.0007)^{b}	0.0064 (0.0008)^{B}
Absorbed (%D)	0.29 (0.04)^{b}	0.63 (0.04)^{a}	0.27 (0.07)^{b}	0.35 (0.04)^{b}	0.38 (0.04)^{B}
Peak flux (%D/min)	0.0017 (0.0002)^{bc}	0.0036 (0.0004)^{a}	0.0014 (0.0002)^{c}	0.0024 (0.0001)^{b}	0.0023 (0.0002)^{B}

Note. Means with the same letter are not significantly different. Lowercase letters represent comparisons within parameters across fuel types. Uppercase letters represent comparisons only within the last column across markers.

McCarley and Bunge, 1998; Riviere *et al.*, 1995a: Williams and Riviere, 1995), however a discussion of such kinetic interactions is beyond the scope of the present work. The important point to be taken from these studies is that compound absorption and penetration must be assessed in all skin compartments since only looking at the absorbed fraction (e.g., perfusate) may produce very misleading conclusions.

One can appreciate the difference seen for a rapidly penetrating compound like naphthalene vs slower penetrating substances such as dodecane and hexadecane. It is not surprising that a low molecular weight aromatic such as naphthalene would have an enhanced absorption compared to less volatile long-chain aliphatic hydrocarbons such as dodecane and hexadecane. Based on data for these three compounds, the percutaneous absorption is relatively low with the greatest estimated penetration being only 1.5% of the applied dose. However, estimating total *in vivo* absorption is not only a function of the applied dose, but also of the surface area of skin to which the jet fuel is exposed. Thus exposure to large surface areas for prolonged contact times could potentially result in significant systemic absorption.

There is limited data in the literature on the percutaneous absorption of these three hydrocarbons in other experimental models or vehicles. Percutaneous absorption studies of neat naphthalene in humans or laboratory animals had not been reported in a recent toxicological profile (ATSDR, 1993). Absorption was inferred from the occurrence of toxicity after dermal application. A study of neat naphthalene absorption in rats suggested that 50% of the applied dose was excreted in urine by 12 h, with the predominant urinary metabolites being 2,7- and 1,2-dihydroxynaphthalene (Turkall *et al.*, 1994). Naphthalene was also included in an *in vitro* monkey skin study comparing the percutaneous absorption in acetone using a series of aliphatic compounds (Sartorelli *et al.*, 1998). Log octanol/water partition coefficients were correlated to permeability constant, with vapor pressure and molecular weight not adding any significant increase in correlation. In the context of the present studies, these correlations would be to the observed perfusate absorption. Evaluation of perfusate fluxes alone, a procedure often done with *in vitro* diffusion cell studies, would mask the significant absorption which ultimately could occur with dodecane and especially hexadecane when skin depots are factored in.

These experimental data suggest that both aliphatic compounds have a propensity for partitioning into skin and forming relatively slowly equilibrating pools that ultimately could be absorbed. Previously, hexadecane has been reported to bind to the stratum corneum (Singh, 1998), a phenomenon which would explain the elevated hexadecane levels seen in stratum corneum (Fig. 5). In contrast, naphthalene is rapidly absorbed and has minimal propensity to stay in skin, although it tends to partition into subcutaneous fat after absorption. The volatility of these compounds could also be an important factor in determining skin concentrations. Both dodecane and hexadecane have significantly higher residual surface concentrations which result in longer surface residence times on skin, and thus in effect longer dosing times. These different mechanisms of absorption and deposition impact on interpreting what absorption and penetration mean. Compounds with enhanced skin residence, if inherently bioactive, might be expected to have a greater propensity for inducing skin irritation than those compounds which do not form skin depots. All of these hydrocarbons, and especially the composite fuels, have the potential to extract epidermal lipids thereby altering the barrier properties of skin. Such an effect was reported in a preliminary study of JP-8 toxicity (Singh, 1998) and is consistent with toxicological findings in our laboratory that transepidermal water loss (TEWL) increased with chronic jet fuel exposure (unpublished data).

These findings suggest that if toxicology studies of individual components are conducted, the disposition of an aromatic such as naphthalene cannot be used to extrapolate absorption estimates to a long-chain aliphatic such as dodecane. The optimal approach would be to select marker compounds that are characteristic of groups of fuel components based on structure–activity relationships, and then assess absorption, cutane-

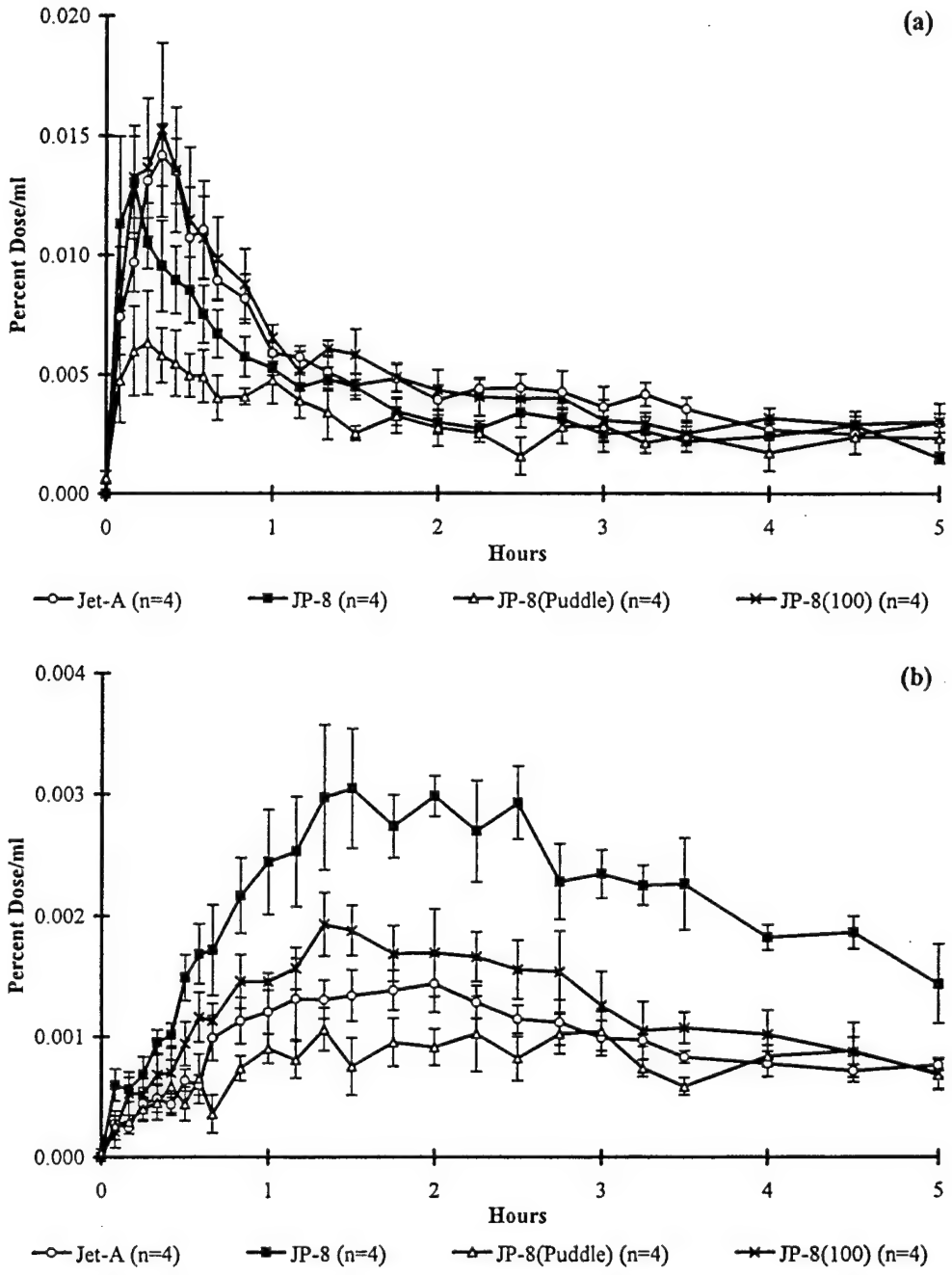

FIG. 6. Naphthalene (a) and dodecane (b) perfusate absorption (mean % dose/ml ± SEM) after dosing in Jet-A, JP-8, JP-8(puddle), and JP-8(100) jet fuels.

ous disposition, as well as toxicological parameters (Basak and Grunwald, 1998).

A surprising finding was the difference in naphthalene and dodecane absorption and skin deposition between the three fuels studied, since these fuels are predominantly composed of similar hydrocarbon components with different additive combinations. Absorption of dodecane was greater from JP-8 than from Jet-A or JP-8(100), while overall penetration of naphthalene was greatest from JP-8(100). Aging of the JP-8 by 24 h evaporation decreased the absorption for both of these markers compared to the other fuel types.

These findings suggest that one or more of the additives combined with Jet-A to make JP-8 modulated dodecane absorption but had minimal effect on naphthalene absorption. The total additive package [corrosion inhibitor DCI-4A, antistatic compound Stats 450, the deicing additive diethylene glycol monomethyl ether (DIEGME)] composes only a small percentage of the final fuel. A common attribute of these three

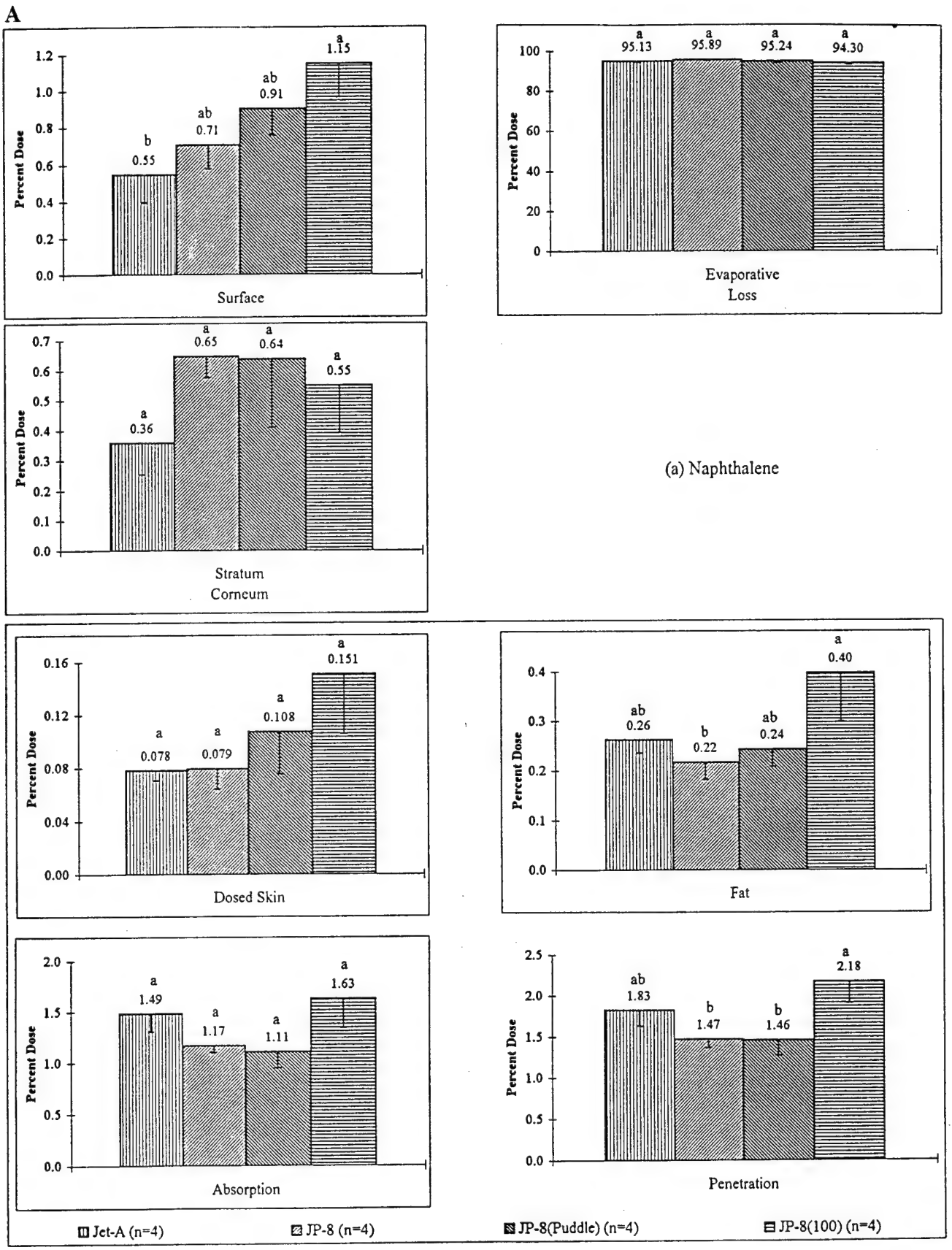

FIG. 7. Pattern of tissue deposition and absorption of naphthalene (a) and dodecane (b) dosed in Jet-A, JP-8, JP-8(puddle), and JP-8(100) jet fuels. All values are expressed as mean % dose ± SEM. Values with different letters are significantly different ($p < 0.05$).

B

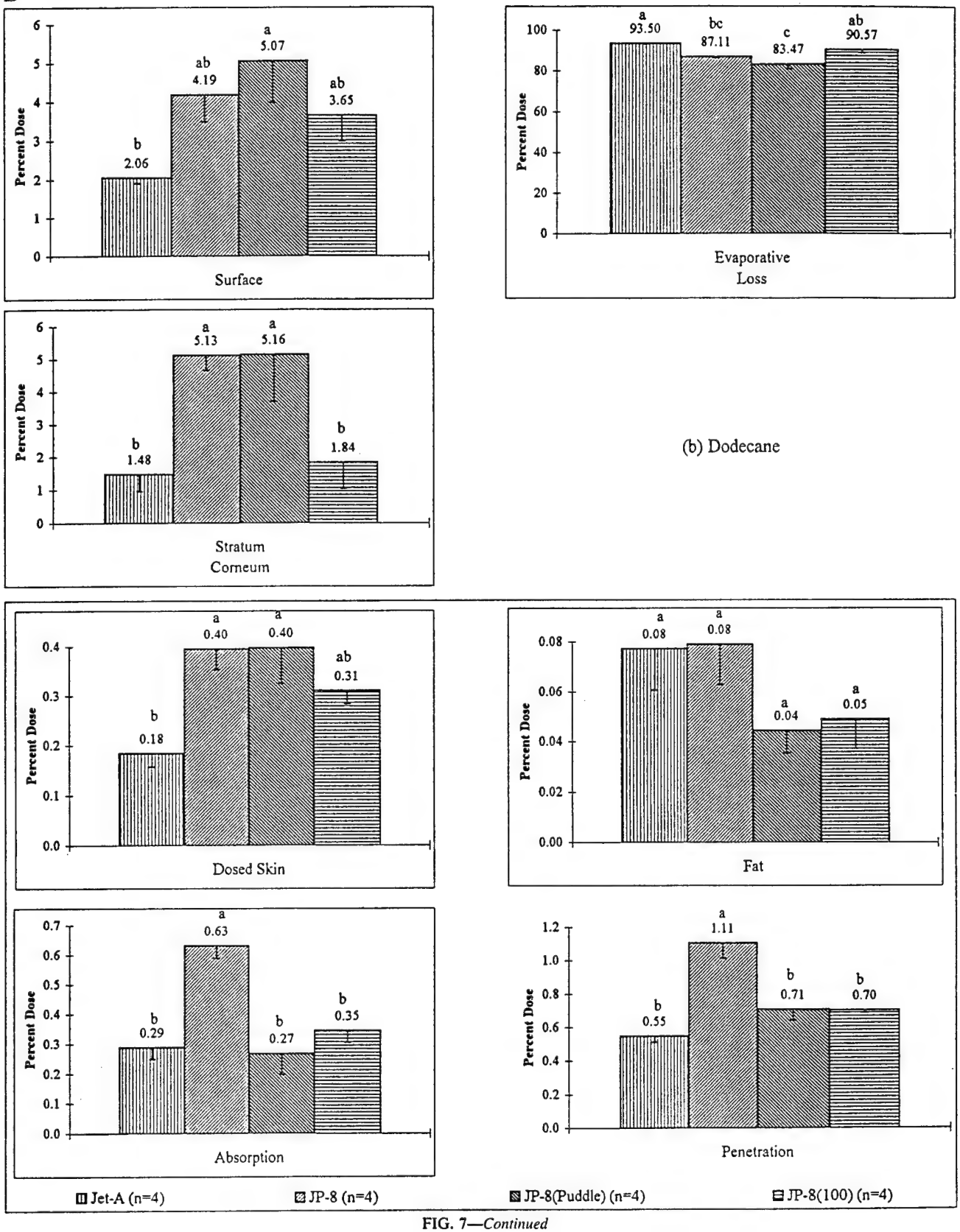

FIG. 7—*Continued*

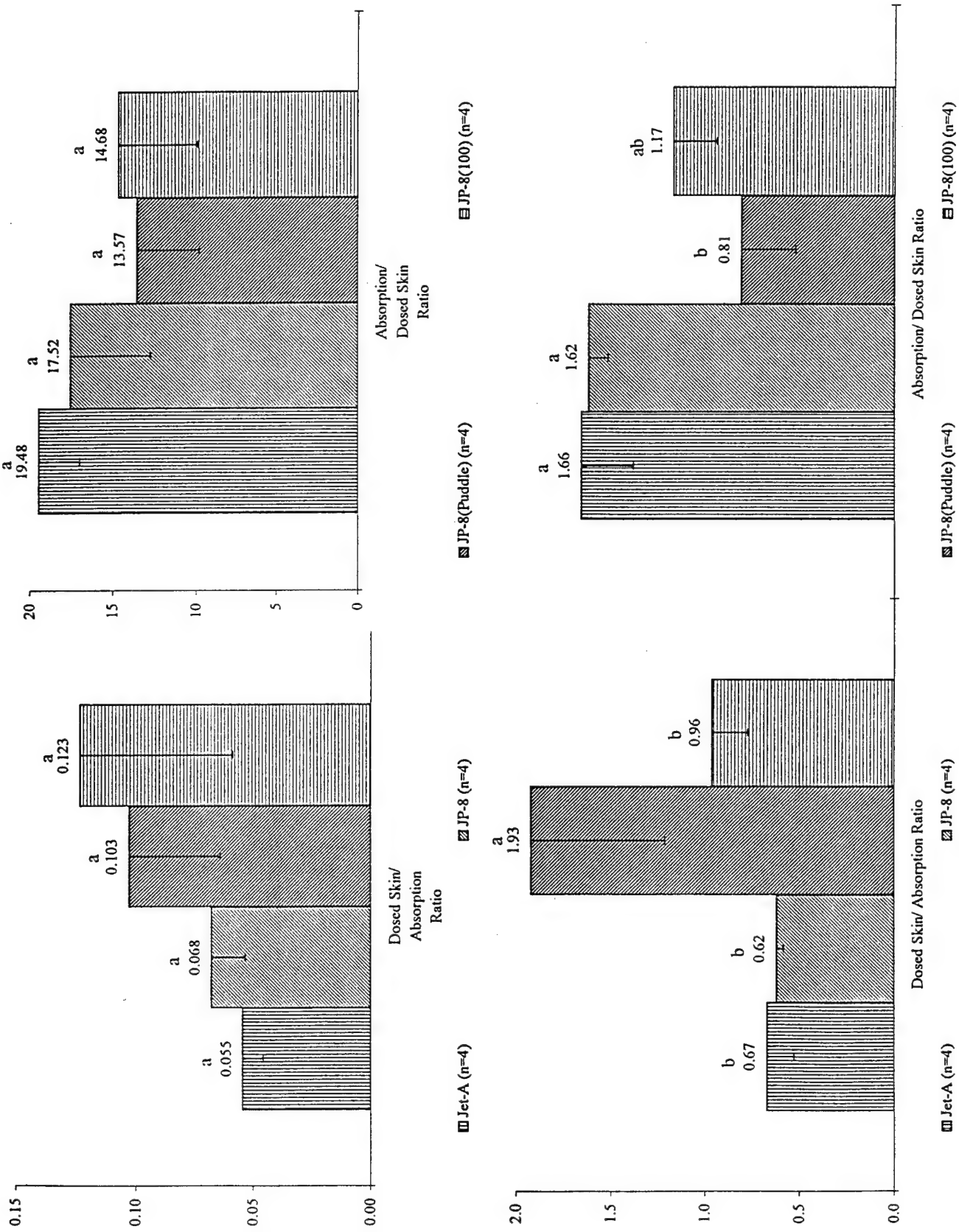

FIG. 8. Absorption to skin deposition ratios (mean ± SEM) of naphthalene (top) and dodecane (bottom) after dosing in Jet-A, JP-8, JP-8(Puddle), and JP-8(100) jet fuels. Values with different letters are significantly different ($p < 0.05$).

TABLE 4

Statistical Significance (p Values) of Napthalene and of Dodecane Absorption and Skin Deposition from Four Jet Fuels

	Napthalene		Contrasts	Dodecane		
	1	2	All	1	2	All
			Original Scale			
Surface	.06	.06	.08	**.021**	.61	.07
Stratum corneum	.18	.66	.53	**.030**	**.024**	**.017**
Dosed skin	.32	.11	.30	**.005**	.22	**.022**
Fat	.72	**.045**	.17	.24	.15	.21
Absorption	.43	.12	.22	**.048**	**.002**	**.0008**
Penetration	.61	**.026**	.07	**.001**	**.0005**	**.0002**
Evaporative loss	.98	.10	.38	**.003**	.13	**.003**
AUC	.11	.12	**.027**	**.013**	**.0002**	**.0001**
Peak flux	.49	.64	.10	**.017**	**.008**	**.0003**
			Ln scale			
Surface	**.036**	.13	.09	**.006**	.59	**.033**
Stratum corneum	.24	.38	.52	**.026**	**.012**	**.012**
Dosed skin	.44	.11	.35	**.001**	.25	**.006**
Fat	.96	.07	.28	.24	.16	.21
Absorption	.34	.17	.24	**.014**	**.015**	**.005**
Penetration	.48	**.025**	.06	**.0007**	**.002**	**.0003**
Evaporative loss	.99	.09	.38	**.004**	.15	**.004**
AUC	.11	.20	**.027**	**.026**	**.001**	**.0001**
Peak flux	.27	.71	**.043**	**.015**	**.029**	**.0002**

Note. Contrasts: (Jet-A, JP-8, JP-8(Puddle), JP-8(100)); 1: Jet-A vs Others (3, −1, −1, −1); 2: JP-8 vs JP-8(100) (0, 1, 0, −1); All: Overall p value from ANOVA for four jet fuels. Bold p values are ≤0.05.

compounds is their relative hydrophilicity compared to the hydrophobic environment of the hydrocarbon jet fuel. DC1-4A is a linoleic acid derivative. Linoleic acid has previously been identified as a skin penetration enhancer for topically applied drugs (Aungst *et al.*, 1986; Mahjour *et al.*, 1989; Schneider *et al.*, 1996). The potential for DIEGME to function as a pharmaceutic enhancer has not been investigated, although in the preliminary study quoted above (McDougal and Miller, 1998), DIEGME had an order of magnitude greater transdermal flux of any hydrocarbon component of JP-8. Enhancers generally have their greatest effect on more nonpolar compounds for which the stratum corneum is a true barrier to absorption. These studies would seem to suggest that dodecane would be more susceptible to enhancement than naphthalene. Individual component absorption studies would have to be assessed to further probe this effect.

Of equal significance is the finding that some of these effects (e.g., dodecane) were apparently reversed in JP-8(100), suggesting further interactions with this more complex additive package. For naphthalene, the additive package which transforms JP-8 into JP-8(100) seemed to have increased its penetration. These findings are not totally unexpected, since we have reported on similar complex interactions when absorption of various organics (parathion, carbaryl, benzidine) was studied from defined chemical mixtures (Baynes *et al.*, 1996, 1997; Qiao *et al.*, 1996; Williams *et al.*, 1996). Possible interactions include chemical binding, chemical effects from surfactants, stratum corneum lipid interactions from enhancers, solvent-mediated lipid extraction, low level irritation, and vasomodulation. Dankovic (1989) had reported on prolonged dermal residence times for benzo[a]pyrene when applied in a mixture of 11 polycyclic aromatic hydrocarbons compared to application in a volatile solvent. All of this previous work suggests that such subtle changes in absorption from mixtures is not unexpected. Finally, the absorption of these additives was not investigated in this study, and their potential biological effects on skin could not be assessed. Since these additives are more polar than the hydrocarbon fuel constituents, they would be expected to be more sensitive to modulation by fuel composition. Further speculation on the mechanism of these jet fuel interactions, and on identifying responsible components, is not warranted at this time but requires further probing.

It must be stressed that these studies were designed only to probe whether absorption of two marker hydrocarbon components of jet fuel were affected by addition of performance additives. It is intriguing that there were some significant differences in absorption of the two markers studied. The absorption of both markers was reduced from the aged JP-8(puddle). This is not totally unexpected since the composition of this fuel would be expected to be the most different from the

other fuels since a large fraction of its most volatile components are lost. This could alter partitioning of the markers from the fuel into the stratum corneum lipids. Second, one must also stress that selection of naphthalene and dodecane was not based on any toxicological property, but only by their virtue of representing a fraction of fuel. It is possible that if any cutaneous toxicity were produced from jet fuel exposure that the additive components themselves could be responsible. If the markers studied, naphthalene and dodecane, were affected by fuel composition, it is entirely feasible that the disposition of the more polar additives could be modulated. This modulation could alter the propensity to induce cutaneous toxicity. This hypothesis has not been evaluated in this work.

In conclusion, assessment of dermal absorption of jet fuels is extremely complex. We have characterized the absorption of three different hydrocarbon marker compounds and demonstrated significant differences in individual component absorption and skin deposition. It must be stressed that we are only looking at 3 of the 228 hydrocarbon components that comprise these fuels and there is no reason to believe that these specific components are toxicologically significant. However, before a complete risk assessment can be made, some estimate of dermal absorption and deposition is required. Second, it is critical that when making these assessments, both absorption into perfusate as well as penetration into skin be assessed to obtain a complete picture of disposition. Finally, the effects of fuel additives on the disposition of naphthalene and dodecane suggests that all fuels cannot be treated as one and furthermore, the mechanisms of these specific interactions deserve clarification.

ACKNOWLEDGMENT

This work was supported by the U.S. Air Force Office of Scientific Research, Grants F49620 and FQ8671.

REFERENCES

ATSDR (1993). Draft Toxicological Profile for Naphthalene - Update. Agency for Toxic Substances and Disease Registry, Atlanta, GA.

ATSDR (1995). Toxicological Profile for Jet Fuels (JP4 and JP7). Agency for Toxic Substances and Disease Registry, Atlanta, GA.

ATSDR (1996). Draft Toxicological Profile for Jet Fuels (JP-5 and JP-8). Agency for Toxic Substances and Disease Registry, Atlanta, GA.

Aungst, B. J., Rogers, N. J., and Shefter, E. (1986). Enhancement of naloxone penetration through human skin in vitro using fatty acids, fatty alcohols, surfactants, sulfoxides and amines. *Int. J. Pharm.* **33,** 225–234.

Basak, S. C., and Grunwald, G. D. (1998). *Clustering of JP-8 Constituents into Structurally Dissimilar Groups: A Novel Computational Strategy for Predictive Toxicology.* Proceedings of AFOSR JP-8 Jet Fuel Toxicology Workshop, Tucson, AZ.

Baynes, R. E., Brownie, C., Freeman, H., and Riviere, J. E. (1996). In vitro percutaneous absorption of benzidine in complex mechanistically-defined chemical mixtures. *Toxicol. Appl. Pharmacol.* **141,** 497–506.

Baynes, R. E., and Riviere, J. E. (1997). Inert ingredients in pesticide formulations influence the dermal absorption of carbaryl. *Am. J. Vet. Res.* **59,** 159–169.

Clark, C. R., Walter, M. K., Ferguson, P. W., and Katchen, W. (1988). Comparative dermal carcinogenesis of shale and petroleum-derived distillates. *Toxicol. Ind. Health* **4,** 11–22.

Dankovic, D. A., Wright, C. W., Zangar, R. C., and Springer, D. L. (1989). Complex mixture effects on the dermal absorption of benzo[a]pyrene and other polycyclic aromatic hydrocarbons from mouse skin. *J. Appl. Toxicol.* **9,** 239–244.

Harris, D. T., Sakiestewa, D., Robledo, R. F., and Witten, M. (1997). Short-term exposure to JP-8 jet fuel results in long term immunotoxicity. *Toxicol. Ind. Health.* **13,** 559–570.

Hsu, J. C. (1996). *Multiple Comparisons: Theory and Methods.* Chapman and Hall, London, UK.

Mahjour, M., Mauser, B. E., and Fawzi, M. B. (1989). Skin permeation enhancement effects of linoleic acid and azone on narcotic analgesics. *Int. J. Pharm.* **56,** 1–11.

Manitz, R., Lucht, W., Strehmel, K., Weiner, R., and Neubert, R. (1998). On mathematical modeling of dermal and transdermal drug delivery. *J. Pharm. Sci.* **87,** 873–879.

McCarley, K. D., and Bunge, A. L. (1998). Physiologically relevant one-compartment pharmacokinetic models for skin. I. Development of models. *J. Pharm. Sci.* **87,** 470–481.

McDougal, J. N., and Miller, T. E. (1998). *Dermal Absorption of JP-8 and its Components.* Proceedings of AFOSR JP-8 Jet Fuel Toxicology Workshop, Tucson, AZ.

Pfaff, J., Parton, K., Lantz, R., Chen, H., Hays, A., and Witten, M. (1995). Inhalation exposure to JP-8 jet fuels alters pulmonary function and substance P levels in Fischer 344 rats. *J. Appl. Toxicol.* **15,** 249–256.

Qiao, G. L., Brooks, J. D., Baynes, R. L., Monteiro-Riviere, N. A., Williams, P. L., and Riviere, J. E. (1996). The use of mechanistically defined chemical mixtures (MDCM) to assess component effects on the percutaneous absorption and cutaneous disposition of topically-exposed chemicals. I. Studies with parathion mixtures in isolated perfused porcine skin. *Toxicol. Appl. Pharmacol.* **141,** 473–486.

Riviere, J. E., Bowman, K. F., Monteiro-Riviere, N. A., Dix, L. P., and Carver, M. P. (1986). The isolated perfused porcine skin flap (IPPSF). I. A novel in vitro model for percutaneous absorption and cutaneous toxicology studies. *Fundam. Appl. Toxicol.* **7,** 444–453.

Riviere, J. E., Brooks, J. D., Williams, P. L., and Monteiro-Riviere, N. A. (1995a). Toxicokinetics of topical sulfur mustard penetration, disposition, and vascular toxicity in isolated perfused porcine skin. *Toxicol. Appl. Pharmacol.* **135,** 25–34.

Riviere, J. E., Monteiro-Riviere, N. A., and Williams, P. L. (1995b). Isolated perfused porcine skin flap as an in vitro model for predicting transdermal pharmacokinetics. *Eur. J. Pharm. Biopharm.* **41,** 152–162.

Riviere, J. E., and Monteiro-Riviere, N. A. (1991). The isolated perfused porcine skin flap as an in vitro model for percutaneous absorption and cutaneous toxicology. *Critical Reviews in Toxicol.* **21,** 329–344.

Riviere, J. E., Williams, P. L., Hillman, R., and Mishky, L. (1992). Quantitative prediction of transdermal iontophoretic delivery of arbutamine in humans using the in vitro isolated perfused porcine skin flap (IPPSF). *J. Pharm. Sci.* **81,** 504–507.

Sartorelli, P., Aprea, C., Cenni, A., Novelli, M. T., Orsi, D., Palmi, S., and Matteucci, G. (1998). Prediction of percutaneous absorption from physiochemical data: A model based on data of in vitro experiments. *Ann. Occup. Hyg.* **42,** 267–276.

Schneider, I. M., Dobner, B., Neubert, R., and Wohlrab, W. (1996). Evaluation of drug penetration into human skin ex vivo using branched fatty acids and propylene glycol. *Int. J. Pharm.* **145,** 187–196.

Singh, J. (1998). *Skin Permeability, Biophysics, and Irritation from JP-8.* Proceedings of AFOSR JP-8 Jet Fuel Toxicology Workshop, Tucson, AZ.

Swallow, W. H. (1984). Those overworked and oft-misused mean separation procedures-Duncan's, LSD, etc. *Plant Dis.* **68,** 919–921.

Turkall, R. M., Skowronski, G. A., Kadry, A. M., and Abdel-Rahman, M. S. (1994). A comparative study of the kinetics and bioavailability of pure and soil-adsorbed naphthalene in dermally exposed rats. *Arch. Environ. Contam. Toxicol.* **26,** 504–509.

Wester, R. C., Melendres, J., Sedik, L., Maibach, H. I., and Riviere, J. E. (1998). Percutaneous absorption of salicylic acid, theophylline, 2,4-dimethylamine, diethyl hexylphthalic acid and *p*-aminobenzoic acid in the isolated perfused porcine skin flap compared to man. *Toxicol. Appl. Pharmacol.* **151,** 159–165.

Williams, P. L., Carver, M. P., and Riviere, J. E. (1990). A physiologically relevant pharmacokinetic model of xenobiotic percutaneous absorption utilizing the isolated perfused porcine skin flap (IPPSF). *J. Pharm. Sci.* **79,** 305–311.

Williams, P. L., and Riviere, J. E. (1995). A biophysically-based dermatopharmacokinetic compartment model for quantifying percutaneous penetration and absorption of topically applied agents. *J. Pharm. Sci.* **84,** 599–608.

Williams, P. L., Thompson, D., Qiao, G. L., Monteiro-Riviere, N. A., Baynes, R. L., and Riviere, J. E. (1996). The use of mechanistically defined chemical mixtures (MDCM) to assess component effects on the percutaneous absorption and cutaneous disposition of topically-exposed chemicals. I. Development of a general dermatopharmacokinetic model for use in risk assessment. *Toxicol. Appl. Pharmacol.* **141,** 487–496.

Identification of Early Biomarkers of Inflammation Produced by Keratinocytes Exposed to Jet Fuels Jet A, JP-8, and JP-8(100)

D. G. Allen, J. E. Riviere, and N. A. Monteiro-Riviere

Center for Cutaneous Toxicology and Residue Pharmacology, North Carolina State University, 4700 Hillsborough St., Raleigh, NC 27606; Tel: 919–513–6426; Fax: 919–513–6358; E-mail: Nancy_Monteiro@ncsu.edu

Received 18 February 2000; revised 14 April 2000; accepted 5 May 2000

ABSTRACT: The purpose of this study was to identify biomarkers of inflammation in normal human epidermal keratinocytes (NHEK) exposed to three jet fuel mixtures, Jet A, JP8, and JP8(100). NHEK were treated over 24 hours with 0.1% jet fuels, and mRNA production and protein release of two proinflammatory cytokines, IL-8 and TNF-α, were determined. Using an enzyme-linked immunosorbent assay (ELISA), NHEK were found to release both TNF-α and IL-8 in response to exposure to all three jet fuels. IL-8 release was noted within 8 hours and continued to rise through 24 hours compared to controls. Maximal levels of TNF-α release were seen at 4 hours and decreased in a time-dependent manner, although these levels remained above control levels at all time points assayed. mRNA for IL-8 was elevated 4 hours following exposure to the fuels, which was detected via a quantitative competitive reverse transcriptase-polymerase chain reaction (RT-PCR). mRNA for TNF-α was detected at all time points assayed but was not quantified. These results demonstrate that jet fuels induce the production and release of proinflammatory cytokines in NHEK and thus create the potential for chronic inflammation, which may contribute to the development or progression of disease states in the skin. © 2000 John Wiley & Sons, Inc. J Biochem Toxicol 14:231–237, 2000

KEY WORDS: **Epidermal Keratinocyte; Cytokine; Jet Fuel; Biomarkers; Inflammation**

INTRODUCTION

The toxicity of jet fuels has primarily centered on damage due to pulmonary exposure. Airway inflammation, immune dysfunction, and memory disturbances are among the adverse effects created by inhalation of aerosolized fuels [1,2]. However, there are few animal studies that have focused on the dermatotoxicity of jet fuels. With the recent advances in fuel mixtures that include an expanding number of compounds, increased concern is being given to the potential dermatotoxicology of jet fuels. The three fuels used in this study represent both commercial (Jet A) and military [JP8, JP8(100)] aircraft fuels. Jet A is a kerosene-cut jet fuel base composed of a complex mixture of 228 aliphatic and aromatic hydrocarbon compounds. JP-8 is a mixture of Jet A plus three additives, an icing inhibitor (diethylene glycol monomethyl ether), an antistatic compound (Stadis 450), and a corrosion inhibitor (DC1-4A). JP-8(100) contains JP-8 and an additional additive package (an antioxidant, chelator, detergent, and dispersant). From skin painting studies using middle distillates such as kerosene, researchers have determined that these chemicals cause edema, erythema, blisters, and burning sensations following acute exposure [3]. Absorption studies using in vitro models such as the isolated perfused porcine skin flap (IPPSF) have demonstrated that a significant fraction of topically applied jet fuel mixtures crosses the epidermal barrier for potential access to the dermal vasculature [4].

It is well documented that keratinocytes release many proinflammatory cytokines, chemokines, and growth factors [5], and this "network" of soluble molecules is responsible for the initiation of the inflammatory response in the skin [6,7]. Many of these molecules are produced constitutively in the keratinocyte, but are upregulated in response to an inflammatory agent [8]. One issue that should be of major concern when examining the toxicity of dermally applied com-

Correspondence to: Dr. Nancy A. Monteiro-Riviere.
Contract Grant Sponsor: U.S. Air Force Office of Scientific Research.
Contract Grant Number: FQ8671-98-000-462.

pounds is the potential for excessive cytokine production yielding chronic inflammation, which may contribute to the development or the progression of disease states (e.g., psoriasis) [9]. Furthermore, one must examine each inflammatory agent individually because their cytokine profiles may be quite different when comparing multiple agents [10].

A major effector in the development of inflammation in the skin is keratinocyte-derived interleukin-8 (IL-8). Primarily renown for its role in neutrophil chemotaxis, IL-8 has also been shown as a chemoattractant for T cells and basophils [11,12]. IL-8 has also been implicated in keratinocyte proliferation by modulating cytosolic free Ca^{2+} transients [13]. Finally, intradermal IL-8 injections resulted in an inflammatory response, characterized by the accumulation of neutrophils and lymphocytes at the injection site [14,15]. The induction of IL-8 release from keratinocytes is normally precluded by the release of tumor necrosis factor alpha (TNF-α). TNF-α can also act in autocrine fashion to stimulate the production and secretion of multiple cytokines and chemokines, as well as adhesion molecules such as ICAM-1. Therefore, TNF-α can modulate other cell types in the skin and activate infiltrating cells (e.g., macrophages). The purpose of this study was to evaluate the expression of IL-8 and TNF-α from cultured keratinocytes at the mRNA and protein levels following exposure to three different jet fuel mixtures, Jet A, JP8, and JP8(100). As early mediators of inflammation, these cytokines were selected as potential early biomarkers of an impending inflammatory response.

MATERIALS AND METHODS

Cell Culture/Chemical Treatment

Cryopreserved adult normal human epidermal keratinocytes (NHEK) were purchased from Clonetics, Corp. (San Diego, CA) and maintained in serum-free, calcium-free keratinocyte basal media (KBM, Clonetics) supplemented with human epidermal growth factor (0.1ng/mL), insulin (5μg/mL), bovine pituitary extract (0.4%), GA-1000 (gentamycin: 50μg/mL; amphotericin-B: 50ng/mL) to create keratinocyte growth media (KGM-2, Clonetics). 0.06 mM $CaCl_2$ was added back to the cultures for optimal growth without initiating Ca^{2+}-induced differentiation of the cells. Cells were cultured in 75cm^2 flasks and grown until 70–80% confluency. Third passage NHEK were plated onto 24-well plates (protein assays) or 12-well plates (mRNA assays) and were maintained in a humidified incubator at 37°C with a 95% O_2/5% CO_2 atmosphere. Upon reaching approximately 80–90% confluency, fresh KGM-2 was added, and test chemicals were added ($n = 3$) to appropriate wells in duplicate for 1–24 hours. Jet fuels were dissolved in 100% ethanol prior to their addition to KGM-2 at a final concentration of 0.1%. Previous experiments in our laboratory indicated that effects of ethanol-only treatment were not significantly different than control ($p < 0.05$, N. A. Monteiro-Riviere, unpublished observations, 1979). Control wells consisted of KGM-2 only. Treatment with 0.1% jet fuel exposure caused no apparent reduction in cell viability (as measured by trypan blue exclusion).

Enzyme-Linked Immunosorbent Assay (ELISA)

To determine secreted protein from NHEK in response to jet fuel exposure, a sandwich enzyme-linked immunosorbent assay (ELISA) assay was used for both IL-8 and TNF-α. NHEK were plated onto 24-well plates prior to treatments. At each time interval following dosage, the supernatant was removed and assayed immediately or frozen at −70°C for later assay. One freeze-thaw cycle showed no adverse effects on protein detected. 96-well plates coated with anti-IL-8 or anti-TNF-α were obtained from a commercial source (Biosource, Camarillo, CA). 100 μL of cell culture supernatant was added in triplicate to each well and incubated for 2 hours at room temperature. Following extensive washing, biotinylated anti-IgG antibodies were added to each well and incubated for 1 hour at room temperature. A streptavidin-peroxidase conjugate was then added to each well to bind to the biotin molecules. After adding a stabilized chromagen, the plates were read at 450 nm on a Multiskan RC plate reader (Labsystems, Helsinki, Finland). For both ELISA assays, a recombinant human IL-8 or TNF-α was diluted to create a standard reference curve. To ensure that neither the culture media nor the dosed chemicals adversely affected the efficiency of the ELISA, a sample from each treatment group was spiked with a known concentration of the recombinant proteins and measured for accuracy.

Statistics

Protein concentrations were expressed as pg cytokine/mL media as determined using Genesis Lite Version 3 for Windows software (Labsystems). Statistical differences in protein release were determined using ANOVA (SAS 6.12 for Windows; SAS Institute, Cary, NC) at the 0.05 level of significance.

Isolation of RNA and Reverse Transcription

Keratinocytes were plated onto 12-well plates and treated ($n = 3$) with test chemicals for various time

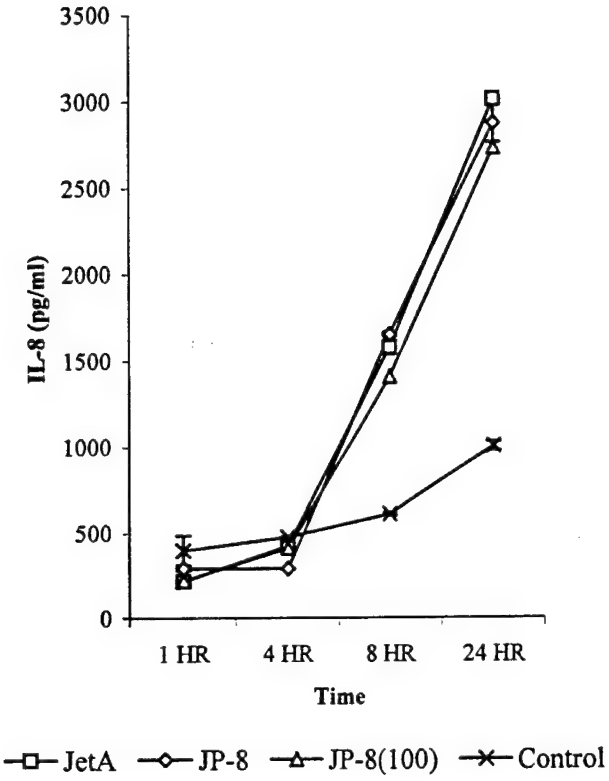

FIGURE 1. IL-8 protein released by NHEK increased in a time-dependent manner following exposure to Jet A, JP-8, and JP-8(100) jet fuels.

intervals (15 minutes, 30 minutes, 1 hour, 2 hours, 4 hours). At each time point, the supernatant was removed and lysis buffer (Qiagen, Valencia, CA, USA) was added directly to the wells. Cells were homogenized by passing them through a 20 cc syringe five times. Lysates from each treatment ($n = 3$) were pooled for RNA extraction. Total RNA was extracted using RNeasy spin columns per manufacturer instructions (Qiagen) and quantified spectrophotometrically. Each sample was then treated with DNase to remove potential genomic DNA contaminants. Following heat inactivation of the DNase by incubating at 65°C for 10 minutes, first strand cDNA synthesis was performed by combining approximately 1 μg of total RNA with 500 pg of Oligo $(dT)_{15}$ and heating to 70°C for 10 minutes, then quickly chilling on ice. The sample volume was then adjusted to 20 μL by the addition of 50 mM Tris-HCl (pH 8.3), 75 mM KCl, 3 mM $MgCl_2$, 10 mM DTT, 0.5 mM each dNTP, and 200 U of Superscript II reverse transcriptase (Gibco/BRL, Rockville, MD). This mixture was heated to 42°C for 50 minutes, and then the reaction was inactivated by heating to 70°C for 15 minutes. An Armored RNA Competicon (Ambion, Austin, TX) for both IL-8 and TNF-α was also reverse transcribed as described previously, and the resultant competitive fragments were serially diluted for use in competitive quantitative RT-PCR experiments (CQRT-PCR).

PCR

A common cocktail for each PCR reaction was used in order to minimize intersample variability. Each sample tube contained 10× PCR reaction buffer (Promega, Madison, WI; 10 mM Tris-HCl, 50 mM KCl), 1.5 mM $MgCl_2$, 0.2 mM each dNTP (Boerhinger Mannheim, Indianapolis, IN, USA), 0.4 μM each forward and reverse gene specific primer (Ambion), 2 U Taq DNA polymerase (Promega), 1 μL of sample cDNA, and sterile H_20 to a final volume of 49 μL. To obtain an initial range of the amount of mRNA present in each sample, the cDNA Competicon produced in the RT reaction was diluted by 2-log increments, and 1 μL was added to each sample tube. PCR was performed using the "hot start" method using the following cycling profile: (1) Soak at 94°C for 3 minutes; (2) 35 cycles at 94°C for 1 minute, 60°C for 1 minute, and 72°C for 2 minutes; (3) 72°C for 7 minutes. DNA products were electrophoresed in a 2% agarose gel, stained with ethidium bromide, and visualized by UV transillumination. Band intensities were quantified using the Alphaimager 2200 quantitative imaging system (Alpha Innotech Corp., San Leandro, CA). The approximate copy number of the sample mRNA corresponded to the Competicon dilution that yielded a band of similar intensity to the sample band. Once an approximate copy number had been established, the appropriate 5-fold dilution was further serially diluted 2-fold, and the above procedures were repeated. PCR reactions using gene-specific primers for a housekeeping gene (β-actin) and the above cycling parameters were performed with each sample cDNA to its quality prior to performing CQRT-PCR experiments. Positive controls consisted of gene-specific wild-type control DNA (Ambion). Negative controls without template were run to control for contaminants in the PCR components. Negative controls without reverse transcriptase were performed on each sample RNA to control for genomic DNA contamination.

RESULTS

Cytokine Release

Jet fuel exposure to keratinocytes caused a time-dependent increase in IL-8 release (Figure 1). During the first 4 hours of exposure, the release of IL-8 was slightly delayed. However, a significant increase was detected at 8 hours as compared to control cells ($p <$

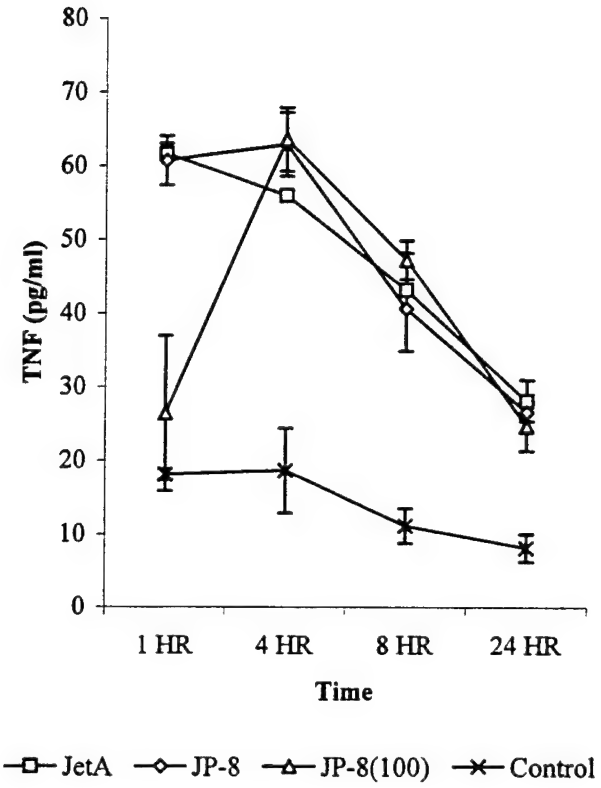

FIGURE 2. TNF-α protein released by NHEK increased at early time points following exposure to Jet A, JP-8, and JP-8(100) jet fuels and then decreased in a time-dependent manner.

0.05). All three fuel types resulted in a 2-fold increase in IL-8 release at 8 hours, and a 3-fold increase was detected at 24 hours. Although slight differences among each fuel type were seen, these differences were not significant ($p < 0.05$). A low level of spontaneous IL-8 release was seen in control cells, which increased slightly in a time-dependent manner.

Maximal TNF-α release was seen at the first hour of exposure to Jet A, and at 4 hours in the JP8 and JP8(100)-treated keratinocytes (Figure 2). After reaching their maximal release, these levels decreased in a time-dependent manner over 24 hours, but were significantly higher than control at all time points ($p < 0.05$). As seen with IL-8, control cells also spontaneously released TNF-α at low levels, which followed the same time-dependent decrease over the 24 hour exposure seen in the jet fuel treated cells.

Cytokine mRNA

Transcripts for both IL-8 and TNF-α were detected as early as 15 minutes in both treated and control cells. A constitutive level of IL-8 mRNA production was detected in control cells. Exposure to all three jet fuels types [Jet A, JP8, and JP8(100)] resulted in an increase in IL-8 mRNA production at 4 hours (Figures 3 and 4). Slightly higher levels of IL-8 mRNA were detected in JP-8 treated cells as compared with cells treated with JP-8(100) and Jet A.

TNF-α mRNA was detected in both treated and control cells (Figure 5). However, although we were unable to quantitate the amount of mRNA produced in response to all jet fuel exposures, the levels of TNF-α mRNA appeared to be relatively unaltered over time.

PCR experiments using primers for a housekeeping gene (β-actin) confirmed the presence of cDNA in all samples following reverse transcriptase and that its constitutive expression was consistent in response to jet fuel treatment.

DISCUSSION

Our results demonstrate that NHEK are activated by three different jet fuel mixtures to synthesize and release the proinflammatory cytokines IL-8 and TNF-α. These cytokines have been attributed to inflammatory and hyperproliferative disorders such as acute contact dermatitis [9] and psoriasis [16]. A major function of cutaneous IL-8 in the inflammatory response is its activity as a chemotactic factor for neutrophils as well as activating neutrophil functions [17]. Studies have shown that keratinocytes are capable of producing very large amounts of IL-8 [16,18] and that IL-8 production occurs in response to a wide variety of compounds including irritants, sensitizers, and allergens [19]. Our studies demonstrate that NHEK release a baseline level of IL-8, proportional to the levels detected by [19] using primary human keratinocytes. We saw an increase (at much lower levels) in the control cells that mimicked the release profile seen in the jet fuel treated cells. One potential explanation for this trend is the fact that fresh media was added to each sample well at the start of the study. Therefore, the profile seen may represent NHEK reaching a steady state level of IL-8 release that exists in unstimulated cells. To test this hypothesis, we sampled supernatants from unstimulated NHEK in culture for three days without changing the media. The IL-8 levels detected were between those detected at 8 and 24 hours. This implies that upon reaching a maximum (24 hours), IL-8 levels decline to a baseline level in which a continuous low-level production and release of IL-8 occurs in unstimulated cells. This is further supported by the IL-8 mRNA production profile we detected, in which IL-8 mRNA in control NHEK was maximal at 30 minutes and then decreased to basal levels by 4 hours.

IL-8 has been shown to promote the proliferation of normal epidermal keratinocytes [13]. Our lab has shown using in vivo swine that jet fuels induced a hy-

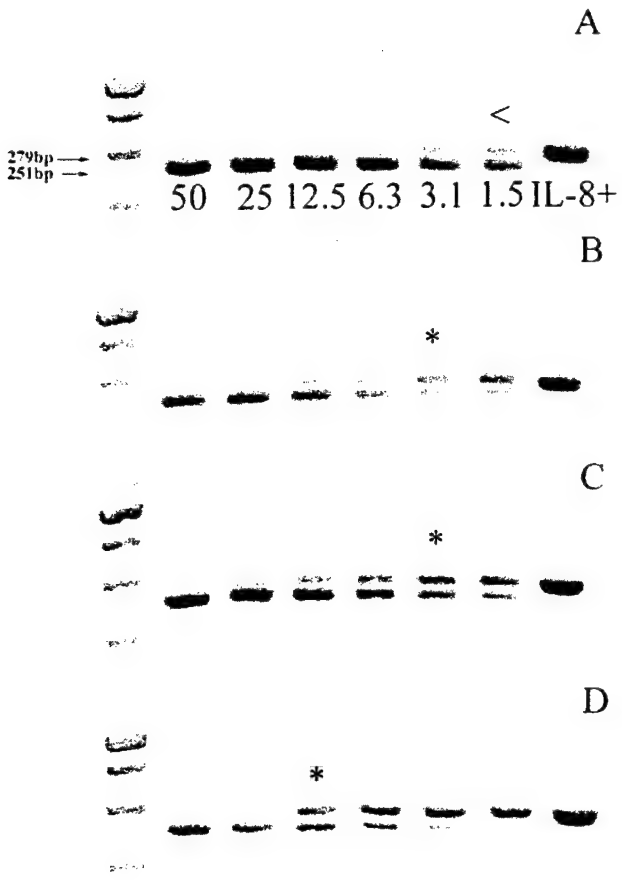

FIGURE 3. IL-8 mRNA production by NHEK 30 minutes following exposure to Jet A, JP-8, and JP-8(100) jet fuels (values are approximate mRNA copy number × 10^5; <, less than lowest competitor concentration examined). A, JP-8; B, Jet A; C, JP-8(100); D, control. Top band corresponds to sample cDNA, bottom band corresponds to competitive fragment cDNA. Band intensities are measured and compared to approximate the two most equal bands, representing the approximate mRNA copy number for that sample (denoted by *).

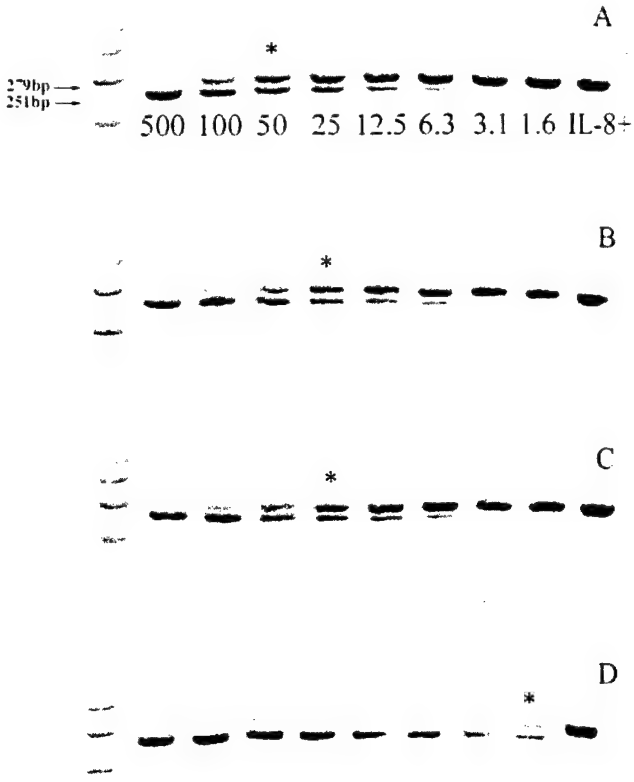

FIGURE 4. IL-8 mRNA production by NHEK 4 hours following exposure to Jet A, JP-8, and JP-8(100) jet fuels (values are approximate mRNA copy number × 10^5). A, JP-8; B, Jet A; C, JP-8(100); D, control. Top band corresponds to sample cDNA, bottom band corresponds to competitive fragment cDNA. Band intensities are measured and compared to approximate the two most equal bands, representing the approximate mRNA copy number for that sample (denoted by *).

perproliferative state after four days of occluded topical treatment [20]. These findings correlate well with our current findings that IL-8 production and secretion in NHEK is upregulated in response to jet fuels, and imply that IL-8 may be partially responsible for the epidermal hyperproliferation seen in vivo.

Our results also demonstrated the production and release of TNF-α following exposure to jet fuels. The TNF-α gene is an immediate early gene that, when induced, is expressed without requiring de novo protein synthesis. This implies that the factors involved in TNF-α expression are pre-existing in the unstimulated cell [21]. Indeed, unstimulated keratinocytes express very low levels of TNF-α mRNA and consequently release only small amounts [6]. This would explain the constitutive TNF-α mRNA and secreted protein seen in our results with control NHEK. TNF-α biosynthesis is very strictly regulated to ensure that it is expressed only under the appropriate conditions. Therefore, several possibilities exist for the mechanism of increased TNF-α seen in response to jet fuel exposure. TNF-α is produced as a biologically inactive 26 kD membrane peptide that is cleaved by a metalloproteinase, TACE (TNF-α converting enzyme) yielding the soluble, biologically active 17 kD TNF-α [22]. Certain metalloproteinase inhibitors can block the release of soluble TNF-α [23,24]. Perhaps the jet fuels actually act in an opposite fashion by enhancing TACE expression or upregulating its activity and therefore increasing TNF-α release. Induction of TNF-α expression is also regulated by the transcription factor, NF-κB. In the unstimulated cell, NF-κB is complexed to I-κB and resides in the cytoplasm. However, upon stimulation by an irritant, NF-κB is activated by rapidly being released from I-κB by a kinase enzyme that allows NF-κB to translocate into the nucleus of the cell and bind to the up-

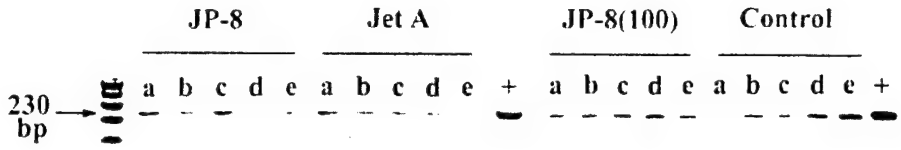

FIGURE 5. TNF-α mRNA production by NHEK exposed to Jet A, JP-8, and JP-8(100) jet fuels. (a) 15 minutes; (b) 30 minutes; (c) 1 hour; (d) 2 hours; (e) 4 hours; (+) TNF-α wild-type positive control.

stream promoter region of the TNF-α gene [8]. As irritants, jet fuels could potential affect cytokine transcription by upregulating the kinase enzyme. Finally, contact irritants cause disturbances to the mitochondrial electron transport chain resulting in the generation of reactive oxygen species. These highly reactive intermediates in turn activate transcription factors, which results in the synthesis of many proinflammatory cytokines, including TNF-α [8,25].

The release of TNF-α in response to jet fuel exposure had a very different profile than that of IL-8. Peak levels of TNF-α release were detected within 4 hours of jet fuel exposure and then declined steadily up to 24 hr. However, at all time points, TNF-α release was significantly higher than control cells. As mentioned previously, the initial release is probably attributed to "prepackaged" TNF-α. Keratinocytes possess the p55 TNF-α receptor, and therefore it is highly plausible that a negative feedback loop exists in keratinocytes to prevent excessive TNF-α release. The fact that we found TNF-α mRNA levels that were below the detection limit of the QCRT-PCR assay further supports the potential for "prepackaged" release.

In most examples of the keratinocyte cytokine cascade, IL-8 production and release is precluded by the release of TNF-α [6]. Our results show that IL-8 release increases within 8 hours of exposure to jet fuels, which is precluded by the release of TNF-α, which is released within 4 hours. The continued increase in IL-8 release during the decline in TNF-α release indicates the possibility of autocrine positive feedback occurring in the keratinocytes via the IL-8 receptor that is found on NHEK. However, studies have demonstrated that certain topical irritants (phenol, croton oil) can prompt IL-8 production in the absence of TNF-α [10]. Therefore, IL-8 release may be independent of TNF-α release.

The three fuels used in this study represent both commercial (Jet A) and military [JP8, JP8(100)] aircraft fuels. Each fuel is a complex mixture of 228 aliphatic and aromatic hydrocarbon compounds. The two military fuels are composed of Jet A to which several performance additives have been added. Among the three fuel types, no significant differences in IL-8 production and release were seen. With respect to production and release, JP8(100) treated keratinocytes was significantly reduced at the 1 hour time point. The complex chemical composition of these mixtures makes the identification of a single component responsible for such a difference impossible. Due to the petroleum-based nature of all three fuels, they are very insoluble in water and therefore required mixing with ethanol to cause them to go into the culture media solution. Even in the presence of ethanol, because of the extreme variability in component hydrophobicity, a gradient of mixture components was most likely established in the media such that some components were denied access to the cell surface. However, the components of JP8(100) include JP8 with an additional additive package that includes antioxidant, chelator, detergent, and dispersant components [4]. It is feasible that some or all of these additives modify the solubility of JP8(100) in ethanol such that a different spectrum of components reaches the keratinocyte monolayer than with Jet A or JP8, resulting in less TNF-α release in the first hour. A recent study investigated the absorption of marker components from the three fuels and found significant differences among the fuels [4]. The authors noted differences in absorption of the marker components among the fuels and postulated the potential for the additives in JP8(100) modulating skin absorption [4]. Finally, contact irritants have been shown to induce an increase in intracellular Ca^{2+} uptake [8]. The resulting alteration in cellular Ca^{2+} homeostasis is then followed by the formation of reactive oxygen species, which activate NF-κB. It is very possible that the chelating component of JP8(100) restricts the early uptake of Ca^{2+} and thus the production and release of TNF-α is delayed.

These results are the first to demonstrate that jet fuel mixtures result in proinflammatory cytokine production and release by keratinocytes. The dermal absorption of marker components of these fuels has been demonstrated previously [4], and therefore concern must be given to the potential for their toxicological significance in skin. Proinflammatory cytokines play a major role in the development of an acute inflammatory response, as well as in the maintenance of a chronic inflammatory response in the presence of continued stimulation. This implies that jet fuels may contribute to the development of disease states in the skin.

Furthermore, these results demonstrate subtle differences in the response among different fuel mixtures. Additional studies focusing on additive components among the fuels may elucidate the significance of such findings.

ACKNOWLEDGMENTS

This work represents partial fulfillment of the requirement for the degree of Doctor of Philosophy (D. Allen). Portions of this work were presented at the 39th Annual Meeting of the National Society of Toxicology in March 2000. The authors wish to thank Jason Pirone for his assistance with the statistical analysis.

REFERENCES

1. Agency for Toxic Substances and Disease Registry (ATSDR). Draft toxicological profile for jet fuels (JP-5 and JP-8). Atlanta: Agency for Toxic Substances and Disease Registry; 1996.
2. Harris DT, Sakiestewa D, Robledo RF, Witten M. Short-term exposure to JP-8 jet fuel results in long term immunotoxicity. Toxicol Ind Health 1997;13:559–570.
3. Koschier FJ. Toxicity of middle distillates from dermal exposure. Drug Chem Toxicol 1999;22(1):155–164.
4. Riviere JE, Brooks JD, Monteiro-Riviere NA, Budsaba K, Smith CE. Dermal absorption and distribution of topically dosed jet fuels Jet-A, JP-8, and JP-8(100). Toxicol Appl Pharmacol 1999;160:60–75.
5. Kondo S. The roles of keratinocyte-derived cytokines in the epidermis and their possible responses to UVA-irradiation. J Invest Dermatol Symp Proc 1999;4:177–183.
6. Luger TA, Schwarz T. Evidence for an epidermal cytokine network. J Invest Dermatol 1990;95:110S–104S.
7. Nickoloff BJ. The cytokine network in psoriasis. Arch Dermatol 1991;127:871–833.
8. Corsini E, Galli CL. Cytokines and contact dermatitis. Toxicol Lett 1998;102–103:277–282.
9. Nickoloff BJ. Pathophysiology of cutaneous inflammation. Arch Dermatol Res 1992;284:S10–S11.
10. Wilmer JL, Burleson FG, Kayama F, Kanno J, Luster MI. Cytokine induction in human epidermal keratinocytes exposed to contact irritants and its relation to chemical-induced inflammation in mouse skin. J Invest Dermatol 1994;102:915–922.
11. Larsen CG, Anderson AO, Appella E, Oppenheim JJ, Matsushima K. The neutrophil-activating protein (NAP-1) is also chemotactic for T lymphocytes. Science 1989;243:1464–1466.
12. Leonard EJ, Skeel A, Yoshimura T, Noer K, Kutvirt S, Van Epps D. Leukocyte specificity and binding of human neutrophil attractant/activator protein-1. J Immunol 1991;144, 1323–1330.
13. Tuschil A, Lam C, Haslberger A, Lindley I. Interleukin-8 stimulates calcium transients and promotes epidermal cell proliferation. J Invest Dermatol 1992;99:294–298.
14. Leonard EJ, Yoshimura T, Tanaka S, Raffeld M. Neutrophil recruitment by intradermally injected neutrophil attractant/activator protein-1. J Invest Dermatol 1991; 96:690–694.
15. Swensson O, Schubert C, Christophers E, Schroder J-M. Inflammatory properties of neutrophil-activating protein-1/interleukin-8 (NAP-1/IL-8) in human skin: a light and electron microscopic study. J Invest Dermatol 1991;96:682–689.
16. Nickoloff BJ, Karabin GD, Barker JNWN, Griffiths CEM, Sarma V, Mitra RS, Elder JT, Kunkel SL, Dixit. Cellular localization of interleukin-8 and its inducer, tumor necrosis factor-alpha, in psoriasis. Am J Pathol 1991;138(1), 129–140.
17. Atta-ur-Rahman, Harvey K, Siddiqui RA. Interleukin-8: an autocrine inflammatory mediator. Curr Pharm Des 1999;5:241–253.
18. Kondo S, Kono T, Sauder DN, McKenzie RC. Il-8 gene expression and production in human keratinocytes and their modulation by UVB. J Invest Dermatol 1993; 101:690–694.
19. Mohamadzadeh M, Muller M, Hultsch T, Enk A, Saloga J, Knop J. Enhanced expression of IL-8 in normal human keratinocytes and human keratinocyte cell line HaCaT in vitro after stimulation with contact sensitizers, tolerogens, and irritants. Exp Dermatol 1994;3:298–303.
20. Monteiro-Riviere NA, Inman AO, Rhyne BN, Riviere JE. Cutaneous irritation of topically applied jet fuels in the pig. Toxicol Sci 2000;54:151.
21. Zhang M, Tracey K. Tumor necrosis factor. In: A. Thomson, editor. The cytokine handbook, 3rd ed. New York: Academic Press Ltd; 1998. p 517–548.
22. Patel IR, Attur MG, Patel RN, Stuchin SA, Abagyan RA, Abramson SB, Amin AR. TNF-α convertase enzyme from human arthritis-affected cartilage: isolation of cDNA by differential display, expression of the active enzyme, and regulation of TNF-α. J Immunol 1998;160:4570–4579.
23. Mohler KM, Sleath PR, Fitzner JN, Cerrettl DP, Alderson M, Kerwar SS, Torrance DS, Otten-Evans C, Greenstreet T, Weerawarna K, Kronheldm SR, Petersen M, Gerhart M, Kozlosky CJ, March CJ, Black RA. Protection against a lethal dose of endotoxin by an inhibitor of tumor necrosis factor processing. Nature 1994;370:218.
24. Williams LM, Gibbons DL, Gearing A, Maini RN, Feldmann M, Brennan FM. Paradoxical effects of a synthetic metalloproteinase inhibitor that blocks both p55 and p75 TNF receptor shedding and TNF-α procesing in RA synovial membrane cell cultures. J Clin Invest 1996; 97:2833–2841.
25. Corsini E, Terzoli A, Bruccoleri A, Marinovich M, Galli CL. Induction of tumor necrosis factor-α in vivo by a skin irritant, tributyltin, through activation of transcription factors: its pharmacological modulation by anti-inflammatory drugs. J Invest Dermatol 1997;108:892–896.

Toxicology Methods, 10:313–332, 2000

1051-7235/00 $12.00 + .00

COMPASS PLOTS: A COMBINATION OF STAR PLOT AND ANALYSIS OF MEANS TO VISUALIZE SIGNIFICANT INTERACTIONS IN COMPLEX TOXICOLOGY STUDIES

Kamon Budsaba and Charles E. Smith
Department of Statistics, North Carolina State University Raleigh, North Carolina, USA

Jim E. Riviere
Center for Cutaneous Toxicology and Residue Pharmacology, North Carolina State University, Raleigh, North Carolina, USA

The Compass Plot, a new graphical method that combines the advantages of the star plot and the analysis of means (ANOM), has been introduced for displaying the results of experiments. In contrast to the star plot, this plot allows statistical inferences to be made for treatment and for factor effects. In contrast to ANOM, this plot is good for comparison in multiresponse experiments, a scenario becoming more commonplace in toxicology with the advent of increasing numbers of chemical mixture studies. An example of a 2^3 factorial chemical exposure experiment is considered here.

Keywords analysis of means, Bonferroni method, chemical mixtures, 2^p factorial experiments, Kimball inequality, parathion, star plot, Yates algorithm

As the performance capabilities of statistical software packages expand, users face increasing difficulty in comprehending the analyzed data. Usually, results are communicated as numbers, which require the user to build a mental model and extract critical information. Statistical visualization tries to bridge the communication gap by creating visual displays that help audiences comprehend in more natural, intuitive ways the extensive amount of data coming from computers. Visualization techniques that help audiences see patterns and deviations can enable researchers to reach the "big picture" more intuitively and get to the main point of a problem quickly. This need has become evident in complex toxicology experiments involving chemical mixtures.

Many data analysis applications involve several or many variables. In reality, it is crucial to consider more than two variables at a time in a study. Many coding schemes can be devised for portraying two or more

Received 20 April 2000; accepted 15 July 2000.
This work was supported by U.S. Air Force Office of Scientific Research grants F49620 and FQ8671.
Address correspondence to Kamon Budsaba, Department of Statistics, North Carolina State University, Raleigh, NC 27695-8203, USA. E-mail: kbudsab@stat.ncsu.edu

variables simultaneously in the plotting symbols. The main purpose of multicode schemes is to obtain a symbol with a distinctive shape for each group, so that an audience can look for pairs or groups of symbols with similar shapes or individuals that are very different from the rest (Chambers et al., 1993). In many scenarios encountered in toxicology, it is the presence of interactions that is particularly significant and has to be stressed.

Radial plots for multivariate data have been introduced as descriptive tools (star and profile plots by Chambers et al. (1993) and by Henry (1995), glyphs by Toit et al. (1986), polyplots by Blazek et al. (1987), florigraphs by Barton (1992), and Kiviat diagrams by Douglas (1994). For applications with a relatively small number of independent variables, some success in multidimensional visualizing has been achieved through the use of so-called Kiviat diagrams, or star plots (Douglas, 1994). In such diagrams, we assign the variables, on same scale or different measurement scales, to the rays of the star. The values of the variables are coded into the lengths of rays. Plotted values are then connected by lines to form an enclosed figure. The normal condition can be indicated by a symmetrical polygon.

The objective of this study was to create a graphical method for the presentation of the results of a 2^p balanced factorial experiment that could illustrate treatment and factor effects under a fixed effects model (Model I). This method combines the advantages of the star plot and of the analysis of means (ANOM); we call it the compass plot. The name "compass plot" was first introduced for the presentation of the results of a chemical mixtures experiment (Qiao, 1996). However, in that paper compass plots were used only as a descriptive tool. They lacked the ability to make statistical inferences; that ability is presented here. The ANOM is summarized subsequently, followed by a discussion of the methods of using compass plots to detect the treatment effects and factor effects; examples of compass plots and ANOM-style plots; and a comparison of compass plots and ANOM-style plots, including their extensions.

ANALYSIS OF MEANS

ANOM is a statistical procedure that has been used mainly for solving industrial problems and analyzing the results of experiments. Ott introduced the ANOM technique in 1967 (reprinted in Ott, 1983) to test the equality among k means. Schilling (1973) extended this technique to what he called the analysis of means for treatment effects (ANOME). P. R. Nelson (1982, 1983) and L. S. Nelson (1983) presented exact critical values for the ANOM. Further applications, tests for interaction effects, and extensions have also been investigated (Nelson, 1988; Wludyka, 1997).

The determination of a significant difference is made by creating a chart to compare points representing the k sample means, with upper and lower lines drawn parallel to the line of the grand mean. If all the plotted points fall between the upper and lower decision lines, it is interpreted as representing only random variability. If a point falls outside of either of these decision lines, it is considered evidence of nonrandomness—that is; treatment means are significant differences with risk α. The meaning of this in the setting of toxicology is illustrated later.

The ANOM and the analysis of variance (ANOVA) are not exactly equivalent (Nelson, 1983). Although the ANOVA has some theoretical advantage over the ANOM test, namely that of having a superior ability to detect differences in the k means and thus being more useful for a complex design. The effectiveness of the ANOVA is limited because it lacks the kind of appealing graphical visualization produced by the ANOM (Lapin, 1997).

ANOM is easy to learn and use because it is a logical extension of the Shewhart control chart, which is well known to industrial practitioners (Snee, 1983) and is commonly used in clinical chemistry labs. Ott (1983) summarized the advantages of ANOM as follows: It provides a direct study of effects by dealing with means instead of variances. It provides a comparison of the relative magnitude of the factors as well as their statistical significance. It provides a graphical comparison of effects which indicates the source of nonrandomness, whereas ANOVA must usually be followed by some additional analysis to detect the important factors. Finally, ANOM can be extended when there is no replication due to the missing values, a situation that arises in toxicological studies. However, although ANOM is appropriate for factors involving fixed effects, it is inappropriate for factors involving random effects. Also, the exact critical values for ANOM are limited to balanced designs and are limited in the values of the risk α and k, the number of treatments. For unbalanced designs, approximate critical values can be obtained (Nelson, 1983).

METHODS

The following section investigates treatment effects for single-factor experiments or one-way ANOVA models. The next section investigates factor effects primarily for 2^p factorial experiments.

Investigation of Treatment Effects: Model I

As in ANOM, the idea of detecting treatment effects by using a compass plot involves comparing all treatment means with the grand mean.

Following Neter et al. (1990), the single-factor ANOVA cell means model may be considered in a balanced experiment as follows:

$$Y_{ij} = \mu_i + \epsilon_{ij} \tag{1}$$

where

Y_{ij} is the value of the response variable in the jth trial for the ith treatment or factor level
μ_i is the parameter representing the mean of the ith treatment
ϵ_{ij} is the independent random error term and $N(0,\sigma^2)$
$i = 1, \ldots, k; j = 1, \ldots, n$

The factor effects model, given below, is an alternative equivalent formulation of the cell means model.

$$Y_{ij} = \mu_. + \tau_i + \epsilon_{ij} \tag{2}$$

where $\tau_i = \mu_i - \mu_.$ is the effect of the ith treatment and $\mu_.$ is the grand mean. This definition implies that $\sum_{i=1}^{k} \tau_i = 0$. To test for equality of treatment means, the hypotheses are as follows:

H_0: $\tau_1 = \tau_2 = \ldots = \tau_k = 0$
H_a: not all τ_i equal zero

For $i = 1, \ldots, k$, let contrast i be $L_i = \mu_i - \mu_.$. An unbiased estimator of L_i is $\hat{L}_i = \bar{Y}_{i.} - \bar{Y}_{..}$. Under model I; $\mathrm{Var}(\hat{L}_i) = (1 - 1/k)\mathrm{Var}(\bar{Y}_{i.}) = (k-1)(\sigma^2)/(k)(n)$. The Bonferroni inequality then implies that the confidence coefficient is at least $1 - \alpha$ and that the following confidence limits for the k linear combinations L_i are all correct:

$$\hat{L}_i \pm t_{1-\frac{\alpha}{2(k)};k(n-1)} s(\hat{L}_i) \tag{3}$$

where $s^2(\hat{L}_i) = (k-1)(MSE)/(k)(n)$ and MSE is the pooled sample variance calculated from each treatment group.

These confidence intervals are smaller than those from the Scheffe method because the number of contrasts to be estimated is equal to the number of factor levels (Neter, 1990, p. 588).

Under H_0, it implies that for each i, $i = 1, \ldots, k$, after some rearranging of terms,

$$\bar{Y}_{..} - t_{1-\frac{\alpha}{2(k)};k(n-1)} s(\hat{L}_i) \le \bar{Y}_{i.} \le \bar{Y}_{..} + t_{1-\frac{\alpha}{2(k)};k(n-1)} s(\hat{L}_i).$$

Hence, the plot of treatment means, along with its lower and upper limits as inner and outer polygons, respectively, can be used in the

compass plot to detect the significance of treatment effects. Said another way, our compass plot for treatment means is simply an ANOM plot mapped to a regular polygon. The inner and outer polygons can be regarded as the lower and upper decision lines in ANOM. If any of the k treatment means falls outside the inner and outer polygon, we can conclude that there is a statistically significant difference among the means.

Instead of using the Bonferroni inequality, we can obtain the exact critical value, $h_{\alpha.k.df}$, from the table in L. S. Nelson (1983) at type I risk α, number of mean k, and degrees of freedom $k(n-1)$. Hence, the lower and upper limits are

$$\text{Lower limit} = \bar{Y}_{..} - h_{\alpha.k.k(n-1)}s(\hat{L}_i)$$

$$\text{Upper limit} = \bar{Y}_{..} + h_{\alpha.k.k(n-1)}s(\hat{L}_i).$$

The compass plot provides a similar graphical representation to investigate factor effects as well, as is shown in the next section.

Investigation of Factor Effects: Model I

Extensions of ANOM to examine the factor effects were presented in Schilling (1973) and Ramig (1983) and are denoted as ANOME. Additional work on testing for interactions via a series of ANOM-like plots was introduced by Nelson (1988). In contrast to these studies, which require several plots to examine the factor effects, the compass plot allows one type of plot to examine all main effects and interactions simultaneously. The compass plot is particularly useful for 2^p factorial experiments.

To detect the factor effects by means of a compass plot, each fitted effect is represented as a deviation from the grand mean. The mean response for a given treatment in a balanced two-factor study is denoted by μ_{ij}, where i refers to the level of factor A ($i = 1, \ldots, a$), and j refers to the level of factor B ($j = 1, \ldots, b$). Let

$$\mu_{i.} = \frac{\sum_{j=1}^{b} \mu_{ij}}{b} \tag{4}$$

$$\mu_{.j} = \frac{\sum_{i=1}^{a} \mu_{ij}}{a} \tag{5}$$

$$\mu_{..} = \frac{\sum_i \sum_j \mu_{ij}}{ab} = \frac{\sum_i \mu_{i.}}{a} = \frac{\sum_j \mu_{.j}}{b}. \tag{6}$$

Now consider the factor effects ANOVA model for two-factor studies:

$$Y_{ijk} = \mu_{..} + \alpha_i + \beta_j + (\alpha\beta)_{ij} + \epsilon_{ijk} \tag{7}$$

where

Y_{ijk} is the value of the response variable in the kth trial when factor A is at the ith level and factor B is at the jth level.
$\mu_{..}$ is an overall constant representing the grand mean.
$\alpha_i = \mu_{i.} - \mu_{..}$ are constants and $\Sigma_i \alpha_i = 0$ (main effect of factor A at ith level).
$\beta_j = \mu_{.j} - \mu_{..}$ are constants and $\Sigma_j \beta_j = 0$ (main effect of factor B at jth level).
$(\alpha\beta)_{ij} = \mu_{ij} - (\mu_{..} + \alpha_i + \beta_j) = \mu_{ij} - \mu_{i.} - \mu_{.j} + \mu_{..}$ are constants and $\Sigma_i(\alpha\beta)_{ij} = 0$, $\Sigma_j(\alpha\beta)_{ij} = 0$ (interaction effect when factor A is at the ith level and factor B is at the jth level).
ϵ_{ij} are independent random error terms, and $N(0,\sigma^2)$.
$i = 1,\ldots,a$; $j = 1,\ldots,b$; $k = 1,\ldots,n$.

Because of the way factorial effects sum to 0 over levels of any factor involved, estimating one effect of each type is sufficient to test the hypothesis in a two-level experiment. To test for main effects and interactions in the case of a 2^2 factorial, the hypotheses are as follows:

H_0: $\alpha_2 = \beta_2 = (\alpha\beta)_{22} = 0$;
H_a: not all of them equal zero.

Consider the following contrasts: $L_1 = \alpha_2 = \mu_{2.} - \mu_{..}$, $L_2 = \beta_2 = \mu_{.2} - \mu_{..}$, and $L_3 = (\alpha\beta)_{22} = \mu_{22} - (\mu_{..} + \alpha_2 + \beta_2) = \mu_{22} - \mu_{2.} - \mu_{.2} + \mu_{..}$. Least squares estimates of each L are $\hat{L}_1 = \bar{Y}_{2.} - \bar{Y}_{..}$, $\hat{L}_2 = \bar{Y}_{.2} - \bar{Y}_{..}$, and $\hat{L}_3 = \bar{Y}_{22} - (\bar{Y}_{..} + \hat{\alpha}_2 + \hat{\beta}_2)$. Because these contrast are orthogonal, the Kimball inequality then implies that the confidence coefficient is at least $1 - \gamma$ and that the following confidence limits for the 3 linear combinations L_i, i =1,2,3, are all correct:

$$\hat{L}_i \pm t_{1-\frac{\gamma i}{2};k(n-1)} s(\hat{L}_i) \tag{8}$$

where $\gamma = 1 - (1 - \gamma_i)^3$, and $s^2(\hat{L}_i) = MSE/2^2 n$. Under H_0, after some rearranging of terms, it implies that

for the A main effect, $\bar{Y}_{..} - t_{1-\frac{\gamma 1}{2};k(n-1)} s(\hat{L}_1) \le \bar{Y}_{2.} \le \bar{Y}_{..} + t_{1-\frac{\gamma 1}{2};k(n-1)} s(\hat{L}_1)$;
for the B main effect, $\bar{Y}_{..} - t_{1-\frac{\gamma 2}{2};k(n-1)} s(\hat{L}_2) \le \bar{Y}_{.2} \le \bar{Y}_{..} + t_{1-\frac{\gamma 2}{2};k(n-1)} s(\hat{L}_2)$;
for the AB interaction, $\bar{Y}_{..} - t_{1-\frac{\gamma 3}{2};k(n-1)} s(\hat{L}_3) \le \bar{Y}_{22} - (\hat{\alpha}_2 + \hat{\beta}_2) \le \bar{Y}_{..} + t_{1-\frac{\gamma 3}{2};k(n-1)} s(\hat{L}_3)$.

Note that the quantity that is compared with the lower and upper limits is the grand mean plus fitted effect, which is the predicted value of Y when only that effect is considered in the model ($\hat{Y}_E$); that is, $\hat{Y}_A =$

$\bar{Y}_{2.} = \hat{\mu}_{..} + \hat{\alpha}_2$, $\hat{Y}_B = \bar{Y}_{.2} = \hat{\mu}_{..} + \hat{\beta}_2$, and $\hat{Y}_{AB} = \bar{Y}_{22} - (\hat{\alpha}_2 + \hat{\beta}_2) = \hat{\mu}_{..} + \hat{\alpha}\beta_{22}$. Hence, plotting $\hat{Y}_E$ along with its lower and upper limits as inner and outer polygons can be used in the compass plot to detect the significance of factor effects. Our procedure is reminiscent of the use of the Yates algorithm to generate, for the high levels of all factors, one fitted effect of each type for a 2^p dataset (Vardeman, 1994).

In summary, to detect the treatment effects, we plot each treatment mean as a ray on the compass plot. Vertex order follows the Yates algorithm. Then we construct contrasts to compare each treatment mean with the grand mean. After setting an appropriate experimentwise error rate, we then construct simultaneous confidence intervals by using the Bonferroni method or the exact critical value (Nelson, 1983) to get the inner and outer bound around the grand mean. If all treatment means are inside this band, it indicates no significant difference among treatments. Similarly, to detect the factor effects, the grand mean plus each fitted effect is then used instead of the treatment means, and the Kimball inequality is used to construct the simultaneous intervals. If any effect is outside the band, it implies that the effect is significant at a particular risk level alpha.

Earlier, we used the inner and outer polygons in the factor effects compass plot to detect significant interactions. We can also qualitatively determine the presence or absence of interactions by using the compass plot for treatment means and "squareness" in the way parallelism is used in the usual means plot. The parallelism in the means plot becomes a square in the compass plot by using a folding technique when no interaction is present. Lack of parallelism or presence of interaction becomes an inside rectangle for non-crossover interaction and an outside rectangle for crossover interaction (Gail, 1985).

EXAMPLE

The following example is a factorial experiment assessing chemical/chemical interactions in a study of topical mixture absorption across skin. Basically, we are interested in the factor effects rather than in the treatment effects. Treatment effects are usually investigated when significant interactions are presented. We begin with an investigation of the treatment effects and then consider the factor effects according to the presentation sequence discussed earlier.

There is a 2^3 factorial experiment in each vehicle (Qiao, 1996). To access the risk of cutaneous exposure to chemical mixtures, acetone or dimethylsulfoxide (DMSO) was used as a vehicle. Percutaneous absorption and cutaneous disposition of parathion (PA) were studied following PA dosing on isolated perfused porcine skin as mechanistically defined chemical mixtures consisting of

TABLE 1. Treatment Means for Each Parameter of PA Cutaneous Disposition in Acetone

Treatment	(1)	a	b	ab	c	ac	bc	abc	$\bar{Y}_{..}$	MSE
Y1	1.0567	1.8033	0.6700	1.7933	0.6667	2.7333	0.8033	0.8600	1.2983	0.8792
Y2	3.0233	4.4700	1.2700	3.9967	1.2867	4.3000	1.4767	2.6100	2.8042	1.8670
Y3	0.7833	2.1933	0.4067	1.5367	0.3400	0.7433	0.4467	1.1933	0.9554	0.3328
Y4	0.0031	0.0056	0.0022	0.0058	0.0023	0.0128	0.0028	0.0036	0.0048	0.000020

Factor A: the surfactant sodium lauryl sulfate (SLS; absence or presence)
Factor B: the rubefacient methyl nicotinate (MNA; absence or presence)
Factor C: the reducing agent stannous chloride ($SnCl_2$; absence or presence)

The original design was a full 2^4 factorial with three replicates that included vehicle as another factor. The vehicle was significant in most of the PA cutaneous disposition parameters, so it is appropriate to compare the effects and interactions between each vehicle.

Some of the parameters of PA cutaneous disposition over the 8-h experimental period are as follows:

Y1: the total absorption (% dose)
Y2: the total penetration (% dose)
Y3: the dosed skin residue (% dose)
Y4: the peak flux rate (% dose/min)

Treatment means are shown in Tables 1 and 2. The treatment labeled (1) denotes the treatment combination in which all factors are at a low level (absence of all those factors). The treatment labeled a denotes the treatment combination in which only factor A is at a high level (presence of SLS). Similarly, the treatment labeled ab denotes the treatment combination in which both SLS and MNA are presented.

For example, to detect treatment effects of Y1 for acetone, $s^2(\hat{L}_i) = (k-1)(MSE)/(k)(n) = (7)(0.8792)/(8)(3) = 0.2564$. If $\alpha = .05$, by using the table in L. S. Nelson (1983), $h_{.05.8.16} = 3.09$. Hence, for i = a, b, ab, c, ac, bc, abc:

$$1.2983 - (3.09)\sqrt{0.2564} \le \bar{Y}_i \le 1.2983 + (3.09)\sqrt{0.2564}$$

$$-0.2664 \le \bar{Y}_i \le 2.8630.$$

TABLE 2. Treatment Means for Each Parameter of PA Cutaneous Disposition in DMSO

Treatment	(1)	a	b	ab	c	ac	bc	abc	$\bar{Y}_{..}$	MSE
Y1	1.3900	3.2733	0.9367	0.2933	0.6433	0.9133	1.0933	1.2867	1.2288	1.3755
Y2	5.3433	5.9767	3.9933	1.6333	3.4800	2.7867	2.7933	3.8900	3.7371	1.4589
Y3	3.5400	1.9133	2.5467	1.1600	2.2033	1.5433	1.3100	2.2433	2.0575	0.4720
Y4	0.0072	0.0144	0.0031	0.0013	0.0031	0.0038	0.0042	0.0041	0.0051	0.000024

For acetone, there is no significant difference among total absorption means. The compass plots for all the treatment effects in each parameter for both acetone and DMSO are shown in Figures 1 and 3. The ANOM-style plots, using the same lower and upper limits as compass plots, are shown in Figures 2 and 4.

For acetone, only dosed skin residue (Y3) at a and peak flux rate (Y4) at ac are significant, but for DMSO there is a significant difference among treatment means in each parameter—that is, total absorption (Y1), total penetration (Y2), and peak flux rate (Y4) at a but dosed skin residue (Y3) at (1).

For factor effects, the fitted effects $\hat{E}$ and $\hat{Y}_E$ of Y1 for acetone can be obtained as in Table 3. We assign the plus sign to the factors in columns A, B, and C when the treatment contains that factor at a high level (a string of letters for that treatment code matches the letter of that particular factor). The sign for an interaction column such as AB was obtained by multiplication of the signs of the particular factors.

For $i = \text{A, B, AB, C, AC, BC, ABC}$, $s^2(\hat{L}_i) = MSE/2^3n = 0.8792/(8)(3) = 0.0366$.

If $\gamma = .10$, by the Kimball inequality, $\gamma_i = .0149$ and hence $t_{1-\frac{.0149}{2};16} = t_{.9926;16} = 2.7265$. Then for each factor effect

$$1.2983 - (2.7265)\sqrt{0.0366} \le \hat{Y}_E \le 1.2983 + (2.7265)\sqrt{0.0366}$$

$$0.7767 \le \hat{Y}_E \le 1.8199$$

For acetone, there is no significant effect on total absorption. The compass plots for all the factor effects in each parameter for both acetone and DMSO are shown in Figures 5 and 7. The ANOM-style plots are also shown in Figures 6 and 8.

For acetone, because no interaction effect is significant, we can conclude that the main effect A is significant in both total penetration (Y2) and dosed skin residue (Y3).

TABLE 3. Calculation of the Fitted Effects, $\hat{E}$, and $\hat{Y}_E$ of the Total Absorption (Y1) in Acetone

Mean	A	B	AB	C	AC	BC	ABC
(1) = 1.0567	−	−	+	−	+	+	−
a = 1.8033	+	−	−	−	−	+	+
b = 0.6700	−	+	−	−	+	−	+
ab = 1.7933	+	+	+	−	−	−	−
c = 0.6667	−	−	+	+	−	−	+
ac = 2.7333	+	−	−	+	+	−	−
bc = 0.8033	−	+	−	+	−	+	−
abc = 0.8600	+	+	+	+	+	+	+
$\hat{E}$	3.9932/8 =0.4992	−2.1334/8 = −0.2667	−1.6332/8 = −0.2042	−0.2600/8 = −0.0325	0.2534/8 = 0.0317	−1.3400/8 = −0.1675	−2.3866/8 = −0.2983
$\hat{Y}_E$	1.7974	1.0316	1.0942	1.2658	1.3300	1.1308	1.0000

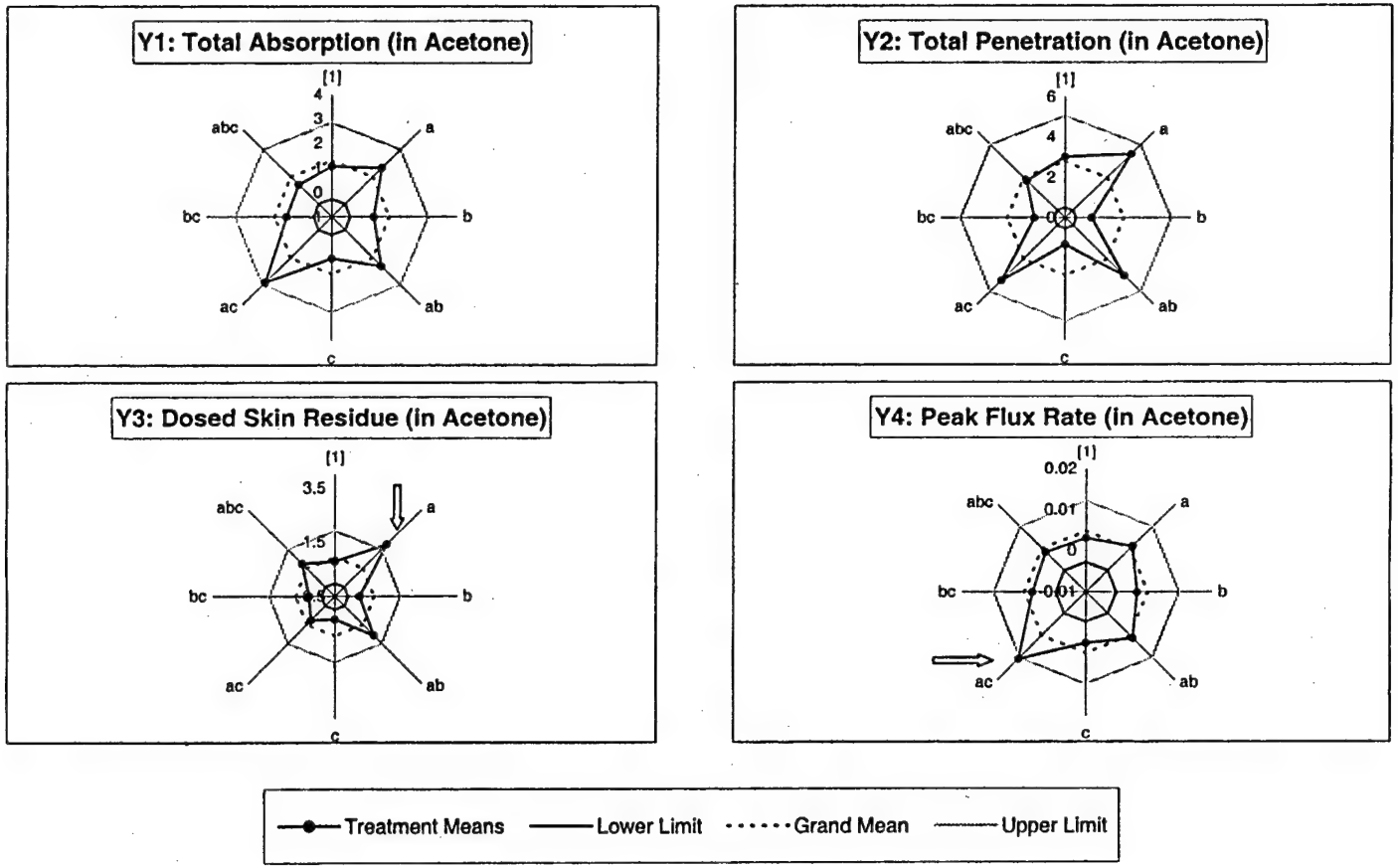

FIGURE 1. Compass plots for detecting the treatment effects in acetone for total absorption, total penetration, dosed skin residue, and peak flux rate (Y1–Y4, respectively). The heavy solid lines are treatment means. The three concentric octagons are the lower limit, grand mean, and upper limit, respectively. Significant treatments are indicated with an arrow. Only dosed skin residue (Y3), at a, and peak flux rate (Y4), at ac, are significant.

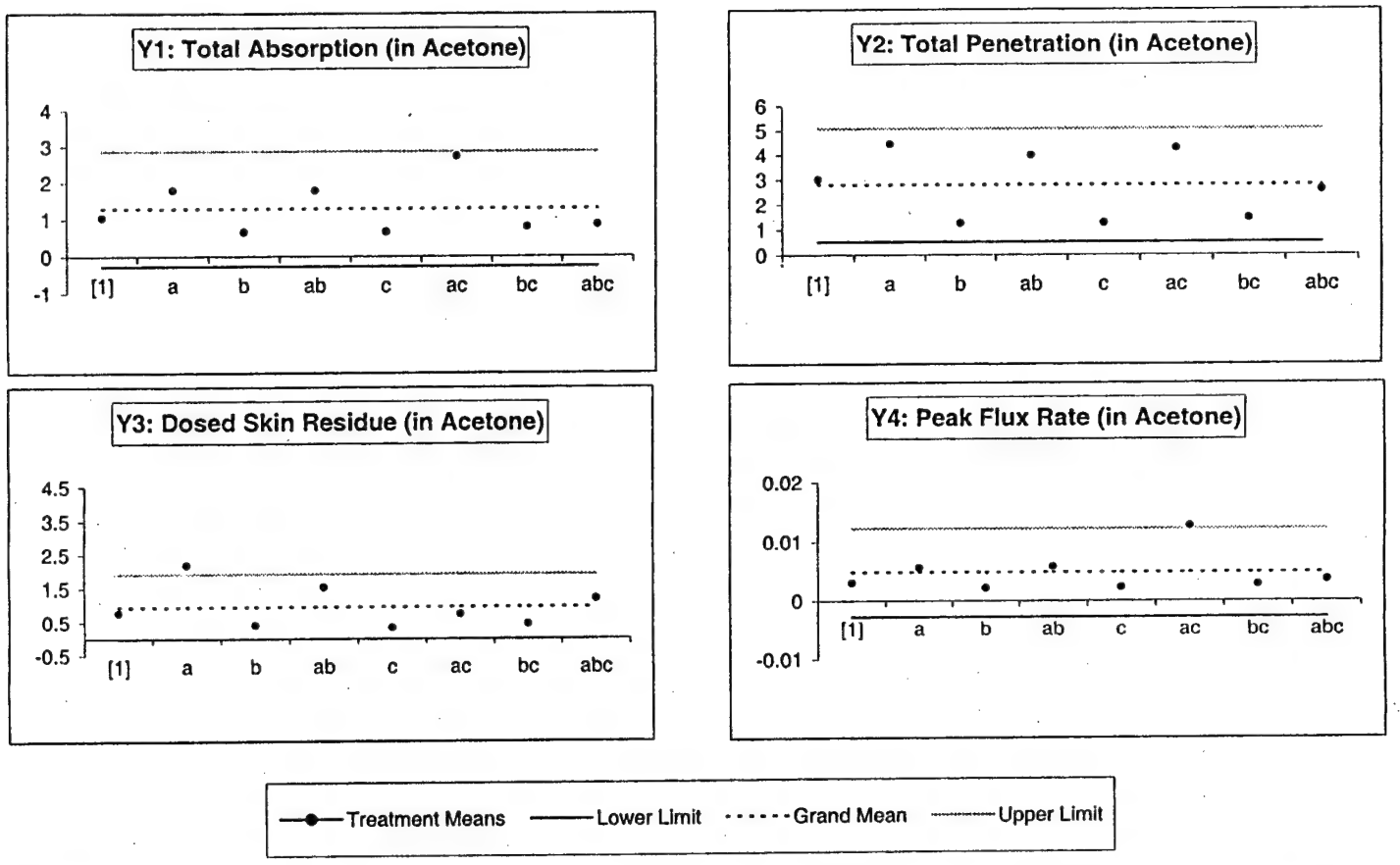

FIGURE 2. ANOM-style plots for detecting the treatment effects in acetone for total absorption, total penetration, dosed skin residue, and peak flux rate (Y1–Y4, respectively). Treatment means are denoted as points. Horizontal lines from top to bottom represent the upper decision line, grand mean, and lower decision line, respectively. Only dosed skin residue (Y3), at a, and peak flux rate (Y4), at ac, are significant.

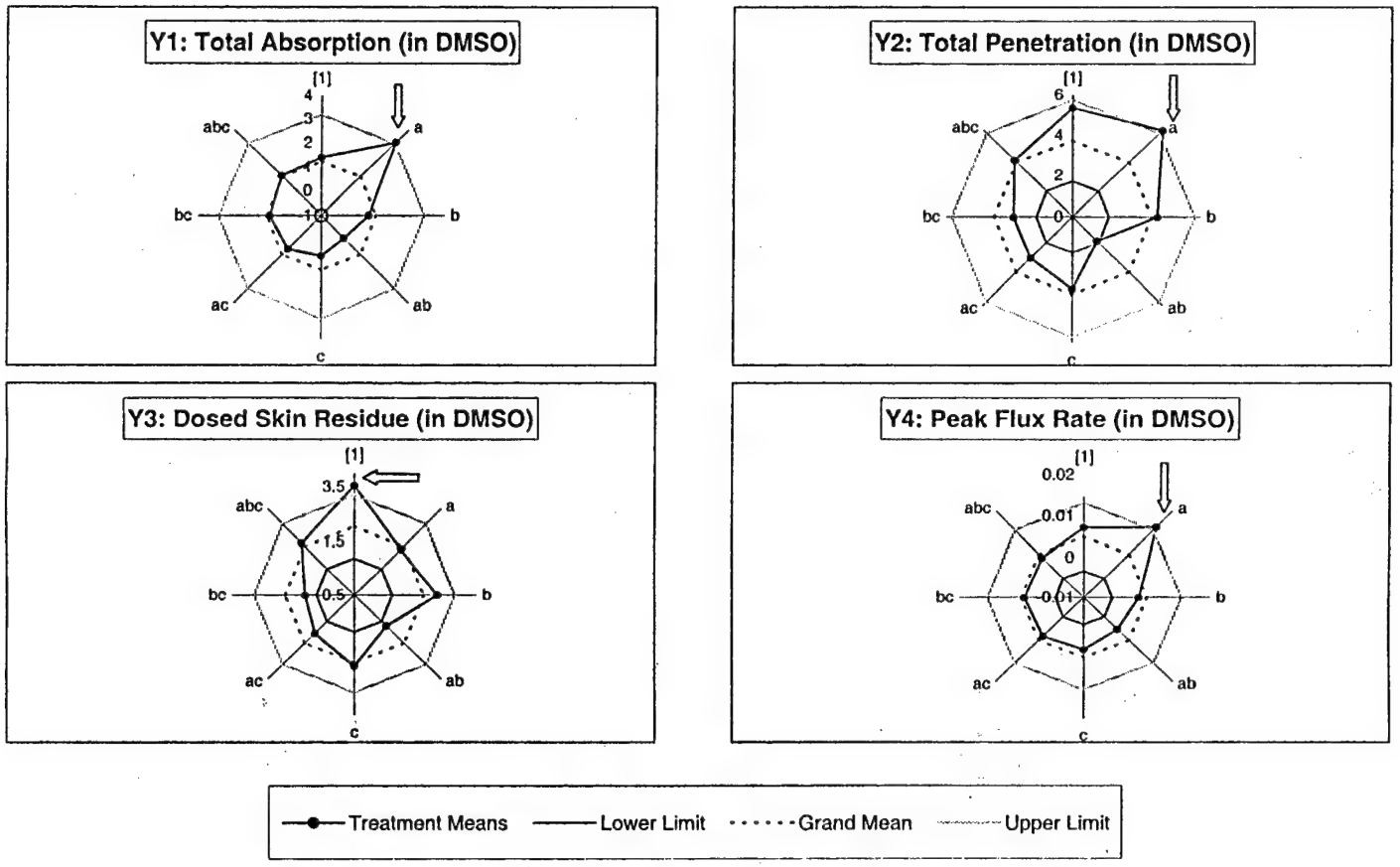

FIGURE 3. Compass plots for detecting the treatment effects in DMSO for total absorption, total penetration, dosed skin residue, and peak flux rate (Y1–Y4, respectively). There is a significant difference among treatment means in each parameter, i.e., total absorption (Y1), total penetration (Y2), and peak flux rate (Y4), at a, but dosed skin residue (Y3) at [1].

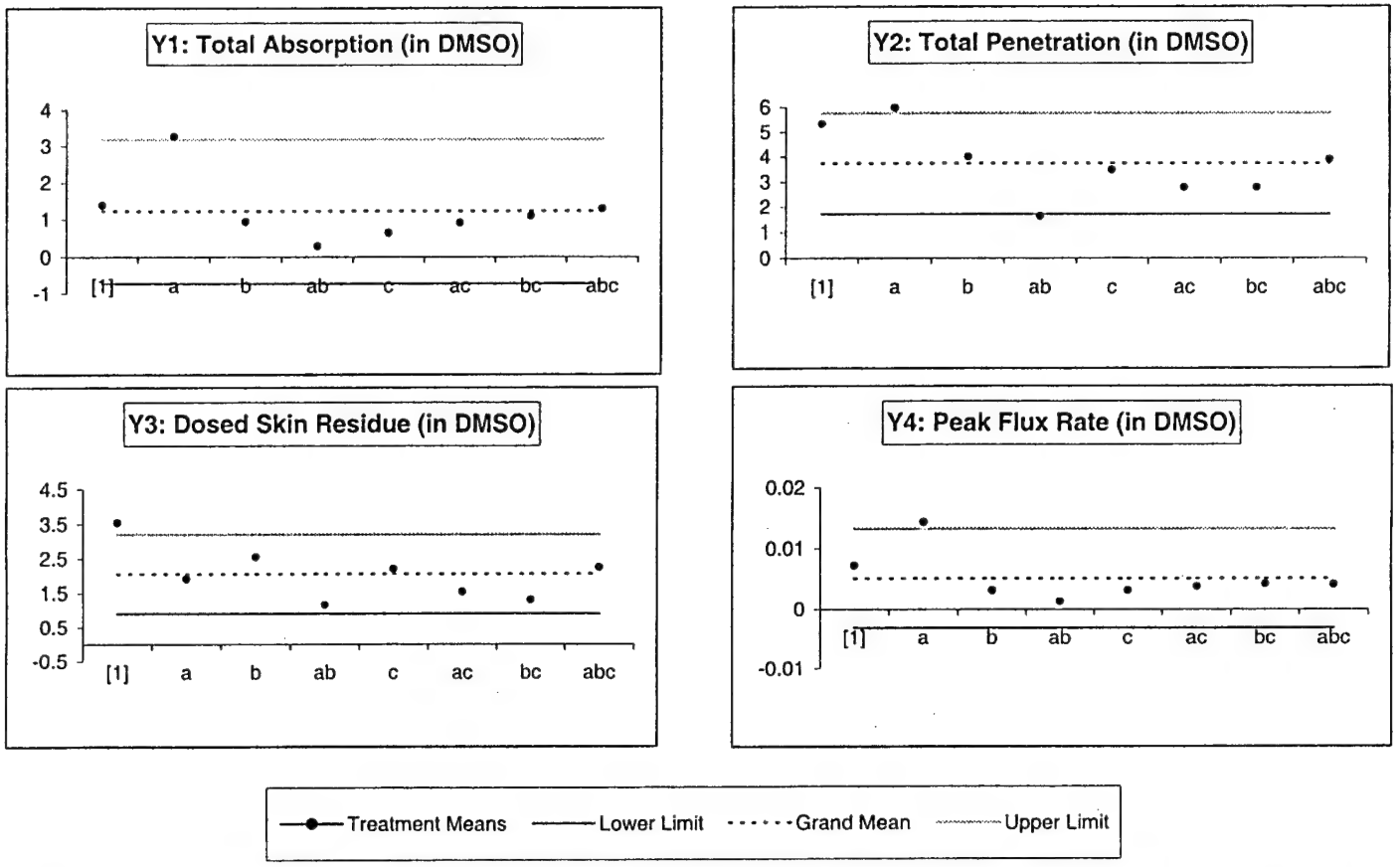

FIGURE 4. ANOM-style plots for detecting the treatment effects in DMSO for total absorption, total penetration, dosed skin residue, and peak flux rate (Y1–Y4, respectively). There is a significant difference among treatment means in each parameter, i.e., total absorption (Y1), total penetration (Y2), and peak flux rate (Y4), at a, but dosed skin residue (Y3), at [1].

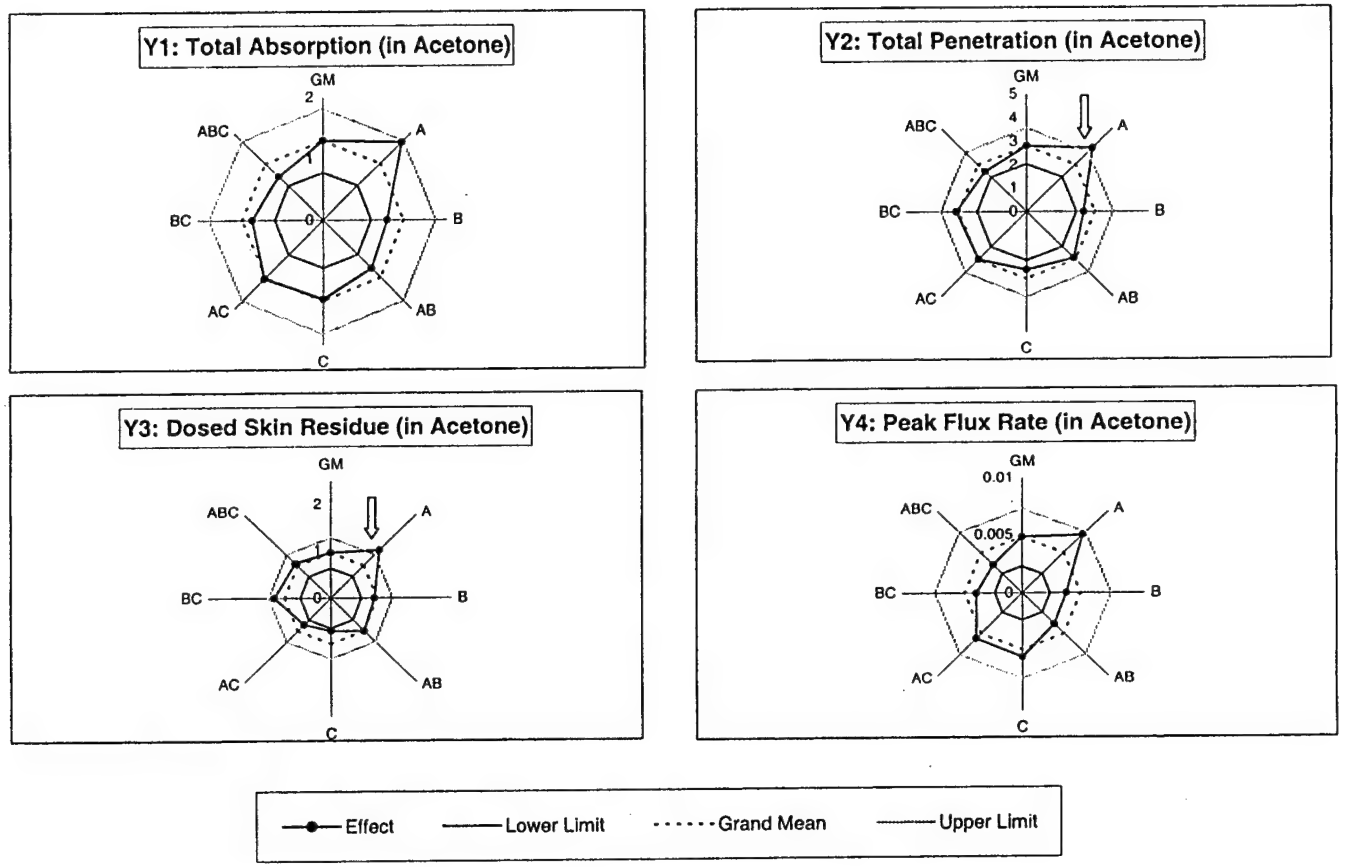

FIGURE 5. Compass plots for detecting the factor effects in acetone for total absorption, total penetration, dosed skin residue, and peak flux rate (Y1–Y4, respectively). Because no interaction effect is significant, the main effect, A, is significant in both total penetration (Y2) and dosed skin residue (Y3).

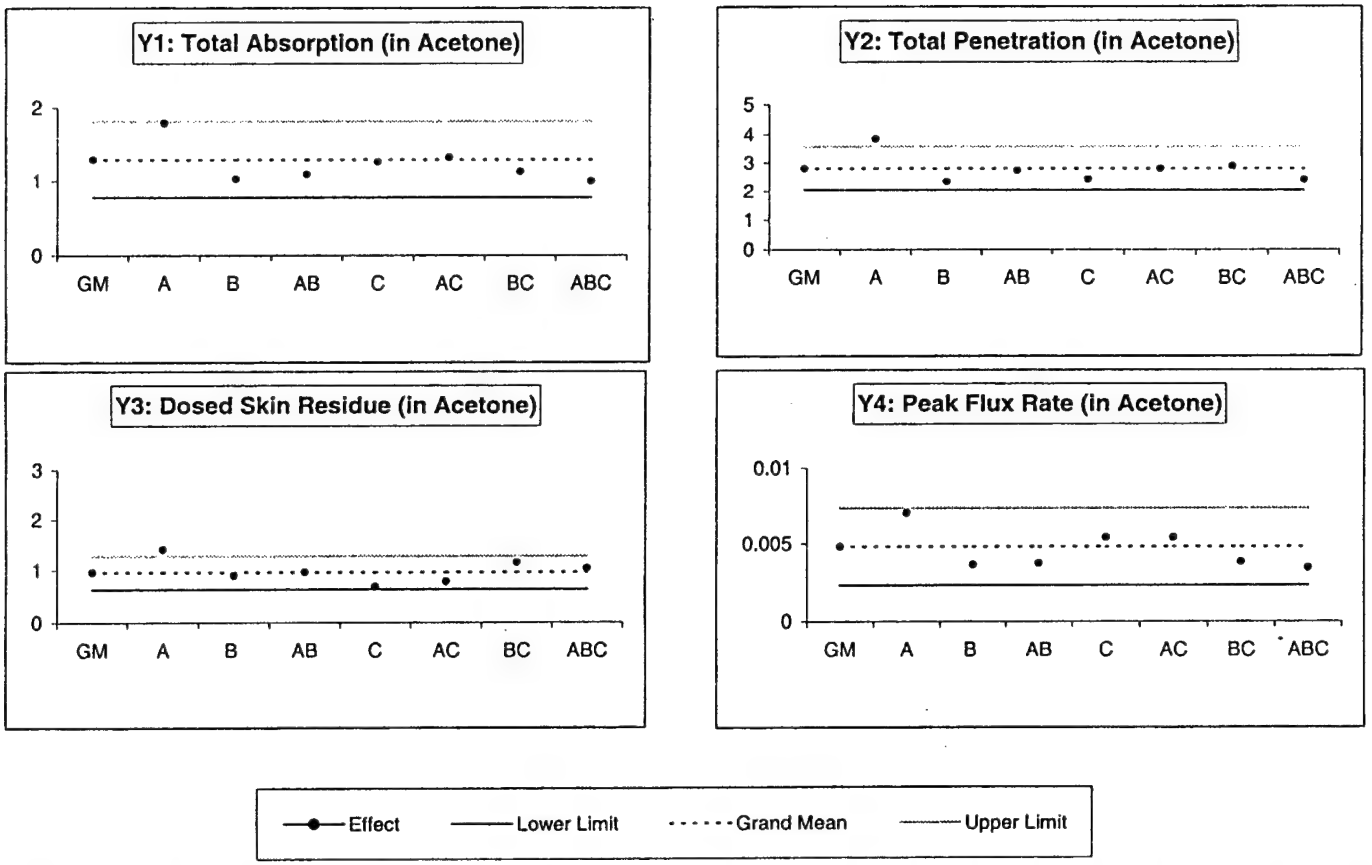

FIGURE 6. ANOM-style plots for detecting the factor effects in acetone for total absorption, total penetration, dosed skin residue, and peak flux rate (Y1–Y4, respectively). Because no interaction effect is significant, the main effect, A, is significant in both total penetration (Y2) and dosed skin residue (Y3).

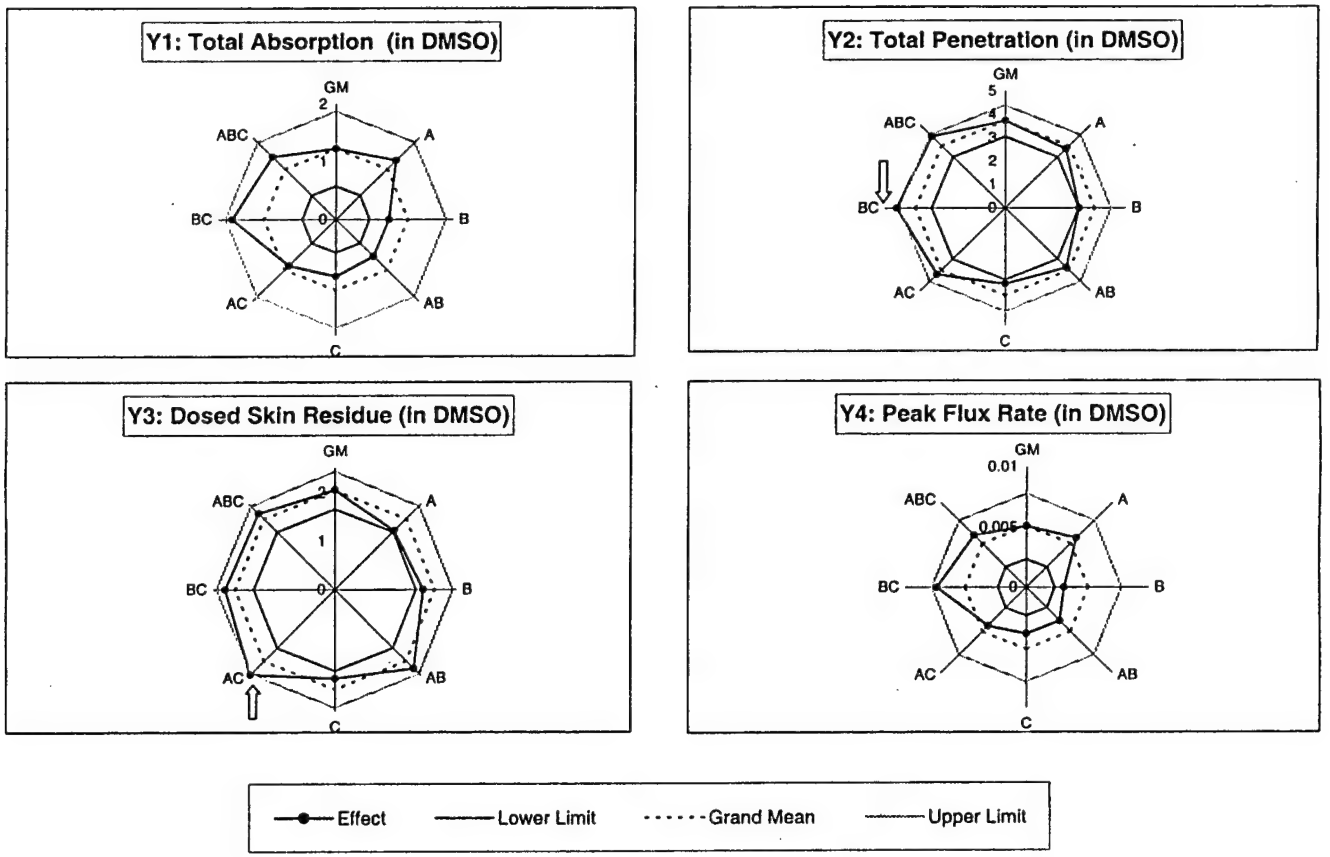

FIGURE 7. Compass plots for detecting the factor effects in DMSO for total absorption, total penetration, dosed skin residue, and peak flux rate (Y1–Y4, respectively). The interaction BC is significant in total penetration (Y2), and interaction AC is significant in dosed skin residue (Y3).

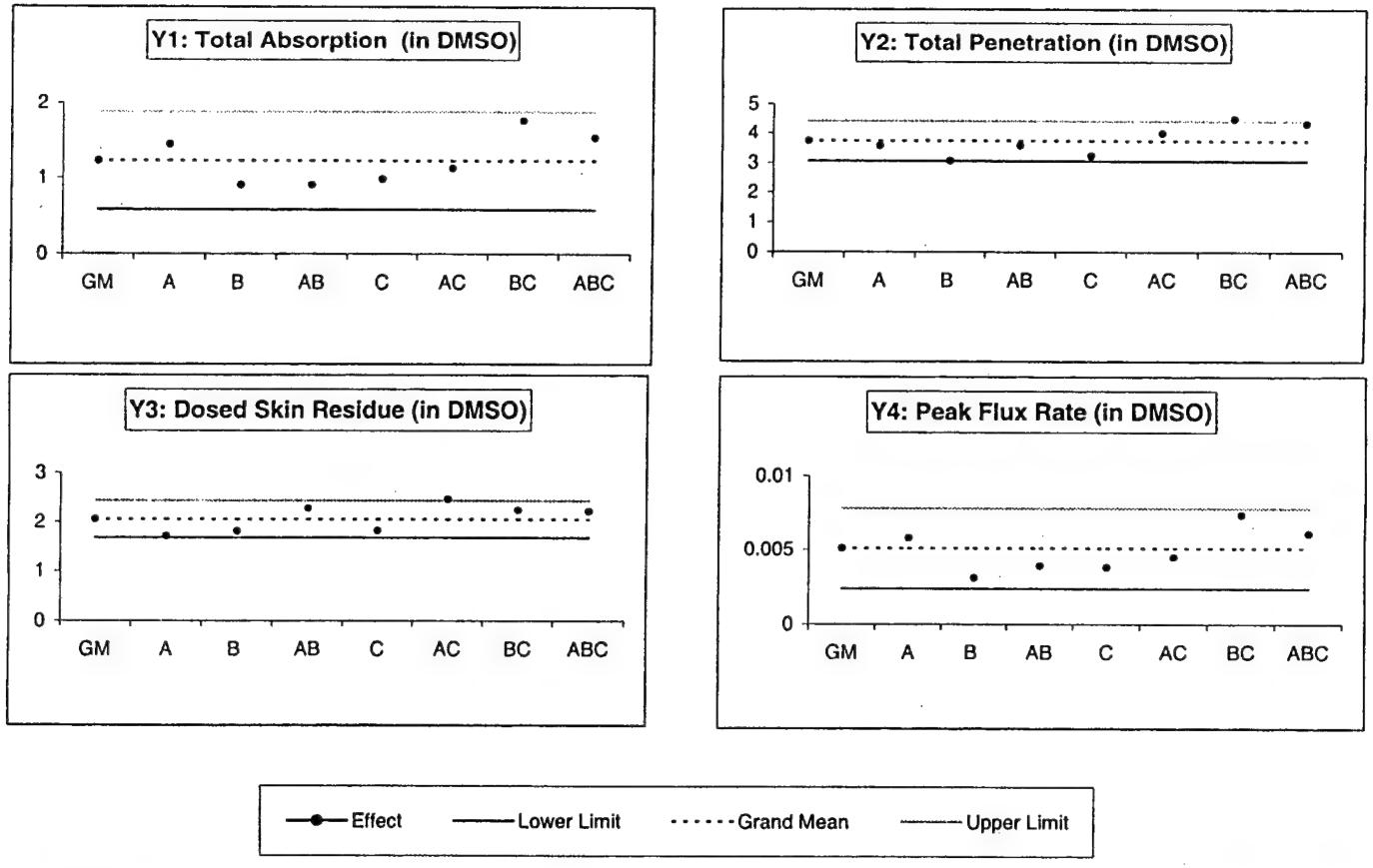

FIGURE 8. ANOM-style plots for detecting the factor effects in DMSO for total absorption, total penetration, dosed skin residue, and peak flux rate (Y1–Y4, respectively). The interaction BC is significant in total penetration (Y2), and interaction AC is significant in dosed skin residue (Y3).

For DMSO, the interaction BC is significant in total penetration (Y2), and interaction AC is significant in dosed skin residue (Y3). This implies that the main effect A is not significant in total penetration (Y2) but we cannot say anything about the significance of the main effects B and C. Similarly, the main effect B is not significant in dosed skin residue (Y3) and we cannot conclude anything about the significance of the main effects A and C.

In summary, factor A (SLS) is a significant effect for the total penetration (Y2) in acetone vehicle but not in DMSO vehicle. SLS also is a significant effect for the dosed skin residue (Y3) only in acetone vehicle. For DMSO vehicle, there is interaction between B (MNA) and C ($SnCl_2$) in total penetration (Y2) and interaction between A (SLS) and C ($SnCl_2$) in dosed skin residue (Y3). There is no evidence to show the effect of factor B (MNA) on the dosed skin residue (Y3) in both vehicles. Also, there is no evidence to show the effect of any factor on the total absorption (Y1) and the peak flux rate (Y4) in both vehicles.

CONCLUSION AND DISCUSSION

A compass plot for treatment effects is a radial plot with the magnitude of each treatment mean determining the length of the ray. The rays are ordered in accordance with the experimental design. To fix the ordering in two-level factorial experiments, we use the ordering in the Yates algorithm. Said another way, the compass plot is essentially a star plot, with the variable being the treatment mean. The unique contribution of the present work is that simultaneous confidence intervals are added to produce inner and outer polygons. A compass plot for the factor effects follows similarly, with the magnitude of each treatment mean replaced by each fitted effect plus grand mean.

Compass plots can, in fact, be regarded as ANOM-style plots in polar coordinates, where the actual magnitude of mean or effect is plotted instead of the deviation from the grand mean. It could be argued that compass plots form a more memorable set of shapes. In particular, it is easier to decide at a glance whether a spike appearing in each of two compass plots corresponds to the same variable. This would be evidence of a significant chemical interaction in a chemical mixture study. However, with ANOM plots, unless the horizontial axes are lined up, it may not be as clear which variable is spiking (Chambers, 1983).

Compass plots are a useful graphical method for displaying the significant results not only for 2^p factorial experiments but also for any other type of experiment using factorials or other designs. For factors with more than two levels, main effects at each level, including their interactions, each with 1 *df*, have to be considered. For example, a 3^2

factorial experiment yields a nonagon shape for treatment means and an octagon shape for the factor effects.

For a univariate response, two-level experiment, other alternatives to the Yates vertex ordering can be used. The shape of the plot and the effectiveness of the whole display can depend critically on this vertex assignment. Replotting the display with a different assignment might emphasize different features and relationship in the data. Vertices can be ordered by the magnitude of treatment means or effects. This will create a spiral shape—it may be compared with the seasonal cobweb plot for time series data (Toit, 1986)—and the significant groups will be in the same neighborhood. For multiresponse experiments, a fixed order such as that provided by the Yates algorithm is better for comparing the response measurements with each other.

We can extend the compass plot to include another factor such as time by stacking successive compass plots. This helps to keep track of how the response at a particular time compares to the response at other times. By letting time (or another third variable, e.g., skin layer in our example) run along the third axis, we thus can form a "compass tube." Such a representation of the compass plot is potentially useful because it gives the viewer a more global perspective of the response data over time (Hackstadt, 1995).

We have presented results for the fixed effects model, but this method can also be extended to the mixed effects model. In the mixed model, each fixed effect has a different standard error, so we have a set of inner and outer polygons for each fixed effect. For the random effects model, interest centers on the variability of the means and the grand mean. Hence, there is little motivation to compare means for the particular μ_i's in the experiment, and compass plots are not very useful in this case.

If the factorial experiment is not balanced, the inner and outer polygons will be irregular; that is, a treatment with fewer replications will have a larger confidence interval at its vertex. Heterogeneity of variances can be handled by transformations. Other choices for multiple comparisons could also be used (Neter, 1990); for example, the Scheffe method could be used instead of the Bonferroni method for treatment effect with simultaneous confidence intervals. In our plot, for significance testing we used polygonal, rather than circular, curves because polygon plots are more widely available in common software such as Microsoft Excel.

In summary, compass plots provide a graphical counterpart to ANOVA tables and mean plots. The plots tend to encourage the design of experiments and are an effective method of presenting the findings, particularly in the case of mutiple responses as seen in toxicological studies involving complex chemical mixtures.

Toxicology Methods, 10:265–281, 2000

1051-7235/00 $12.00 + .00

METHODS OF ASSESSING THE PERCUTANEOUS ABSORPTION OF VOLATILE CHEMICALS IN ISOLATED PERFUSED SKIN: STUDIES WITH CHLOROPENTAFLUOROBENZENE AND DICHLOROBENZENE

Jim E. Riviere and James D. Brooks

Center for Cutaneous Toxicology and Residue Pharmacology, North Carolina State University, Raleigh, North Carolina, USA

Guilin Qiao

Exposure Assessment Branch, Health Effects Laboratory Division, National Institute for Occupational Safety and Health, Morgantown, West Virginia, USA

The experimental determination of dermal absorption of volatile chemicals is fraught with difficulties. The isolated perfused porcine skin flap (IPPSF) is a biologically intact, perfused skin preparation that has been employed to predict dermal absorption of chemicals in humans. The purpose of this work was to explore various experimental dosing strategies for volatile chemicals using dichlorobenzene (DCB) and chloropentafluorobenzene (CPFB) as model compounds. Effects of complete occlusion and various strategies of vapor trapping, vapor dosing, and solvent effects were explored. The results suggest that dosing methodology is a major determinant of dermal absorption and could easily skew results obtained from different systems. A biologically sensitive system such as the IPPSF is particularly sensitive to the manipulations required to ensure precise dosing of these compounds. An interesting finding was that the effects of solvents on compound absorption that are routinely described in liquid dosing scenarios were also detected when both the compound and solvent were exposed during the vapor phase.

Keywords chloropentafluorobenzene, dermal absorption, dichlorobenzene, volatile chemicals

The assessment of the percutaneous absorption and penetration of volatile compounds is experimentally challenging. In many cases, chemical loss is avoided by conducting studies under conditions of occlusion to protect against loss of dose. However, this scenario often does not model

Received 4 February 2000; accepted 15 July 2000.

The authors thank the staff of the Center for Cutaneous Toxicology and Residue Pharmacology for technical support. This research was supported by United States Air Force Office of Scientific Research grants F49620 and FQ8671.

Address correspondence to Jim E. Riviere, Center for Cutaneous Toxicology and Residue Pharmacology, College of Veterinary Medicine, 4700 Hillsborough Street, North Carolina State University, Raleigh, NC 27606, USA. E-mail: Jim_Riviere@NCSU.EDU

the natural exposure conditions, and this poses problems when making risk assessment calculations. Complete occlusion of a dosing site alters absorption profiles (Chang and Riviere, 1993). The isolated perfused porcine skin flap (IPPSF) is an in vitro model system that has been utilized to model compound absorption and skin disposition (Riviere et al., 1986, 1995; Riviere and Monteiro-Riviere, 1991). This model has been validated as being predictive of in vivo human absorption for a large and diverse series of compounds (Riviere et al., 1992, 1995; Wester et al., 1998). The advantage of the system is that all the biological components of skin that could modulate percutaneous absorption (e.g., the stratum corneum barrier, epidermal metabolism, dermal vascular uptake, irritation) are functional in this perfused tissue preparation.

Risk assessment of volatile compounds is generally focused on their primary route of exposure, inhalation. As a result, there are few data available in the literature concerning dermal absorption after topical exposure, as might occur when the skin surface is exposed to a compound. Dichlorobenzene (DCB) is commercially utilized as a space deodorizer, moth repellent, and fungicide. The compound is also used as an intermediate in the synthesis of resins, organic solvents, pesticides, and dyes (ATSDR, 1993). A recent epidemiological survey suggests that 96% of the adult population in the United States has detectable levels of DCB in their blood (Hill et al., 1995). At very high doses, DCB has been associated with kidney and hepatic toxicity and is a putative carcinogen in laboratory animal studies. Its biotransformation has been investigated in the context of its role as a carcinogen (Hissink et al., 1997a, b). Chloropentafluorobenzene (CPFB) is a volatile fluorinated hydrocarbon that has been proposed to be used as a chemical warfare agent simulant because it has a very low level of toxicity, being associated only with mild skin and eye irritation in rabbits (Clewell and Jarnot, 1994). For both of these compounds, dermal penetration has not been adequately assessed in a model system predictive of human absorption.

A second variable often encountered in assessing the absorption and cutaneous toxicity of such compounds is the protocol used to dose low concentrations in laboratory animal studies. In most cases, especially when assessing low-level exposure, vehicles must be used to apply test compounds to skin. It is recognized that vehicles may alter the dermal absorption properties of chemicals so that they differ from those that occur in cases of neat application (Löf and Johanson, 1998), a phenomenon documented in IPPSF studies with phenol and paranitrophenol (Brooks and Riviere, 1996).

The purpose of this project was to develop methodologies that could be used to study volatile compound absorption in the IPPSF. Because of the peculiarities of this model (e.g., sensitivity to handling during an experiment, venous drainage open to the environment, tubular shape,

variability in size due to surgical procedure), a new dosing system was developed for the IPPSF that allowed more controlled exposure to these chemicals. The process of conducting these experiments involved (1) development of a cradle chamber to trap the evaporated compound in the area next to the skin, (2) assessment of the amount of chemical absorbed into the perfusate from the chemical that evaporated from excised skin, (3) exposure of the IPPSF to neat test compound and to test compound in a vehicle, (4) assessment of the amount of test compound in the perfusate as a result of exposure to the volatile compound vapor, and (5) development of a dosing dome that allowed dosing a vapor to skin without vapor uptake directly into the perfusate. Model compounds for these experiments were CPFB and DCB, dosed neat and in vehicles.

MATERIALS AND METHODS

Experiment Scenarios

A number of experimental scenarios were set up to investigate the effects of different dosing strategies on compound absorption in the IPPSF. Table 1 lists the experiment scenarios studied. Compounds were applied neat or in varying concentrations in vehicles, generally using $n = 4$ replicates per treatment condition. Ethanol was the vehicle for DCB experiments; however, it was necessary to use acetone in the CPFB experiments because of analytical interference resulting from the fact that the elution times of ethanol and CPFB are similar during gas chromatography (GC) analysis. In scenario A, compound was dosed on IPPSFs perfused in open chambers. In scenario B, compound was dosed on the IPPSF and the entire dosing site was immediately occluded with

TABLE 1. Experimental Scenarios Investigated

Protocol number	Compound	Exposure conditions	Dose	Vehicle	*n*
A	CPFB	Nonoccluded	20 μL liquid	Neat	4
B	CPFB	Occluded patch	20 μL liquid	Neat	4
C	CPFB	Cradle chamber	20 μL liquid	Neat	4
D	CPFB	Cradle chamber (excised skin)	20 μL liquid	Neat	4
E	CPFB	Cradle chamber	20 μL liquid	Neat	6
F	CPFB	Cradle chamber	2 μL liquid	Neat	4
G	CPFB	Cradle chamber	2 μL liquid	8 μL acetone	4
H	CPFB	Cradle chamber	10 μL liquid	10 μL acetone	4
I	DCB	Cradle chamber	20 μL liquid	Neat	4
J	CPFB	Dosing dome	20 μL vapor	Neat	7
K	DCB	Dosing dome	20 μL vapor	Neat	4
L	DCB	Dosing dome	50 μL vapor	Neat	4
M	DCB	Dosing dome	10 μL vapor	10 μL ethanol	3
N	DCB	Dosing dome	20 μL vapor	20 μL ethanol	2

cellophane tape. In C, compound was dosed using the cradle chamber as described later. In D, compound was dosed onto excised, nonperfused skin in a cradle chamber, with perfusate flowing through the chamber in order to assess evaporation into perfusate. Treatments E, F, G, and H compared CPFB absorption in the cradle chamber at two doses and coadministered in acetone vehicles. Treatment I assessed DCB absorption in the cradle chamber. Treatments J, K, L, M, and N utilized the dosing dome described later and assessed neat CPFB and DCB at two doses in ethanol vehicles.

Isolated Perfused Porcine Skin Flap

The routine two-stage surgical procedure was used to create IPPSFs (Riviere et al., 1986). The flap was then transferred to a temperature- and humidity-regulated perfusion system. In the chamber, the perfusion flow rate, pH, temperature, and relative humidity were maintained at a perfusation flow rate of 1 mL/min/flap (3–7 mL/min/100 g tissue), a pH of 7.4, a temperature of 37°C, and a relative humidity of 60 to 80% in a nonrecirculating perfusion configuration. Flow rate and perfusion pressure (arterial, 30–70 mmHg) were recorded every 30 min during experiments. The perfusion medium was a Krebs-Ringer bicarbonate buffer (pH 7.4, 350 mOsm/kg) containing albumin (45 g/L) and glucose (80–120 mg/dL).

Figure 1A depicts the configuration of the cradle chamber, which allowed the volatile compound to evaporate and be trapped in an environment around the skin flap. A 1 × 3-cm dosing area was drawn on the surface of the skin flap. The maximum dose that could be applied to this area was 20 μL. The cradle chamber was then secured in place with a parafilm gasket. The cannula end of the cradle was sealed to minimize evaporation from the cradle chamber. The skin flap was dosed via the slit in the top of the cradle chamber, and the slit was immediately covered with tape. Vapor samples (0.5 mL) were taken from this slit via a 25-gauge needle through the tape, and the hole in the tape was sealed with tape immediately after sampling. Care was taken at every step to minimize loss of the vapor of the test compound. Perfusate entered the arterial supply via the cannula and the venous drainage was collected in a funnel built into the floor of the cradle because cannulation of the draining veins is not feasible in routine studies. This configuration could result in exposure of perfusate to dosed vapor, so nonperfused skin wrapped on a tubular stint was exposed to compound and air, and perfusate samples were monitored over time. These data suggested that this configuration would require a normalization procedure for accurate assessment of skin penetration.

Figure 1B depicts the second approach, which utilized a glass dosing dome that restricted vapor contact to dosed skin. This eliminated the

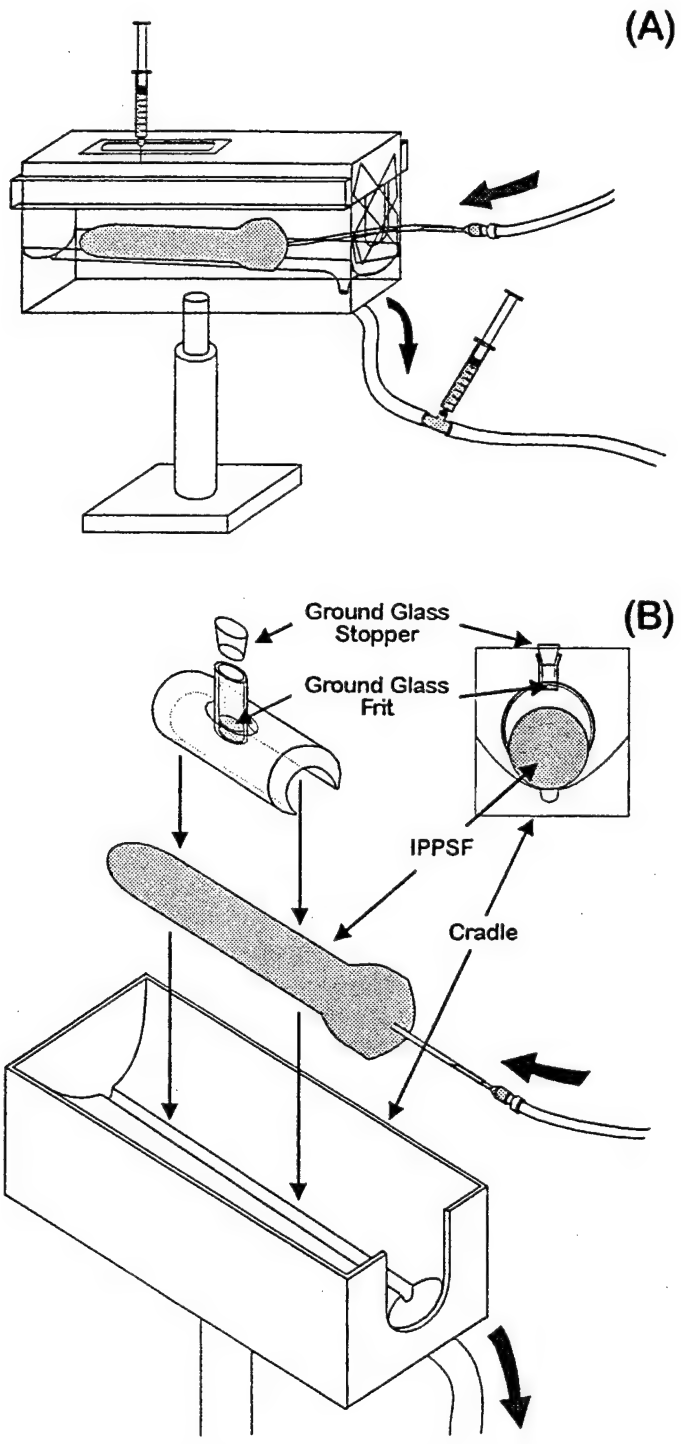

FIGURE 1. Dosing chambers assessed on IPPSFs. A. Cradle chamber dosing allows a volatile chemical to evaporate from the dosing site and be trapped in the environment around the skin flap. B. The glass dosing dome exposes a defined skin surface area to volatilized compound that is applied at the ground glass frit.

need to normalize perfusate concentrations for vapor contact. Several sizes of glass dosing domes have been developed to accommodate various skin flap sizes. (Although care is taken to produce skin flaps that are the same length and diameter, differences in donor pigs and surgical procedures make it impossible to produce absolutely uniform-sized skin flaps.) The glass dosing dome was placed over the skin flap, and the snugness of the fit held the dome in place without overly constricting the flap, which would produce perfusion problems. The ground-glass stopper was removed from the glass dosing dome, and the dose of the volatile test compound was applied to the porous ground-glass frit at the base of the central tube. The glass stopper was replaced immediately after the dose was pipetted. The test compound then volatilized to fill the dome with test compound vapor. Because the glass dosing dome eliminated direct contact between the vapor and the perfusate, the test compound that appeared in the perfusate resulted solely from absorption through the skin.

At termination, several samples were taken for mass balance of the test compounds. The surface of the dosed area was swabbed twice with gauze moistened with a 1% soap solution followed by 12 stratum corneum tape strips. The entire dosed area was removed. A 1 cm × 1 cm core of the dose area was removed and frozen for subsequent studies of depth of penetration. The remaining dosed area was extracted using the appropriate solvent and analyzed for test compound. A sample of the fat under the dosed area and a 1 cm × 1 cm-area of nondosed skin were extracted and analyzed.

Gas Chromatography

Sample analysis was made by means of gas chromatography using a Hewlett Packard 5890 II gas chromatograph and an external standard method. DCB samples were extracted from perfusate and tissues using iso-octane, and CPFB samples using hexane. Air samples were directly injected. An Alltech Capillary Column (SE-30 15 M × 0.53 mm) (Alltech Assoc., Inc., Deerfield, IL) with a column flow rate of 10 mL/min was used; it produced a total flow (column + auxillary) of 50 mL/min. The carrier was 95% argon and 5% methane. The oven temperature was 70°C, the injector temperature 180°C, and the electron capture detector temperature 380°C. Peaks were quantitated using the external standard area method and linear calibration curves for air, perfusate, and tissue samples.

All data are expressed as mean ± SEM.

RESULTS AND DISCUSSION

Figure 2A illustrates the mean CPFB perfusate values over time when IPPSFs were dosed and not occluded (scenario A), placed under an occlusive dressing (scenario B), and placed in the cradle chamber (scenario C) (Table 1). Figure 2B depicts the mean CPFB vapor concentrations

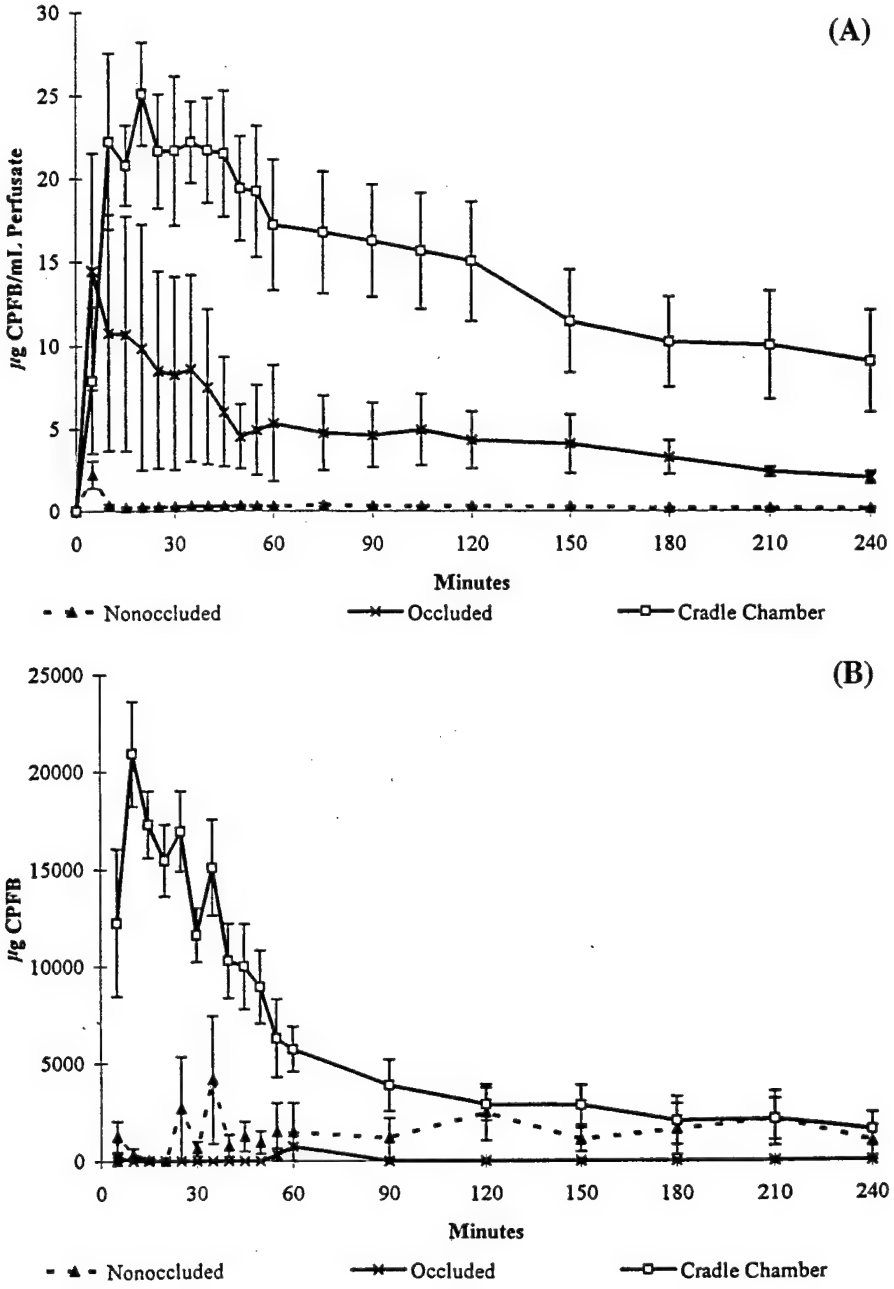

FIGURE 2. CPFB absorption into IPPSF perfusate after dosing in nonoccluded and occluded environments and in the cradle chamber. A. The absorbed dose is expressed as a concentration in perfusate. B. Total mass absorbed from the vapor. Mean ± SEM.

simultaneously collected for the same experiments. Vapor samples were taken from the area over the IPPSF in the nonocluded and occluded systems and from the sampling port in the cradle chamber studies.

A number of observations can be made based on this first series of exposures. The perfusate data demonstrate that only trace amounts of CPFB were absorbed from a totally nonoccluded system (62.4 ± 11.4 μg). CPFB could be detected in the air sampled from the IPPSF chamber despite its relatively large volume (approximately 1 cu. yd). In contrast, occluded dosing produced a rapid increase in perfusate levels and a larger total absorption (1070 ± 477 μg). The lack of continuously detectable CPFB in the vapor samples under occluded dosing supports the efficiency of the occlusion process. The surprising data, which prompted many of the studies in this manuscript, were the high levels of absorption seen when CPFB was dosed in the cradle chamber (2892 ± 620 μg). However, this was accompanied by high vapor concentrations in the cradle chamber. Theoretically, dosing with the use of a completely occlusive dressing should produce maximal absorption. The higher absorption seen in the cradle chamber prompted the hypothesis that absorption was occurring by two routes, through skin at the dosing site and into perfusate from the chamber environment as it exited the flap and collected in the drainage funnel. This exposure of perfusate to exposed vapor was a major limitation of the system and prompted remaining studies to investigate how such data could be handled.

To assess this possibility, in scenario D, CPFB was dosed onto an excised piece of dermatomed pig skin (500 μm thick) applied over a glass cylinder to reproduce the geometry of the IPPSF. This skin was not perfused, so any CPFB appearing in the perfusate must have been secondary to absorption from the cradle chamber environment. In this exposure scenario, total absorption into the perfusate was 1114 ± 349 μg, a value approximately 40% that seen when a perfused IPPSF was dosed. The difference (1778 μg) approached the value seen under occluded dosing.

These observations prompted a second series of studies, scenarios E though H, in which CPFB was dosed using cradle chambers while perfusate and cradle chamber while concentrations were simultaneously monitored. In these studies, additional care was taken to avoid compound loss due to leakage and evaporation from samples. Figure 3A illustrates the mean vapor levels of CPFB inside the cradle chamber over time for four different dosing protocols. Figure 3B illustrates the mean CPFB values in the perfusate. Figure 3C depicts the ratio of CPFB in perfusate divided by CPFB in vapor. A clear plateau in this ratio occurred within 10 min. The following computational approach was then utilized to generate the corrected perfusate absorption profiles depicted in Figure 3D:

1. Determine μg/mL concentrations in vapor and perfusate samples.
2. Determine ratio [Perfusate(μg/mL)]/[Vapor(μg/mL)].

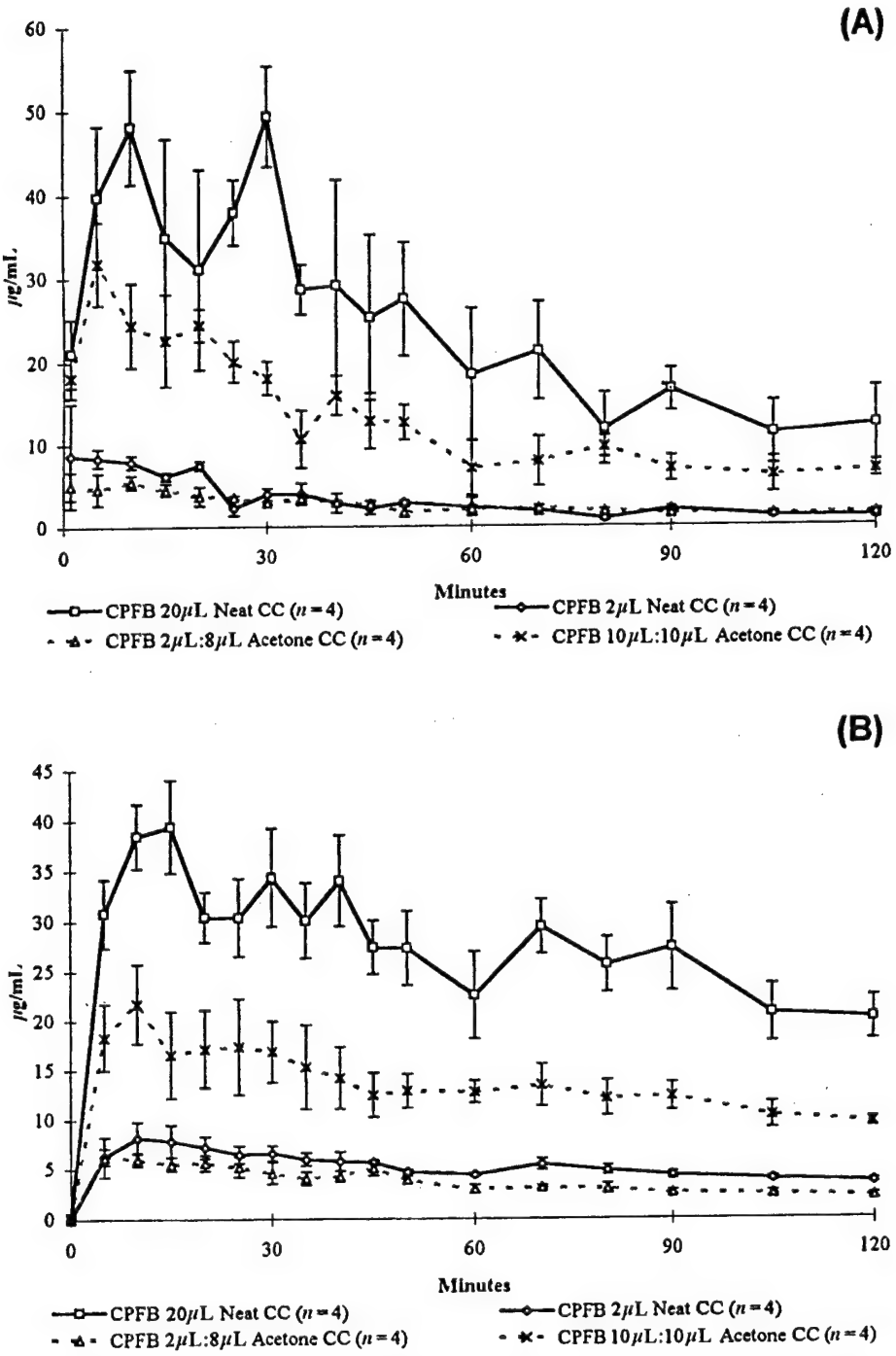

FIGURE 3. Percutaneous absorption of CPFB dosed according to four treatments: 20 μL neat; 2 μL neat; 10 μL CPFB and 10 μL acetone; 2 μL CPFB and 8 μL acetone. A. Concentration in cradle chamber atmosphere. B. Concentration in IPPSF perfusate. *(Continued)*

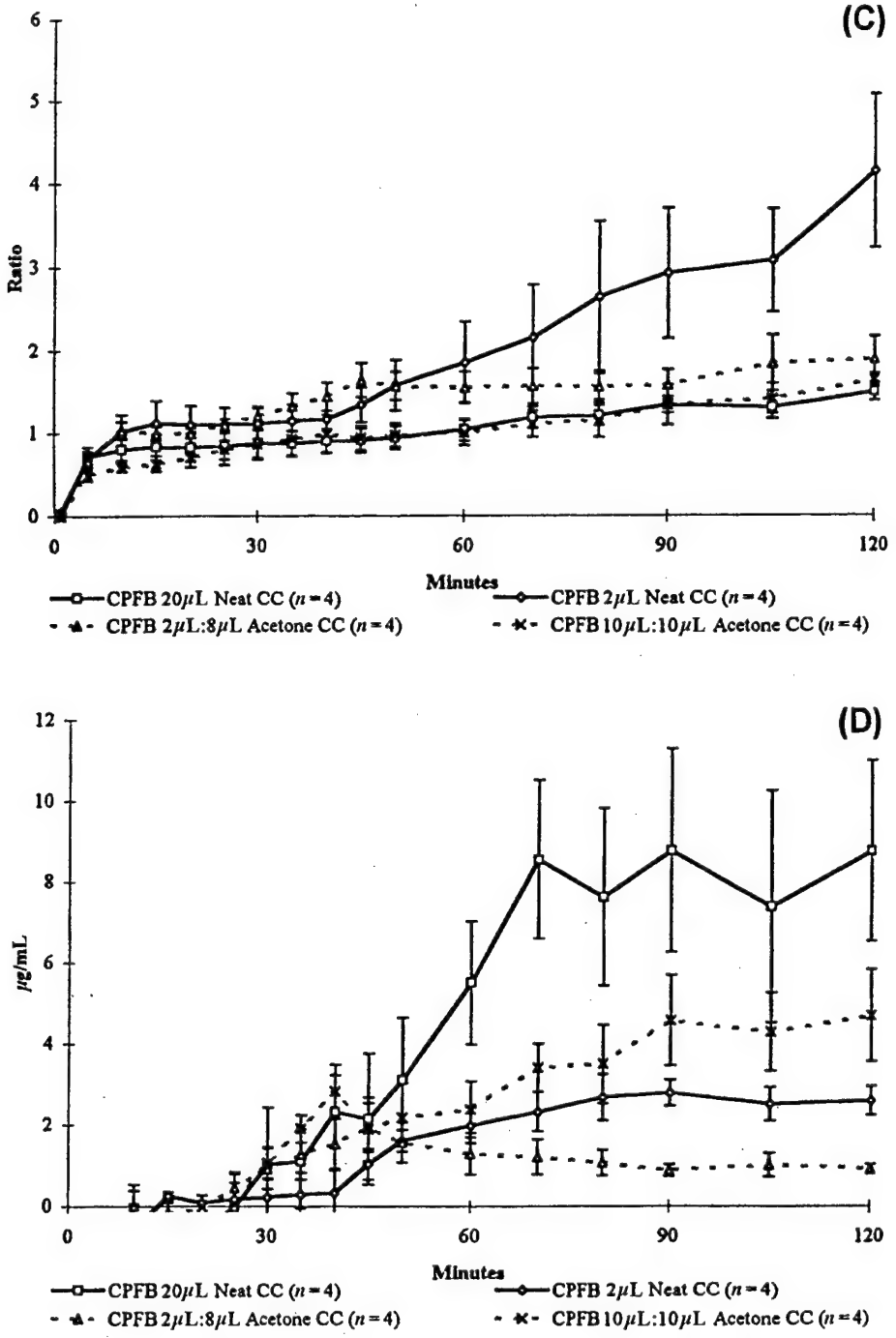

FIGURE 3. (Continued) C. Ratio of CPFB in perfusate to vapor. D. Corrected perfusate concentrations using equation. CC, cradle chamber.

TABLE 2. Percutaneous Absorption of CPFB Liquid Dosed Using Cradle Chambers

	Actual dose	Total absorption into perfusate		Absorption into perfusate from air		Corrected dermal absorption	
Treatment	(μg)	(μg)	(%D)	(μg/mL)	(%D/mL)	(μg)	(%D)
20 μL neat	31,360	3634^{a} (514)	$12^{b,c}$ (2)	700^{a} (121)	2.2[a] (0.14)	2934^{a}	0.81^{a}
10 μL CPFB/ 10 μL acetone	15,680	1857^{b} (287)	$12^{b,c}$ (2)	$409^{b,c}$ (46)	2.6[a] (0.3)	1448^{b}	0.78^{a}
2 μL neat	3136	664^{c} (49)	21^{a} 2	86^{d} (7)	2.7[a] (0.2)	578^{c}	0.18^{b}
2 μL CPFB/ 8 μL acetone	3136	482^{c} (69)	15^{b} (2)	81^{d} (8)	2.6[a] (0.2)	401^{c}	0.13^{b}

Note. Values are mean (SEM). D, dose.
[a,b,c,d]Data with superscripts are compared within columns. Values with the same letter are not significantly different.

3. Determine first plateau of ratios = ratio*.
4. Determine corrected [perfusate] using the following equations:

$$\text{Ratio}^* = [\text{perfusate}]/[\text{vapor}]$$

$$[\text{Perfusate}] = (\text{ratio}^* \times [\text{vapor}])$$

$$\text{Corrected } [\text{perfusate}_{0-120}] = [\text{original perfusate}_{0-120}] - (\text{ratio}^* \times [\text{vapor}_{0-120}])$$

The corrected absorption parameters are listed in Table 2. An insignificant fraction of the applied dose was recovered in any of the stratum corneum tape strips, dosed skin, or fat samples collected. The absorption of CPFB from the cradle chamber into the perfusate was relatively constant across all scenarios (approximately 2.5%). The rank order of absorption was 20 μL neat CPFB >10 μL CPFB in 10 μL acetone >2 μL neat CPFB >2 μL CPFB in 8 μL acetone. As can be seen by comparing absorption with percentage of applied dose, absorption efficiency decreased with higher doses. Dosing in an acetone vehicle reduced the absorption of the lower dose.

In contrast to the highly volatile CPFB, DCB absorption profiles (Figures 4A through D) using this exposure scenario (I) had a minimal vapor effect, and any correction did not significantly alter the absorption profile. Total perfusate absorption was 616 $\pm$ 31 μg. Concentrations were detectable in tissue samples but were uniformly less than 5% of perfusate absorption at the end of an experiment. It is to be noted that in contrast to CPFB, absorption did not plateau with DCB.

There was a great deal of variability in these studies, partially attributable to the difficulty of achieving a constant dosing surface area.

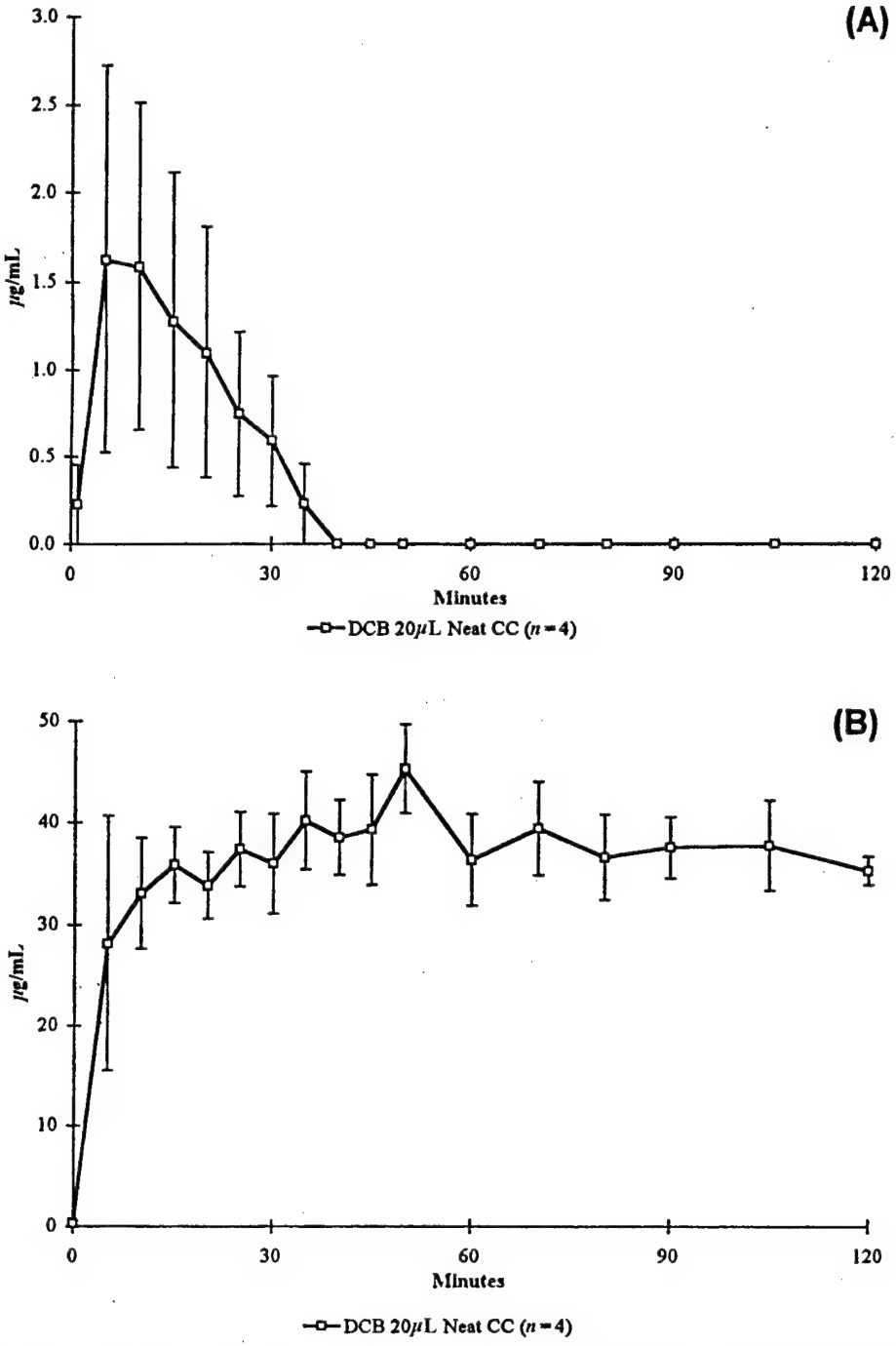

FIGURE 4. Percutaneous absorption of DCB by IPPSF. A. Concentration in cradle chamber atmosphere . B. Concentration in perfusate. *(Continued)*

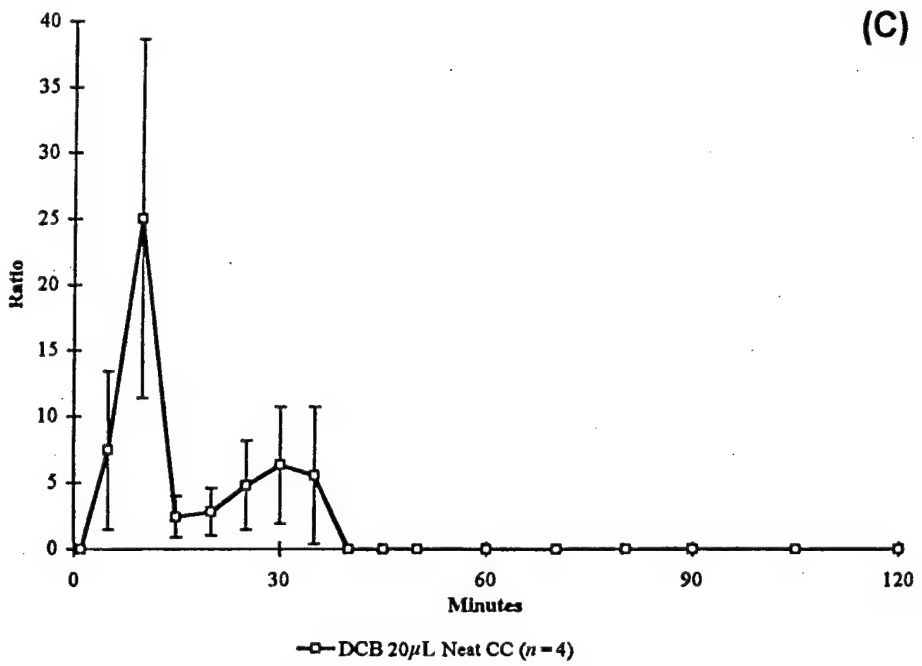

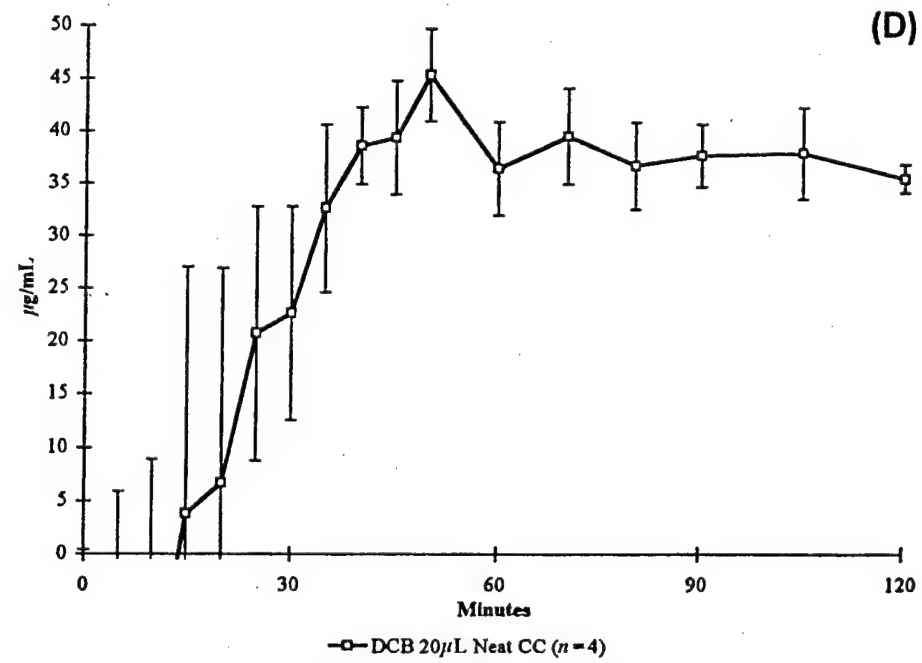

FIGURE 4. (Continued) C. Ratio of DCB in perfusate to vapor. D. Corrected perfusate concentrations using equation. CC, cradle chamber.

DCB beaded on the skin surface, making it impossible to achieve uniform dosing. Even with CPFB, the cylindrical geometry of the IPPSF promoted run-off onto dosing templates.

To address these concerns, the glass dosing dome was utilized. In these cases, neat compound never touched the skin surface; instead, vapor from the applied dose uniformly exposed the skin under the dome. Figures 5A and 6A illustrate the absorption of CPFB (scenario J) and DCB (scenarios K, L, M, and N), respectively, through the skin flap from the glass dosing dome. Figures 5B and 6B compare the dosing dome profiles to the corrected cradle chamber profiles previously presented. The glass dosing dome traps the vapor next to the skin flap, so there is no vapor in contact with the perfusate in the cradle. Notice in Figure 6A that there has been no depletion of the DCB dose, as no defined peak has been demonstrated. This is in contrast to the liquid dosing scenarios in which

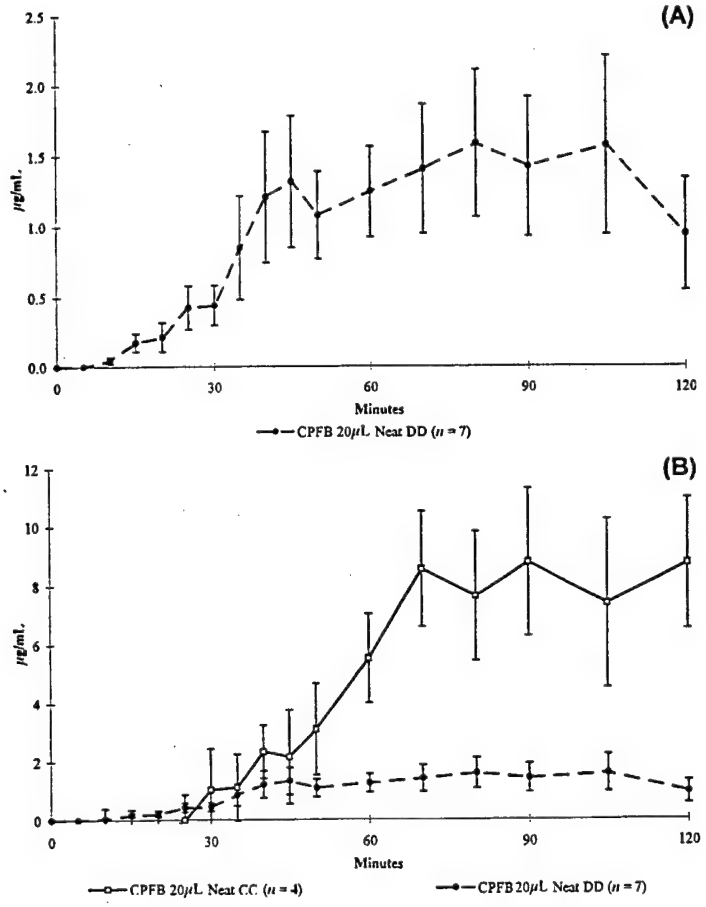

FIGURE 5. A. Percutaneous absorption of neat CPFB dosed in dosing dome. B. Comparison with corrected cradle chamber absorption. DD, dosing dome; CC, cradle chamber.

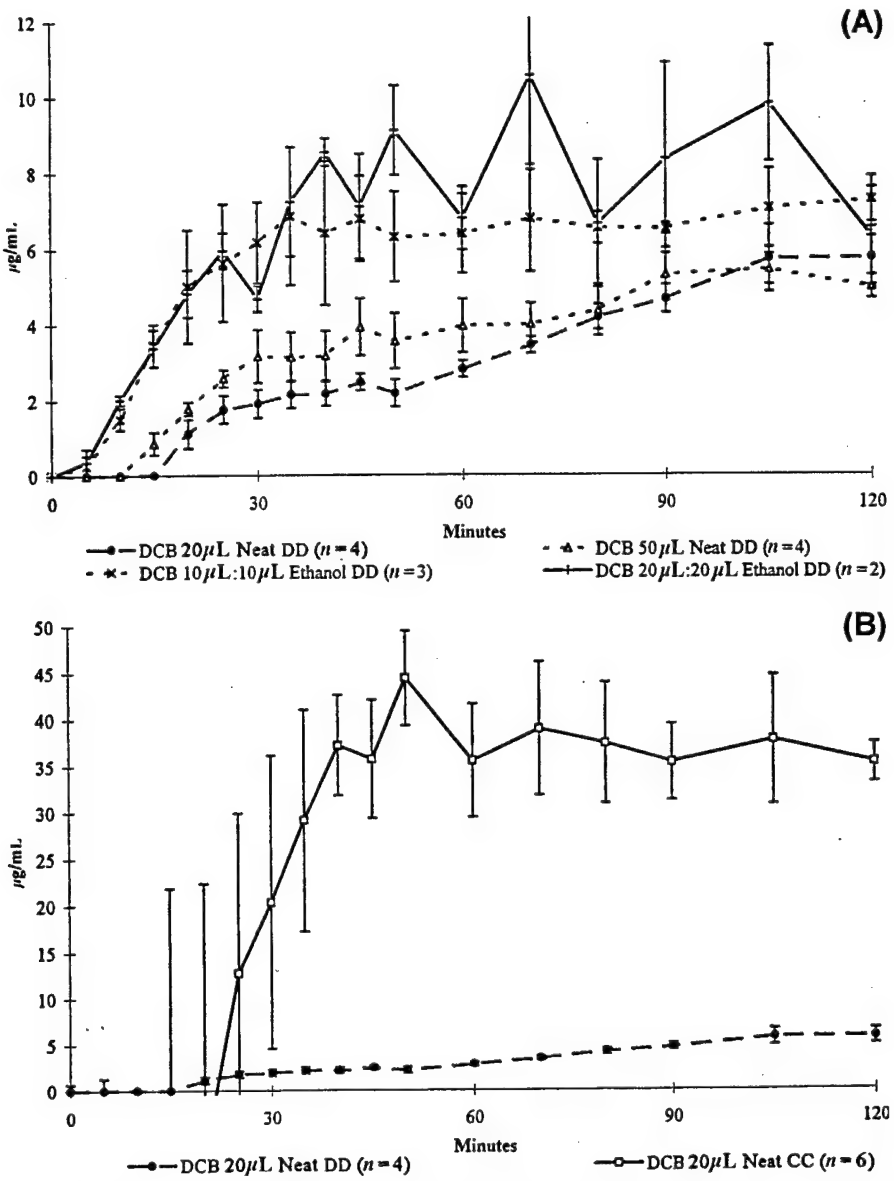

FIGURE 6. A. Percutaneous absorption of DCB dosed according to four treatments: 20 μL neat; 50 μL neat; 10 μL DCB and 10 μL ethanol; 20 μL DCB and 20 μL ethanol. B. Comparison of absorption of 20 μL neat DCB in dosing dome and in corrected cradle chamber. DD, dosing dome; CC, cradle chamber.

evaporation of applied dose depletes available compound for absorption. It is important to note that for both compounds, higher absorption is seen with the liquid cradle chamber dosing than with the vapor dosing dome.

Figure 6A and B depicts the absorption profiles seen with dosing scenarios K (20 μL neat), L (50 μL neat), M (10 μL vapor/10 μL ethanol), and

N (20 μL vapor/20 μL ethanol). With DCB, there is very little dose effect suggesting saturation of absorption. In contrast, dosing with ethanol significantly increased absorption across both doses, suggesting an enhanced permeability of skin in the presence of ethanol vapor.

CONCLUSION

These studies clearly illustrate the complexities involved in assessing the absorption of volatile chemicals across skin. The problems are magnified in a model system such as the IPPSF which imposes restrictions on the type of dosing devices that can be applied to the skin without causing adverse biological effects such as vascular constriction. The initial approach of using the cradle chamber results in absorption data that is confounded by vapor absorption into perfusate. Correction for this effect is possible and reduces some variability; however, it eliminates early time points that may be important for some types of mathematical modeling.

The dosing dome is a simpler approach to this problem, but it allows the assessing of absorption from the vapor phase only. The downside of this technique of experimentation is that a number of domes must be fabricated to fit the different sizes of IPPSFs that are produced from the surgical procedure.

The focus of this work was to compare various dosing methodologies suitable for the IPPSF, not to focus on the mechanism of percutaneous absorption or on its quantification. However, some observations are worth summarizing. As seen with both CPFB and DCB, saturation of absorption is seen when high and low doses are compared. When expressed as percent dose absorbed, the lower doses had higher fractional absorptions. This observation, also seen with many other compounds, must be taken into consideration when such experimental data are utilized in risk assessment calculations. Second, absorption from liquid is not directly comparable with absorption during a vapor phase. Part of this effect could be secondary to the physical chemistry of diffusion, where the driving force in a liquid application is the concentration on the skin surface versus the partial pressure of the compound while it is in a vapor state.

Finally, simultaneous dosing with a vehicle may modulate the absorption profile seen. In the case of DCB in ethanol, higher absorption was seen at both doses when compared to neat DCB application. This confirms the previously alluded to effects of application vehicle (Brooks and Riviere, 1996; Löf and Johanson, 1998). However, all previous studies were done using liquid dosing; thus, this finding is significant because vapor/vapor exposure also results in modulation of absorption.

The mechanism behind vehicle effects is often suggested to be secondary to formulation factors such as solubility in the vehicle and partitioning of the vehicle between the skin surface and the stratum corneum. Finding a vehicle effect when both compounds are in the vapor phase is significant because solution interactions are not present. This suggests that the mechanism is more likely to be secondary to direct interaction of the vehicle with stratum corneum lipids, which results in altered permeability for the penetrating chemical. This observation is important when the absorption of complex mixtures routinely encountered in occupational and environmental exposures is being assessed.

REFERENCES

Agency for Toxic Substances and Disease Registry. 1993. Toxicological Profile for 1,4-dichlorobenzene TP-92/10. Atlanta: U.S. Public Health Service.

Brooks, J. D., and Riviere, J. E. 1996. Quantitative percutaneous absorption and cutaneous distribution of binary mixtures of phenol and *p*-nitrophenol in the IPPSF. *Fundam. Appl. Toxicol.* 32:233–243.

Chang, S. K., and Riviere, J. E. 1993. Effect of humidity and occlusion on the percutaneous absorption of parathion in vitro. *Pharm. Res.* 10:152–155.

Clewell, H. J., and Jarnot, B. M. 1994. Incorporation of pharmacokinetics in noncancer risk assessment: Example with chloropentafluorobenzene. *Risk Anal.* 14:265–276.

Hill, R. H., Ashley, D. L., Head, S. L., Needham, L. L., and Pirkle, J. L. 1995. *p*-Dichlorobenzene exposure among 1000 adults in the United States. *Arch. Environ. Health* 50:277–280.

Hissink, A. M., Oudshoorn, M. J., Van Ommen, B., and Van Bladeren, P. J. 1997a. Species and strain differences in the hepatic cytochrome P450-mediated biotransformation of 1,4-dichlorobenzene. *Toxicol. Appl. Pharmacol.* 145:1–9.

Hissink, A. M., Van Ommen, B., Krüse, J., and Van Bladeren, P. J. 1997b. A physiologically based pharmacokinetic (PB-PK) model for 1,2-dichlorobenzene linked to two possible parameters of toxicity. *Toxicol. Appl. Pharmacol.* 145:301–310.

Löf, A., and Johanson, G. 1998. Toxicokinetics of organic solvents: A review of modifying factors. *Crit. Rev. Toxicol.* 28:571–650.

Riviere, J. E., Bowman, K. F., Monteiro-Riviere, N. A., Carver, M. P., and Dix, L. P. 1986. The isolated perfused porcine skin flap (IPPSF). I. A novel in vitro model for percutaneous absorption and cutaneous toxicology studies. *Fundam. Appl. Toxicol.* 7:444–453.

Riviere, J. E., Monteiro-Riviere, N. A., and Williams, P. L. 1995. Isolated perfused porcine skin flap as an in vitro model for predicting transdermal pharmacokinetics. *Eur. J. Pharm. Biopharm.* 41:152–162.

Riviere, J. E., and Monteiro-Riviere, N. A. 1991. The isolated perfused porcine skin flap as an in vitro model for percutaneous absorption and cutaneous toxicology. *Crit. Rev. Toxicol.* 21:329–344.

Riviere, J. E., Williams, P. L., Hillman, R., and Mishky, L. 1992. Quantitative prediction of transdermal iontophoretic delivery of arbutamine in humans using the in vitro isolated perfused porcine skin flap (IPPSF). *J. Pharm. Sci.* 81:504–507.

Wester, R. C., Melendres, J., Sedik, L., Maibach, H. I., and Riviere, J. E. 1998. Percutaneous absorption of salicylic acid, theophylline, 2,4-dimethylamine, diethyl hexylphthalic acid and *p*-aminobenzoic acid in the isolated perfused porcine skin flap compared to man. *Toxicol. Appl. Pharmacol.* 151:159–165.

Toxicology and Industrial Health (2001) 16, 1–13

www.arnoldpublishers.com/journals

Membrane transport of naphthalene and dodecane in jet fuel mixtures

RONALD E. BAYNES, JAMES D. BROOKS AND JIM E. RIVIERE

Center for Cutaneous Toxicology and Residue Pharmacology (CCTRP), Department of Food Animal Health and Resource Management, College of Veterinary Medicine, North Carolina State University, Raleigh, North Carolina 27606

Jet fuels are formulated with numerous aliphatic and aromatic components that are thought to cause dermal irritation in air force personnel. However, diffusion of these components in such a complex mixture is not well understood. The purpose of this study is to evaluate the physicochemical properties of these mixtures in the context of how they influence partitioning, diffusion, and absorption of aromatic (^{14}C-naphthalene) and aliphatic (^{14}C-dodecane) markers in porcine skin and silastic membranes *in vitro*. In these 5-h flowthrough diffusion studies, Jet-A, JP-8, and JP-8(100) fuels, and weathered JP-8 (JP-8(Puddle)) were tested. In both membrane systems and across all jet fuels tested, naphthalene absorption (1.29–1.84% dose) was significantly greater than dodecane absorption (0.14–0.28% dose). However, significantly more dodecane than naphthalene was observed in the stratum corneum (SC; 4.23–7.23% dose *vs.* 1.88–4.08% dose) and silastic membranes (59.2–81.7% dose *vs.* 30.5–36.7% dose). Naphthalene was least likely to be retained on the skin surface compared to dodecane, while this trend was reversed in silastic membranes. In porcine skin, weathered JP-8 significantly increased dodecane absorption, permeability (0.19×10^{-4} cm/h), and diffusivity, and also naphthalene deposition in the SC compared to other jet fuels. In contrast, weathered JP-8 appears to decrease naphthalene flux (1.56 μg/cm^2/h) and permeability (1.14×10^{-4} cm/h) in skin. There were no differences among the three jet fuels in terms of their ability to influence naphthalene or dodecane disposition in skin and, generally, no significant differences among the four jet fuel mixtures were observed in silastic membranes. In conclusion, these transport studies suggest that absorption and deposition of naphthalene and dodecane are different when dosed in various jet fuel mixtures, and disposition in weathered jet fuel is significantly different from that in commercial and military fuels. These interactions may not only be related to the unique chemistry of these components, but also specific membrane interactions in the SC and viable epidermis. *Toxicology and Industrial Health* (2001) **16.**

Keywords: *absorption, dodecane, jet fuels, mixtures, naphthalene, skin.*

Introduction

Anecdotal reports and preliminary research suggest that topical exposure to liquid jet fuels can cause dermal irritation in U.S. Air Force personnel (Sing, 1998; Zeiger and Smith, 1998). There is, however, no clear evidence as to which jet fuel and what component or combination of components and additives are responsible for causing occupational irritant dermatitis. Preliminary studies in our laboratory demonstrated gross morphological changes *in vivo* in pig's skin exposed to Jet-A, JP-8, and JP-8(100) jet fuels (Monteiro-Riviere et al., 2000) and release of TNF-α and IL-8 in cultured human epidermal keratinocytes (Allen et al., 2000). As jet fuels are effectively chemical mixtures of hundreds of hydrocarbon chemicals, it is important to identify the chemical or group of chemicals that is readily absorbed across skin to illicit the observed health effects. Recent studies have characterized absorption of several JP-8 components and additives in rodent skin (McDougal et al., 2000) and in porcine skin flaps (Riviere et al., 1999). However, these studies did not focus on specific physicochemical interactions and chemical–biological interactions that are unique to these jet fuels.

Jet-A, JP-8, and JP-8(100) are kerosine-based fuels that are essentially chemical mixtures of aliphatic and aromatic components. These include paraffins or alkanes, cycloparaffins, aromatics, and olefins or alkenes (ATSDR, 1996). Although percentage composition can vary between formulations, jet fuels consist mostly of aliphatic compo-

1. Address all correspondence to: Ronald E. Baynes, Center for Cutaneous Toxicology and Residue Pharmacology (CCTRP), Department of Food Animal Health and Resource Management, College of Veterinary Medicine, North Carolina State University, Raleigh, NC 27606. Tel.: +1-919-513-6261. Fax: +1-919-513-6358. E-mail: ronald_baynes@ncsu.edu

Table 1. Comparison of physicochemical properties[a] of naphthalene and dodecane.

Jet fuel component	Molecular weight[b]	Log octanol–water PC[c]	Solubility in water[b,d] (mg/l)
Naphthalene	128.2	3.37	31.7
Dodecane	170.3	7.24	0.0084

[a]Values obtained from [b]The Merck (1996) Index, [c]ATSDR Toxicological Profiles, and [d]Franks (1966).

nents (80–90%) and smaller amounts of aromatics (≈17%). The aromatics are substituted benzenes and naphthalenes, and relatively low levels of highly volatile chemicals such as benzene, toluene, and xylene (Zeiger and Smith, 1998). It should be noted that >93% of the water-soluble fraction of kerosene is composed of the aromatic components including benzene and naphthalenes (ATSDR, 1996). Theoretically, solubility differences between solutes and between vehicle and membrane should result in differences in partitioning and membrane diffusion (Sloan et al., 1986; Hilton et al., 1994). This study focuses on membrane transport of a major aliphatic component of jet fuels, dodecane, (4.7% w/w) and a major aromatic component, naphthalene (1.1% w/w).

The major difference between jet fuel formulations is the inclusion of additives. JP-8 contains many of the aliphatic and aromatic components found in commercial jet fuels, Jet-A, as well as static inhibitors, icing inhibitors, and corrosion inhibitors (DOD, 1992). JP-8(100) is essentially JP-8 fuel with a proprietary additive package (e.g., detergent, chelator, dispersant, antioxidant) designed to increase thermal stability and reduce soot buildup (Zeiger and Smith, 1998). Interestingly, the icing inhibitor, diethylene glycol monomethyl ether (DEGME), does not appear to cause major toxicological changes systematically or in the skin after topical exposure (Hobson et al., 1986), but can influence transdermal delivery of several drugs (Ritschel and Hussain, 1988; Panchagnula and Ritschel,

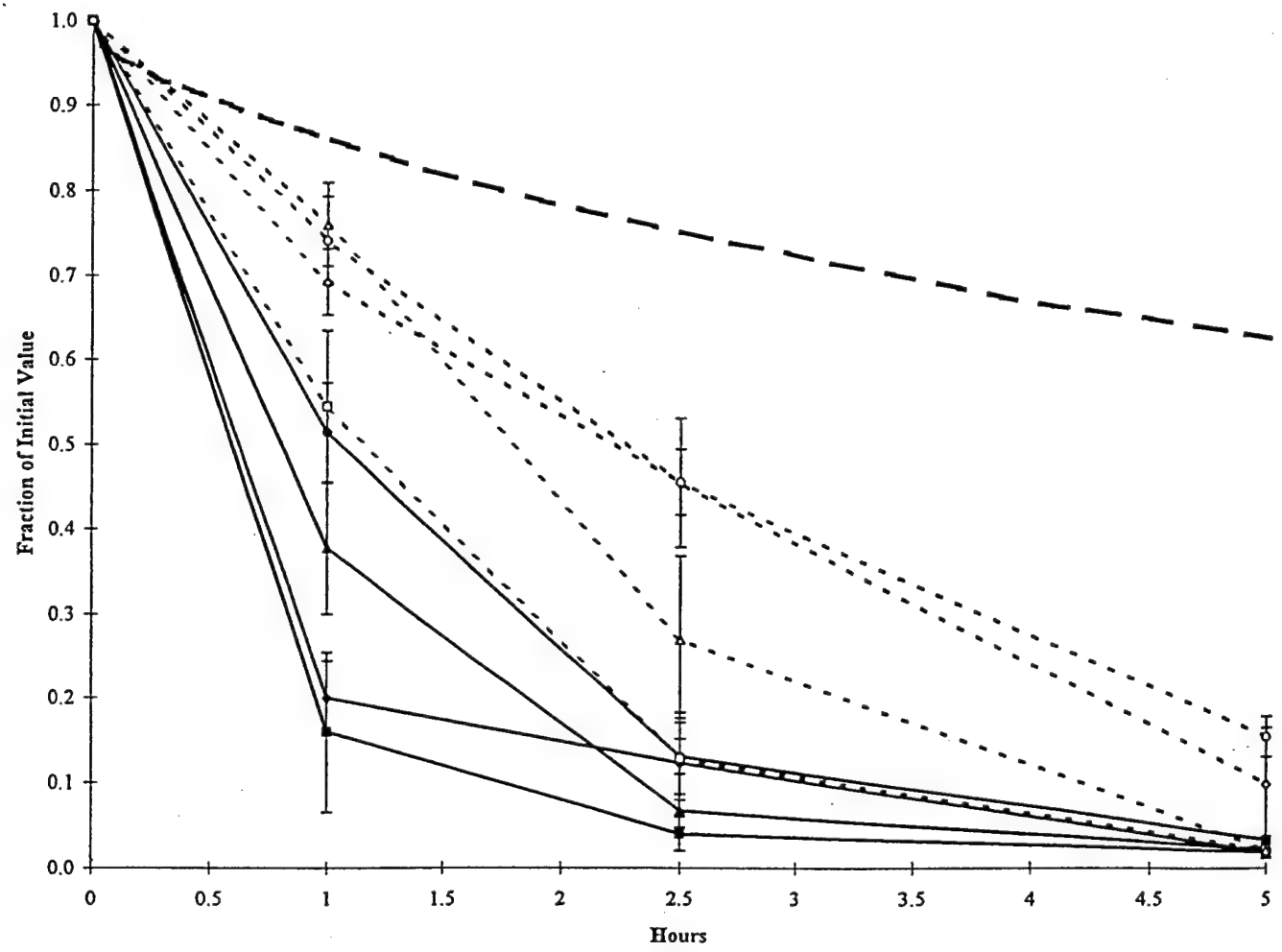

Figure 1. Evaporation of naphthalene from Jet-A (-◆-), JP-8 (-■-), JP-8(100) (-▲-), and JP-8(Puddle) (-●-) jet fuels of dodecane from Jet-A (-◇-), JP-8 (-□-), JP-8(100) (-△-), and JP-8(Puddle) (-○-) jet fuels, and evaporation of total JP-8 (- -) jet fuels.

1991; Yazdanian and Chen, 1995). Very little is known about the corrosive inhibitor, DCI-4A, and the antistatic compound, Stadis 450, and it is difficult to predict how these additives and those in the JP-8(100) additives package influence absorption.

The purpose of this study is to probe for physicochemical and chemical–biological interactions in these three jet fuel formulations or mixtures using skin model systems such as silastic membrane and porcine skin that vary in complexity. In order to assess how chemical interactions influence chemical diffusion independent of biological interactions in skin, an artificial membrane such as a silastic membrane can serve the purpose of assessing diffusion in a simple membrane model system that is hydrophobic. The silastic membrane has been used to extract similar information from various pharmaceutical and cosmetic formulations (Cappel and Kreuter, 1991). Compared to silastic membrane, porcine skin is a more complex model consisting of (1) stratum corneum (SC) that is functionally lipid in character and (2) hydrophilic diffusional layers of the viable epidermis and dermis. Unlike the silastic membrane, porcine skin can respond physiochemically and biochemically to topically applied irritants. However, by using such a membrane with thickness similar to that of skin, diffusion properties independent of biological interactions can be adequately assessed and then compared with those in viable skin. Porcine skin is anatomically and physiologically similar to human skin (Monteiro-Riviere, 1991); therefore, percutaneous absorption of naphthalene and dodecane in jet fuel mixtures through pig skin should reflect absorption in human skin.

Diffusion of jet fuel components in skin is also dependent on the ability of components to partition from the jet fuel mixture into the lipid matrix of the SC. Octanol–water partition coefficients (PCs) can be used to estimate skin permeability (Sartorelli et al., 1998); however, there are often discrepancies in this relationship (Jetzer et al., 1986). Another aim of this study is to empirically determine how aliphatic and aromatic components in jet fuels partition from jet fuel mixtures into the SC and compare these values with those in the literature (Table 1) and diffusion parameters obtained from the flowthrough studies in porcine skin.

Materials and methods

Chemicals

Jet fuels Jet-A, JP-8, and JP-8(100) were kindly supplied by Major T. Miller from Wright Patterson Air Force Base. Weathered JP-8 (JP-8(Puddle)) was produced by allowing JP-8 to evaporate in an open Petri dish in a fume hood for 24 h. Approximately 30% of the initial mass was lost (Figure 1), and the remnant was then spiked with radiochemicals and used in JP-8(Puddle) exposures. Radiolabeled ^{14}C-naphthalene (specific activity=8.1 mCi/mmol) and ^{14}C-dodecane (specific activity=8.3 mCi/mmol) were obtained from Sigma Chemical (St. Louis, MO) and each marker was dissolved in methylene chloride prior to formulation with jet fuels. Radiochemical purity of both compounds ranged from 98% to 100%. Jet fuel mixtures were prepared and 10 μl of these mixtures was topically applied to each diffusion cell to deliver 40–49 and 21–33 μg/cm^2 of ^{14}C-naphthalene and ^{14}C-dodecane, respectively. It should be noted that the added radiochemical compounds had little effect on the final concentration of naphthalene (1.21% instead of 1.1%) and dodecane (4.701% instead of 4.7%).

Jet Fuel Evaporation Experiments

Known amounts of ^{14}C-naphthalene or ^{14}C-dodecane were added to Jet-A, JP-8, JP-8(100), and JP-8(Puddle) and then placed in scintillation vials equilibrated at 37°C. Vials (four replicates per fuel) were then quenched with Ecolume (ICN, Costa Mesa, CA) and capped at 0, 1, 2.5, and 5.0 h. These vials were then counted by Packard

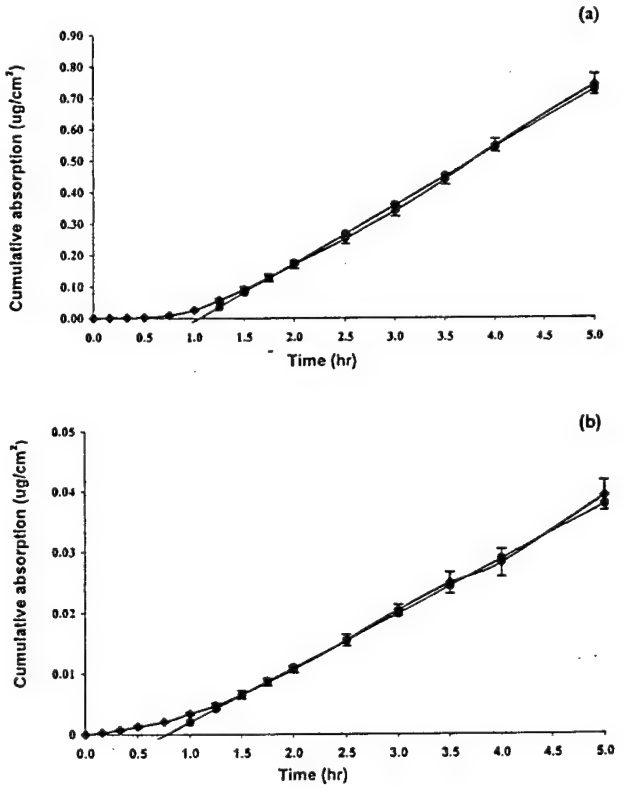

Figure 2. Cumulative absorption (μg/cm^2) *versus* time (h) plot for (a) naphthalene and (b) dodecane in JP-8 following topical application to porcine skin sections in *in vitro* flowthrough diffusion cells. The best-fit straight line was used to calculate the flux for these jet fuel markers.

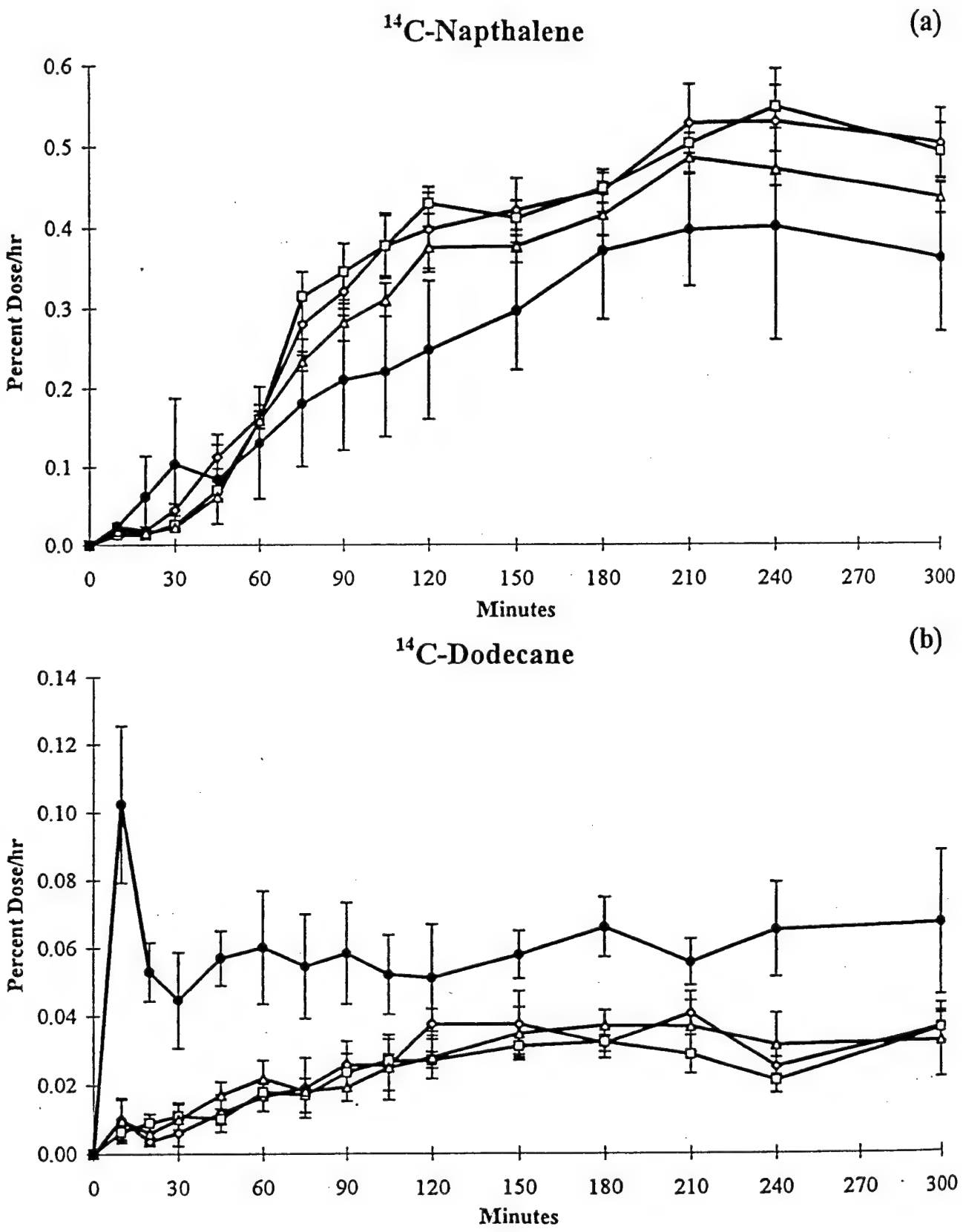

Figure 3. Naphthalene (a) and dodecane (b) perfusate absorption (percent dose/h ± SEM) in porcine skin after dosing in Jet-A (-◇-), JP-8 (-□-), JP-8(100) (-△-), and JP-8(Puddle) (- ● -) jet fuels.

Table 2. Flux, permeability, and diffusivity of naphthalene and dodecane in porcine skin sections exposed to Jet-A, JP-8, JP-8(100), and JP-8(Puddle) fuel mixtures for 5 h.

Fuel	Flux±SEM* ($\times 10^{-1}$) ($\mu g/cm^2/h$)	Permeability±SEM ($\times 10^{-4}$) (cm/h)	Diffusivity±SEM ($\times 10^{-4}$) (cm^2/h)
Naphthalene			
Jet-A	$2.22 \pm 0.12^{a,A}$	$1.68 \pm 0.06^{a,A}$	$0.95 \pm 0.05^{a,b,A}$
JP-8	$1.86 \pm 0.06^{a,b,A}$	$1.44 \pm 0.06^{a,b,A}$	$0.99 \pm 0.05^{a,A}$
JP-8(100)	$1.74 \pm 0.12^{a,b,A}$	$1.32 \pm 0.06^{a,b,A}$	$0.97 \pm 0.04^{a,b,A}$
JP-8(Puddle)	$1.56 \pm 0.3^{b,A}$	$1.14 \pm 0.24^{b,A}$	$0.80 \pm 0.09^{b,A}$
Dodecane			
Jet-A	$0.10 \pm 0.01^{a,B}$	$0.11 \pm 0.01^{b,B}$	$1.24 \pm 0.29^{b,A}$
JP-8	$0.09 \pm 0.01^{a,B}$	$0.09 \pm 0.01^{b,B}$	$1.37 \pm 0.14^{b,A}$
JP-8(100)	$0.11 \pm 0.02^{a,B}$	$0.11 \pm 0.02^{b,B}$	$1.28 \pm 0.18^{b,A}$
JP-8(Puddle)	$0.09 \pm 0.01^{a,B}$	$0.19 \pm 0.03^{a,B}$	$2.22 \pm 1.37^{a,A}$

*Lower case superscripts represent significant differences between treatments within a parameter. Upper case superscripts represent significant differences between naphthalene and dodecane for a specific treatment ($P<0.05$). Means with the same letter are not significantly different. Data were obtained at steady state.

Model 1900TR Liquid Scintillation Counter (Packard Chemical, Downers Grove, IL) for total ^{14}C determination. Radioactivity in each vial was expressed as percent of initial value (Figure 1).

Jet Fuel/SC PC Determination

Dissected skin from the abdomen of a female weanling Yorkshire pig was cut into pieces to fit between preheated aluminum blocks and placed in an oven at 60° for 6–8 min. The SC/epidermis was removed using dissection forceps and placed dermis side down into Petri dishes lined with filter paper and containing 0.25% trypsin (Sigma) to dissolve the epidermis. After 24 h in an incubation oven at 35°C, trypsin inhibitor (Sigma) was added to neutralize trypsin and the SC was washed with distilled water. The SC was dried at room temperature for approximately 24 h before being weighed (5–8 mg sample) and placed in vials. About 500 μl of Jet-A, JP-8, and JP-8(100) with either ^{14}C-naphthalene or ^{14}C-dodecane was added to the SC sample vial ($n=4$), capped, sealed, and allowed to remain undisturbed at room temperature for 24 h. At 24 h, 10 μl of the vehicle was removed for direct counts using Ecolume (ICN). The SC sample was removed, gently blotted on a Kimwipe to remove access solution, then analyzed as described below.

Flowthrough Diffusion Cell Experiments

The flowthrough diffusion cell system, as previously described by Bronaugh and Stewart (1985), was used to perfuse porcine skin and silastic (polydimethylsiloxane) membranes. Porcine skin was obtained from the dorsal area of weanling female Yorkshire pigs. The skin was dermatomed to a thickness of 200–300 μm with a Padgett Dermatome (Padgett Instruments, Kansas City, MO). Silastic membranes (250 μm) were obtained from Dow Corning (Midland, MI). Each circular skin and silastic section was punched to provide a dosing surface area of 0.32 cm^2 and then placed into a two-compartment Teflon flowthrough diffusion cell. Skin and silastic discs were perfused using Krebs–Ringer bicarbonate buffer spiked with dextrose and bovine serum albumin. The temperature of the perfusate and flowthrough cell was maintained at 37°C using a Brinkmann constant temperature circulator (Brinkmann, Westbury, NY). The pH was maintained between 7.4 and 7.5. Perfusate flow rate was 4.0 ml/h and perfusate samples were at 0, 10, 20, 30, 45, 60, 75, 90, 105, 120, 150, 180, 240, and 300 min. At the end of the perfusion, the dose area was swabbed with soapy solution to determine surface content, taped–stripped six times with scotch tape to determine SC content, and then removed from the skin disc with a 0.32-cm^2 punch biopsy to determine dose area skin deposition. These tissue samples, in addition to the remaining peripheral skin, were saved for radiochemical analysis described below.

Chemical Analysis

For determination of ^{14}C-naphthalene and ^{14}C-dodecane, perfusate, swabs, dose skin, and SC samples were combusted in a Packard Model 306 Tissue Oxidizer (Packard Chemical) and then analyzed by Packard Model 1900TR Liquid Scintillation Counter (Packard Chemical) for total ^{14}C determination.

Calculations and Statistics

Absorption was defined as the total percentage of initial dose detected in the perfusate for the entire 5-h perfusion period. *Flux* ($\mu g/cm^2/h$) was determined at steady state from the slope of the cumulative mass per unit area *versus* time (h) curve. An example of how flux and lag times were

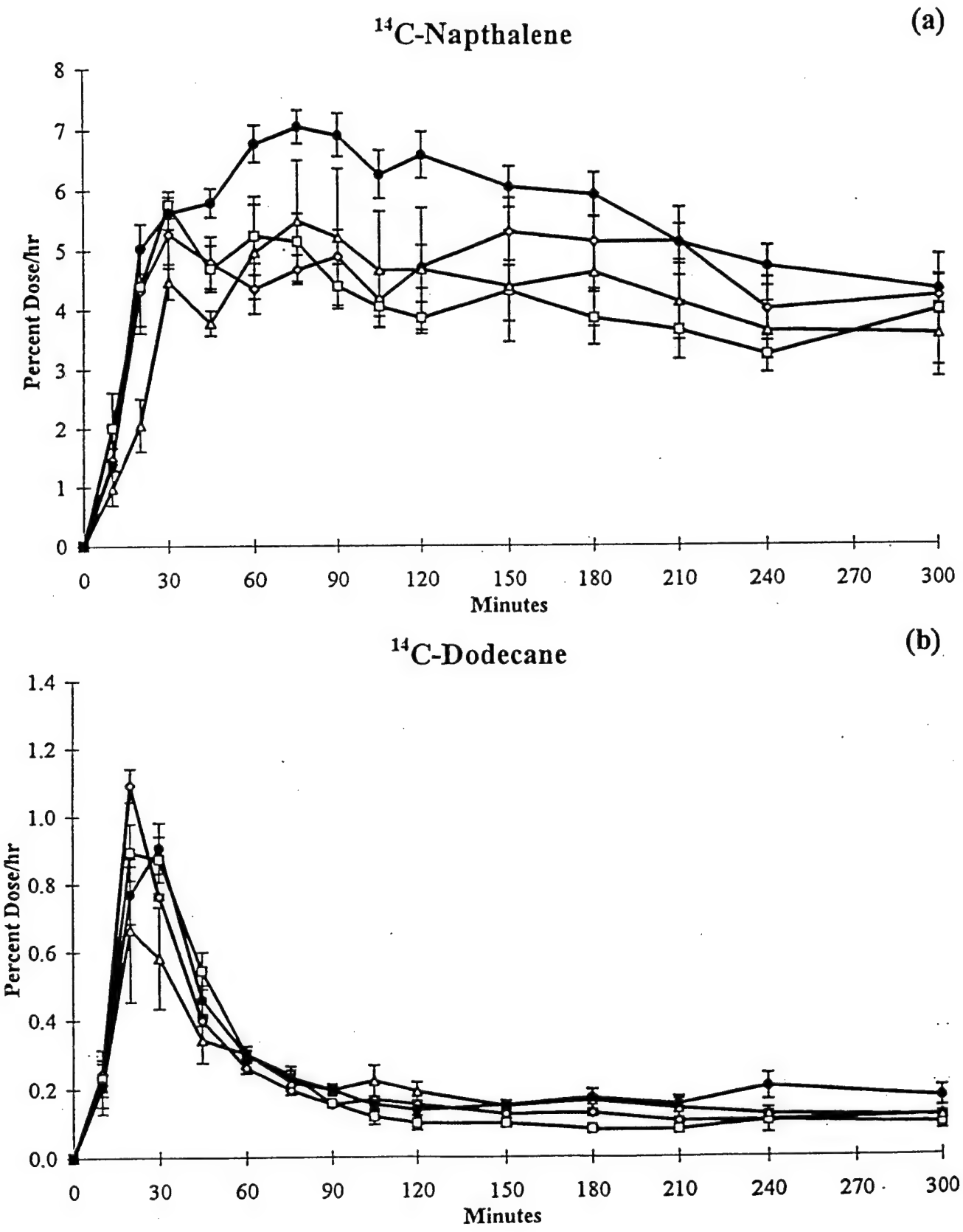

Figure 4. Naphthalene (a) and dodecane (b) perfusate absorption (percent dose/h ± SEM) in silastic membrane after dosing in Jet-A (-◇-), JP-8 (-□-), JP-8(100 (-△-), and JP-8(Puddle) (- ● -) jet fuels.

determined for both markers is presented in Figure 2 depicting cumulative absorption ($\mu g/cm^2$) *versus* time (h) in JP-8 mixture. *Permeability* (cm/h) was determined from the ratio of individual fluxes to the concentration ($\mu g/cm^3$) of the initial topical dose. *Diffusivity* (cm^2/h) was determined by obtaining the lag time before steady-state flux is reached. This lag time (τ) was obtained by extrapolating the steady-state portion of the curve back to the time- or x-axis. This lag time was related to diffusivity (D) and membrane thickness (L) by the following equation: $D=L^2/6\tau$, where $L=250$ μm. *Tissue disposition* parameters such as surface, SC, dosed skin, dosed+peripheral skin were described above. For *partition coefficient* determinations, radioactivity content in the jet fuel and SC were normalized to 1000 mg jet fuel ($C_{\text{Jet Fuel}}$) and 1000 mg SC (C_{SC}), respectively. The Jet Fuel/SC PC was determined from the equation: $PC=C_{\text{Jet Fuel}}/C_{SC}$.

Standard errors were determined for all data sets. For analysis of total absorption, flux, permeability, diffusivity, surface, SC, dosed area, dosed area+peripheral skin data, multiple comparison tests were performed using ANOVA with significance level at 0.05. All analyses were carried out using SAS 6.12 for Windows software (SAS Institute, Cary, NC). A least significant difference (LSD) procedure was used for multiple comparisons on all parameters assessed.

Results

Dermal Absorption, Flux, Permeability, and Diffusivity

Naphthalene versus Dodecane Naphthalene absorption in porcine skin (1.29–1.88% dose) was significantly greater ($P<0.05$) than dodecane absorption (0.13–0.27% dose). The absorption profiles in Figure 3 demonstrate that dodecane absorption in porcine skin was minimal. Peak absorption ranged from 0.02% to 0.1% dose/h for dodecane, while the peak absorption for naphthalene ranged from 0.4% to 0.6% dose/h. Naphthalene achieved steady state within 150–210 min for all mixtures tested, while steady state was achieved for dodecane within 90–120 min. As listed in Table 2, naphthalene flux ($1.56–2.22\times10^{-1}$ $\mu g/cm^2/h$) was significantly greater than that for dodecane ($0.09–0.11\times10^{-1}$ $\mu g/cm^2/h$), and naphthalene permeability ($1.14–1.68\times10^{-4}$ cm/h) was significantly greater than that for dodecane ($0.09–0.19\times10^{-4}$ cm/h). However, naphthalene diffusivity in skin ($0.80–0.99\times10^{-4}$ cm/h) was statistically similar to dodecane diffusivity ($1.24–2.22\times10^{-4}$ cm/h).

Naphthalene and dodecane absorption profiles in silastic membrane (Figure 4) are not only different from each other, but are also different from the corresponding absorption profiles in porcine skin depicted in Figure 3. Generally, naphthalene absorption, flux, permeability, and diffusivity in silastic membranes were significantly greater than those for dodecane (Table 3). For example, naphthalene absorption was, on average, 22-fold greater than dodecane absorption in silastic membranes compared to an average 11-fold difference in absorption between the two markers in porcine skin as previously indicated. By comparing the two membrane systems, naphthalene absorption was, on average, 14-fold greater in silastic membranes than in porcine skin compared to only, on average, sevenfold difference for dodecane (Figure 5).

Jet Fuel Mixture Effects There were no significant differences among Jet-A, JP-8, and JP-8(100) with regards to influencing the absorption, flux, permeability, and diffusivity of naphthalene or dodecane in porcine skin. However, weathered JP-8 (JP-8(Puddle)) significantly

Table 3. Flux, permeability, and diffusivity of naphthalene and dodecane are silastic membranes exposed to Jet-A, JP-8, JP-8(100), and JP-8(Puddle) fuel mixtures for 5 h.

Fuel	Flux ± SEM* ($\times10^{-1}$) ($\mu g/cm^2/h$)	Permeability ± SEM ($\times10^{-4}$) (cm/h)	Diffusivity ± SEM ($\times10^{-4}$) (cm^2/h)
Naphthalene			
Jet-A	$19.98\pm1.44^{a,A}$	$14.34\pm1.14^{b,A}$	$14.19\pm4.76^{a,b,A}$
JP-8	$22.68\pm1.50^{a,A}$	$15.30\pm1.02^{a,b,A}$	$14.97\pm3.98^{a,A}$
JP-8(100)	$22.50\pm4.44^{a,A}$	$16.08\pm3.12^{a,b,A}$	$5.09\pm2.05^{b,B}$
JP-8(Puddle)	$27.00\pm12.6^{a,A}$	$20.46\pm0.90^{a,A}$	$5.80\pm0.93^{a,b,B}$
Dodecane			
Jet-A	$0.95\pm0.02^{a,B}$	$2.15\pm0.04^{a,B}$	$14.76\pm1.39^{a,A}$
JP-8	$1.42\pm0.41^{a,B}$	$3.09\pm0.88^{a,B}$	$11.92\pm2.80^{a,A}$
JP-8(100)	$0.99\pm0.29^{a,B}$	$2.18\pm0.65^{a,B}$	$10.61\pm1.07^{a,A}$
Jp-8(Puddle)	$1.01\pm0.09^{a,B}$	$2.15\pm0.19^{a,B}$	$10.58\pm0.90^{a,A}$

*Lower case superscripts represent significant differences between treatments within a parameter. Upper case superscripts represent significant differences between naphthalene and dodecane for a specific treatment ($P<0.05$). Means with the same letter are not significantly different. Data were obtained at steady state.

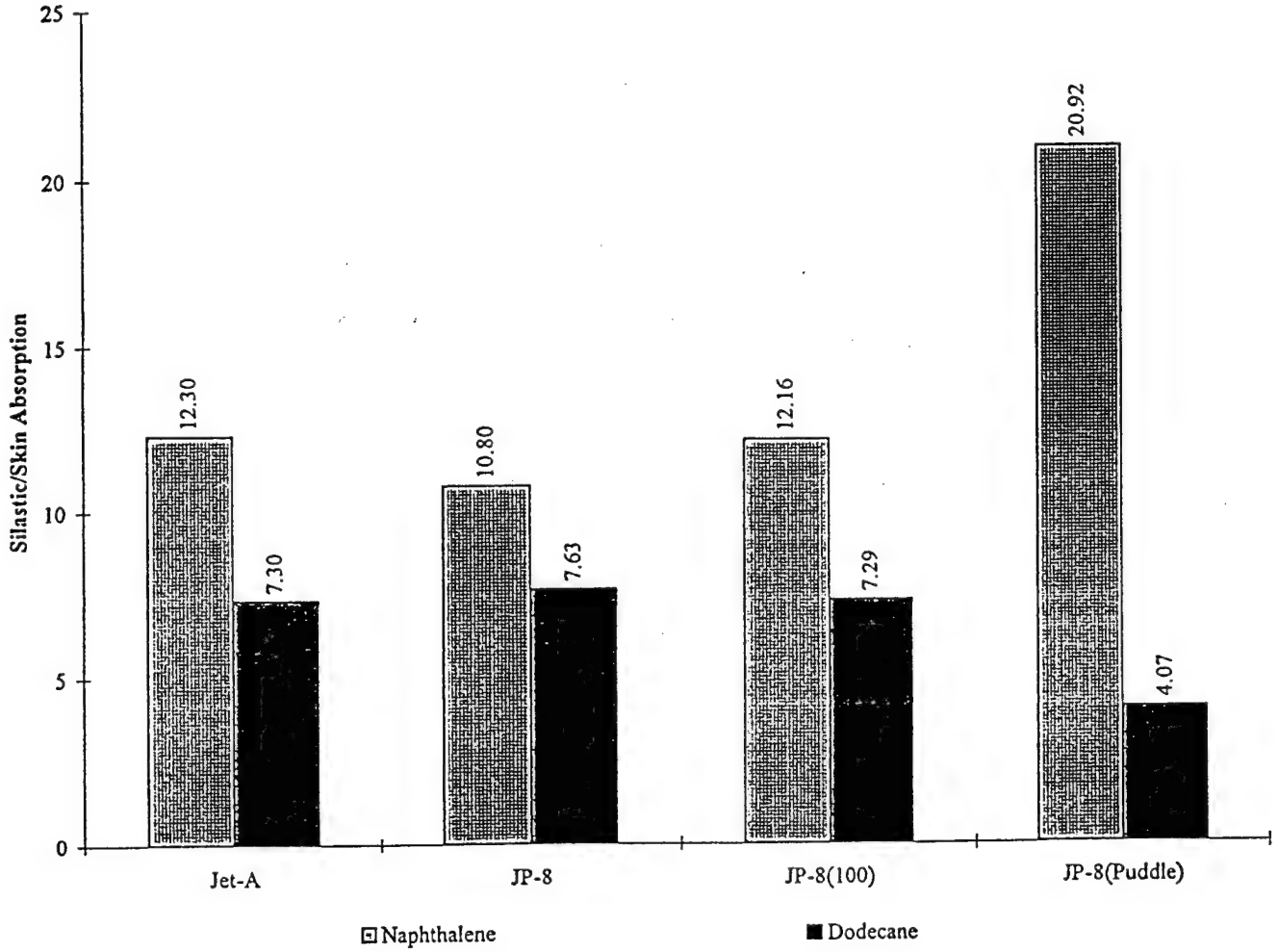

Figure 5. Silastic/skin absorption ratios for naphthalene and dodecane in Jet-A, JP-8, JP-8(100), and JP-8(Puddle) jet fuels.

enhanced dodecane absorption, permeability, and diffusivity in porcine skin compared to JP-8, Jet-A, and JP-8(100). Weathered JP-8 appears to lower all absorption parameters for naphthalene, but not significantly. These trends and specific weathered JP-8 differences between mixtures were not absorbed for naphthalene and dodecane diffusion in silastic membranes. In these inert membranes, naphthalene diffusivity was significantly less in JP-8(100) than in other jet fuel mixtures, and dodecane diffusivity was significantly greater in weathered JP-8 and JP-8(100) compared to naphthalene diffusivity in similar jet fuel mixtures.

Disposition in SC, Skin, and Surface

Naphthalene versus Dodecane Significantly greater levels of dodecane (4.23–7.23% dose) compared to naphthalene (1.88–4.08% dose) were detected in the SC ($P<0.05$) at 5 h after exposure (Figure 6). However, there were no significant differences between naphthalene and dodecane for the radioactivity detected in the dose area or total skin+SC. Significantly more dodecane than naphthalene was retained on the skin surface at 5 h. In the silastic membrane, more dodecane than naphthalene was detected in the membrane, but significantly higher levels of naphthalene were retained on the membrane surface at 5 h (Figure 7).

The jet fuel/SC PC data (Figure 8) showed that jet fuel/SC PC values were significantly greater for naphthalene (1.88–2.61) than for dodecane (0.68–0.97). Naphthalene is also more likely to partition into silastic membranes (JF/Silastic=1.83) than partition into the SC (JF/SC=2.83).

Jet Fuel Mixture Effects Weathered JP-8 significantly enhanced naphthalene deposition in SC compared to the three jet fuel formulations ($P<0.05$). Weathered JP-8 compared to JP-8(100) significantly increased dodecane deposition in the SC. There were no significant differences among Jet-A, JP-8, and JP-8(100) regarding naphthalene and dodecane deposition in the SC or dose skin area.

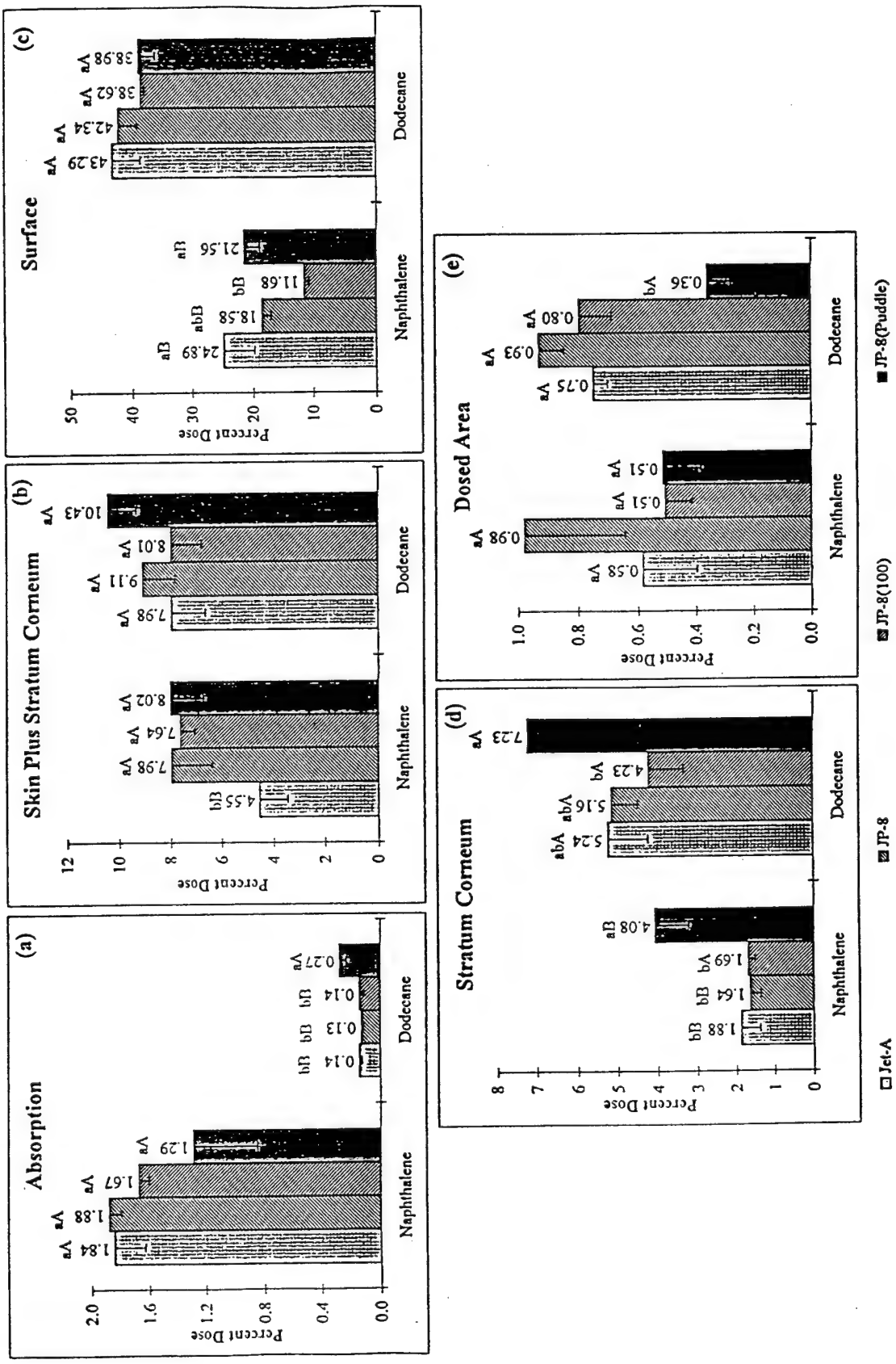

Figure 6. Absorption and tissue disposition of naphthalene and dodecane in porcine skin after dosing in Jet-A, JP-8(100), and JP-8(Puddle) jet fuels.

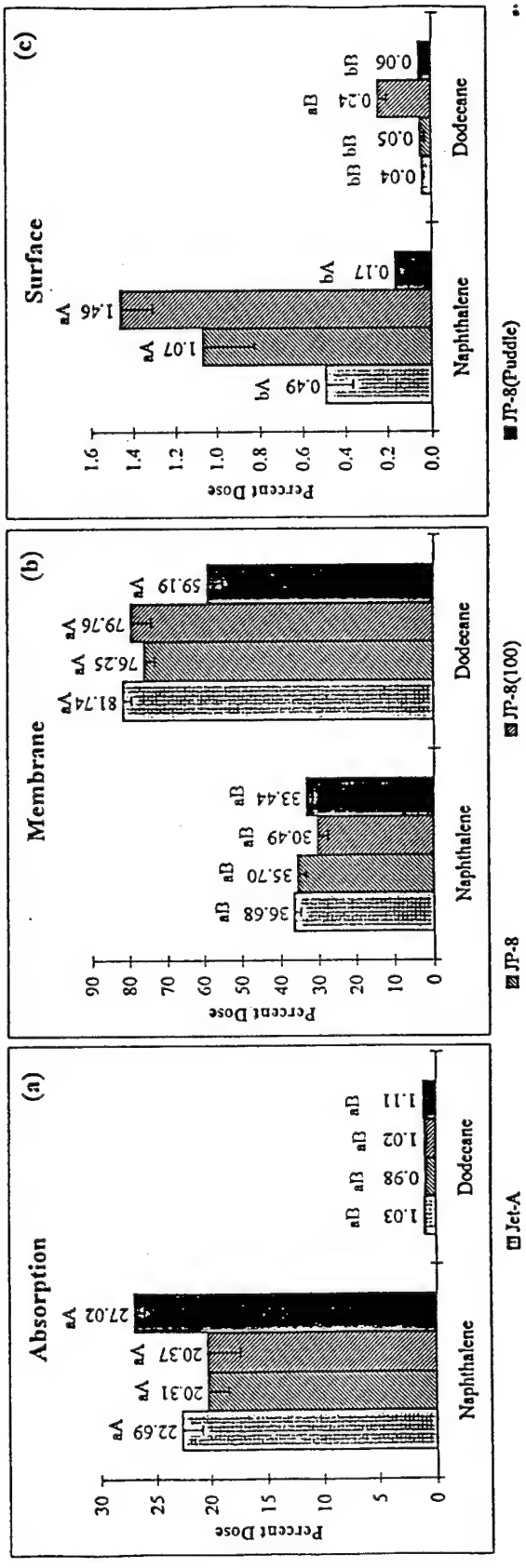

Figure 7. Absorption and tissue disposition of naphthalene and dodecane in silastic membrane after dosing in Jet-A, JP-8, JP-8(100), and JP-8(Puddle) jet fuels.

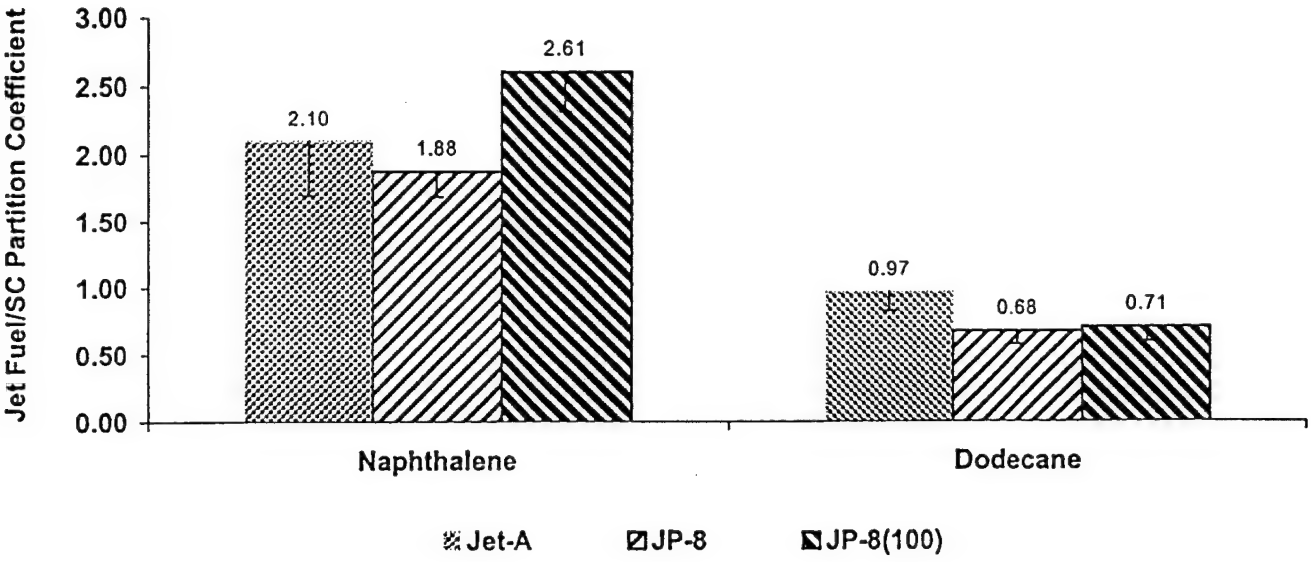

Figure 8. Jet fuel/SC PCs for naphthalene and dodecane in Jet-A, JP-8, JP-8(100) at 24 h.

Surface retention of naphthalene was significantly greater with Jet-A and weathered JP-8 compared to JP-8(100), but there were no significant differences between jet fuel mixtures for dodecane retention on skin surface.

As observed with skin, there were no significant differences among the three jet fuel formulations for naphthalene or dodecane deposition in silastic membranes. However, these three jet fuel formulations, compared to weathered JP-8, significantly increased dodecane deposition in the membrane. It should also be noted that JP-8 and JP-8(100), compared to the other two jet fuel mixtures, significantly enhanced surface retention of naphthalene, while JP-8(100) increased surface retention of dodecane on the membrane.

The evaporation studies (Figure 1) demonstrated that naphthalene was more volatile than dodecane irrespective of the jet fuel formulation. Within 1 h, 15–38% naphthalene and 54–76% dodecane remained to be evaporated. However, at 5 h, only 1.9–3.4% naphthalene and 2.1–15.3% dodecane remained with four- to fivefold differences between naphthalene and dodecane for Jet-A and weathered JP-8.

Discussion

Jet fuels are thought to be dermal irritants, and an understanding of the rate and extent of absorption and distribution in skin of these components in jet fuel mixtures may be useful in assessing the hazard to workers dermally exposed to these fuels. The primary focus of this study was to characterize the dermal diffusion of representative aliphatic (dodecane) and aromatic (naphthalene) components and determine the influence of four jet fuel mixtures on dermal disposition of these marker components. The data from this study demonstrate distinct differences between naphthalene and dodecane in terms of dermal absorption and distribution, and several of these differences can be explained based on known physicochemical differences. This study also identified possible mixture interactions using both porcine skin and silastic membranes that would not have otherwise been identified using more complex skin models.

Synthetic membranes provide additional understanding of mechanistic aspects of skin permeability and the thermodynamic effects of chemical solubility, PC, and chemical–vehicle interaction (Behl et al., 1993). The silastic membrane acts as a nonaqueous pore, and because of its hydrophobic nature, it should be highly permeable to nonionized species. In many respects, it resembles the diffusion environment in the SC. Synthetic membrane models have been successfully used to demonstrate formulation effects on permeability of various drugs and chemicals (Twist and Zatz, 1988, 1990). Chemical interactions between the membrane and ethanol have been previously described (Maitani et al., 1995). Kerosine-based mixture can therefore be expected to alter the lipid and protein components in the SC, but only the hydrophobic component in the silastic membrane.

Naphthalene and Dodecane Disposition

The flux profiles and the absorption data demonstrated that more naphthalene than dodecane was transported across biological and synthetic membranes. A similar trend was recently observed in porcine skin flaps (Riviere et al., 1999) and rat skin *in vitro* (McDougal et al., 2000). While dodecane permeability in pig skin from our study was

comparable to that in rat skin, naphthalene permeability was threefold greater in rat skin than in pig skin. The latter may be a result of rat skin being two to three times more permeable than human or porcine skin (McDougal et al., 1990).

Naphthalene has a smaller molecular weight (Table 1) than dodecane (ATSDR, 1996); therefore, the rate (flux) and extent (% dose) of absorption is expected to be greater than dodecane as demonstrated in this study. However, there were no significant differences between marker diffusivity, which suggests that in jet fuel mixtures specifically, molecular weight differences and molecular structure differences may not be sufficient to influence diffusivity in skin. Solute diffusivity can also be altered by viscosity as demonstrated by using two different membrane systems. The greater diffusivity in the silastic membrane (which is hydrophobic) is suggestive of greater diffusivity in the SC, but significantly reduced diffusivity in skin can occur once the marker enters the viable epidermis. Diffusivity differences between the SC and viable epidermis have been previously proposed in the development of various kinetic models in skin (Bunge and Cleek, 1995), and the viable epidermis can represent the decisive resistance to drug transport (Wenkers and Lippold, 1999). Interpreting diffusivity data in skin and even predicting permeability is therefore complicated by the fact that the SC is a lipid domain and the viable epidermis is comparably a hydrous mass with quasi-like liquid properties (Potts and Francoeur, 1991). Diffusivities in the SC and viable epidermis can also depend differently on molecular weight (Bunge and Cleek, 1995). These differences support the need to sometimes conduct simultaneous skin diffusion studies with artificial membranes to characterize diffusion in homogenous media.

Surprisingly, naphthalene/dodecane diffusivity ratios of approximately 1 were observed in skin and silastic membrane. This suggests that the absorption differences between naphthalene and dodecane are probably more related to partitioning differences on the surface and/or at the membrane–perfusate interface. These physicochemical differences are illustrated by the different silastic/skin absorption ratios for naphthalene and dodecane, with the ratios being always higher for naphthalene than for dodecane irrespective of the jet fuel mixture. This is related to a greater naphthalene flux and permeability in the homogenous silastic membrane compared to slower flux and permeability in skin. The differences between these two membranes are reduced for dodecane because absorption appears to be controlled or modulated by chemical–biological interactions in the SC or silastic membrane.

Differences between naphthalene and dodecane transport can be related to solubility differences (Table 1) in vehicles that play an important role in determining flux and permeability. More importantly, it is the differences in thermodynamic activity of the penetrant in the vehicle. For a chemical that is very soluble in a vehicle (e.g., dodecane in jet fuel), its activity can be less than that for naphthalene that is comparatively less soluble in that vehicle (Smith and Surber, 2000). These interactions can result in a higher rate of transport as observed in this study for naphthalene. The opposite interaction occurs for dodecane. Furthermore, because of the water solubility characteristics of naphthalene, which is inherently hygroscopic, diffusion into the more aqueous epidermis and perfusate is more likely with naphthalene than dodecane. Our data show that there are no differences between these two markers in skin deposition at 5 h, but naphthalene permeability and flux were greater than dodecane. In silastic membranes, the more water-soluble naphthalene is more likely to leave this hydrophobic polymer and enter the perfusate than dodecane. This also explains why the naphthalene/dodecane absorption ratio in the silastic membrane (22-fold) is greater than that in skin (11-fold). Interactions between naphthalene and the aqueous milieu of the viable epidermis in skin are greater than that in the more hydrophobic silastic membrane where the intrinsic leaving potential encourages diffusion into the perfusate.

The log octanol–water PC ($\log_{o/w}$) for naphthalene (3.37) and dodecane (7.24) (ATSDR, 1996) predicted that more dodecane than naphthalene would partition into the SC. This interaction may then limit diffusion of dodecane through the skin. Our data indicated that naphthalene was more likely to remain in the jet fuels than the SC and that dodecane was more likely to partition into the SC than into the jet fuels. These findings are supported by the fact that more dodecane than naphthalene was observed in the SC and hydrophobic silastic membrane. In spite of this preference for dodecane to partition into the SC, naphthalene absorption and permeability were significantly greater than that for dodecane in both membrane systems. This was consistent with data from a permeability study where rat skin was exposed to JP-8 fuel and permeability was greater for JP-8 components with lower $\log_{o/w}$ values than for components with higher $\log_{o/w}$ values (Robinson and McDougal, 2000). These authors concluded that the octanol–water PC had a greater impact on permeability than molecular weight. It can therefore be deduced that because dodecane had a greater affinity for the SC than naphthalene, the interaction between these two lipophilic moieties (dodecane and SC) reduced flux and absorption into the perfusate as well as by surface interaction with the jet fuel as predicted by the $\log_{o/w}$. The surface deposition data indicate that more dodecane than naphthalene remained on the skin surface. This may also be because naphthalene is a more volatile component than

dodecane (National Research Council, 1996), as indicated in our evaporation experiment (Figure 1). The reverse trend in silastic membrane is difficult to explain, but it may be suggestive of unique surface–chemical interaction that is specifically related to the silastic surface.

Mixture Effects

Only the weathered JP-8 mixture appeared to have an effect on marker absorption and distribution in skin. Weathered JP-8 is capable of increasing both dodecane and naphthalene deposition in the SC while at the same time increasing dodecane absorption significantly but decreasing naphthalene absorption. A conceptually similar effect was observed in porcine skin flaps where the ratio of skin deposition to absorption for dodecane from weathered fuels was greater than other fuels, suggesting enhanced depot formation (Riviere et al., 1999). It is possible that weathered jet fuel may contain less volatile aromatic and short-chained aliphatic components. This suggests that the presence of volatile organics may be *a priori* for naphthalene absorption, but their absence significantly enhances aliphatic (dodecane) absorption. However, these effects were not observed in the silastic membrane, and may therefore be related to specific chemical–biological interaction in skin. These effects are significant as workers are most likely to be exposed to weathered jet fuel mixture. It is therefore possible that those fuel mixtures that increased SC or skin deposition of these markers may be associated with occupational irritant dermatitis.

There were no significant differences among the three jet fuels with regards to influencing naphthalene and dodecane disposition in skin. The additives package in JP-8 and JP-8(100), therefore, do not appear to have an effect on absorption of these markers. The additive, DEGME, is known as an enhancer of dermal absorption (Yazdanian and Chen, 1995); however, its presence in high concentrations can reduce absorption of several drugs. It is possible that although DEGME can readily diffuse through skin (51.5 $\mu g/cm^2/h$) in jet fuels (McDougal et al., 2000), its ability to enhance the permeability of jet fuel components may also be reduced in the presence of other additives. Only well-designed factorial studies can evaluate whether such additives or combination of additives can influence absorption of jet fuel components. The ability for JP-8(100) compared to other fuels to selectively retain both markers on the silastic skin may have occupational relevance. JP-8 and JP-8(100) are less volatile than its predecessor fuel (JP-4), and contact with liquid fuel on skin and clothing may result in prolonged exposure (Pleil et al., 2000). The slowly evaporating JP-8 fuel and, more importantly, weathered JP-8 (Figure 1) tend to linger on clothing and skin surface, increasing the chance for systemic absorption. To date, there are no reports of the effects of occlusion, humidity, or hydration on absorption of these marker components. However, it is anticipated that in a more aqueous vehicle, there will be an increased tendency for jet fuel components to move into the more lipophilic SC and probably increase absorption. Further studies are therefore required to understand the contribution of occlusion and formulation additives on absorption of toxicologically important jet fuel components. As observed from this study, dermal disposition cannot always be predicted from known physicochemical properties of individual chemical components. It is very likely that in complex mixtures such as jet fuels, these properties change and so will the parameters used to assess disposition in skin.

Acknowledgments

This research was supported by the United States Air Force, USAFOSR no. FQ8671-98.

References

Allen D.G., Riviere J.E., and Monteiro-Riviere N.A. Induction of early biomarkers of inflammation produced by keratinocytes exposed to jet fuels Jet-A, JP-8, and JP-8(100). *J. Biochem. Mol. Toxicol.* 2000: 14.~~(in press)~~ 231 – 237

ATSDR. Draft Toxicological Profile for Jet Fuels (JP-5 and JP-8). Agency for Toxic Substances and Disease Registry, Atlanta, GA, 1996.

Behl C.R., Char H., Patel S.B., Mehta D.B., Piemontese D., and Malick A.W. *In vivo* and *in vitro* skin uptake and permeation studies. In: Shah V.P., Maibach H.I. (Eds.), Topical Drug Bioavailability, Bioequivalence, and Penetration. Plenum Press, New York, NY, 1993, pp. 225–259.

Bronaugh R.L., and Stewart R.F. Methods for *in vitro* percutaneous absorption studies: IV. The flowthrough diffusion cell. *J. Pharm. Sci.* 1985: 74: 64–67.

Bunge A.L., and Cleek R.L. A new method for estimating dermal absorption from chemical exposure: 2. Effect of molecular weight and octanol–water partitioning. *Pharm. Res.* 1995: 12: 88–95.

Cappel M., and Kreuter J. Effect of ionic surfactants on transdermal drug delivery: I. Polysorbates. *Int. J. Pharm.* 1991: 69: 143–153.

DOD. Military specification: turbine fuel aviation, grades JP-4, JP-5, and JP-5/Jp-8 ST. U.S. Department of Defense, 1992, Document no. MIL-T-5624P.

Franks F. Solute–water interactions and the solubility behavior of long-chain paraffin hydrocarbons. *Nature* 1966: 210: 87–88.

Hilton J., Woolen B.H., Scott R.C., Auton T.R., Trebilcock K.L., and Wilks M.F. Vehicle effects on *in vitro* percutaneous absorption through rat and human skin. *Pharm. Res.* 1994: 11: 1396–1400.

Hobson D.W., D'Addario A.P., Bruner R.H., and Uddin D.E. A subchronic dermal exposure study of diethylene glycol monomethyl ether and ethylene glycol monomethyl ether in the male guinea pig. *Fundam. Appl. Toxicol.* 1986: 6: 339–348.

Jetzer W.E., Huq A.S., Ho N.F., Flynn G.L., Duraiswamy N., and Condie L. Permeation of mouse skin and silicone rubber membranes by phenols: relationship to *in vitro* partitioning. *J. Pharm. Sci.* 1986: 75: 1098–103.

Maitani Y., Sato H., and Nagai T. Effect of ethanol on the true diffusion coefficient of diclofenac and its sodium salt in silicone membrane. *Int. J. Pharm.* 1995: 113: 164–174.

McDougal J.N., Jepson G.W., Clewell H.J., Gargas M.L., and Anderson M.E. Dermal absorption of organic chemical vapors in rats and humans. *Fundam. Appl. Toxicol.* 1990: 14: 299–308.

McDougal J.N., Pollar D.L., Weisman W., Garrett C.M., and Miller T.E. Assessment of skin absorption and penetration of JP-8 jet fuel and its components. *Toxicol. Sci.* 2000: 55: 247–255.

Merck. In: Budavari S. (Ed.), The Merck Index, 12th edn. Merk and Co., Whitehouse Station, NJ, 1996.

Monteiro-Riviere N.A. Comparative anatomy, physiology, and biochemistry of mammalian skin. In: Hobsen D.W. (Ed.), Dermal and Ocular Toxicology: Fundamentals and Methods. CRC Press, Boca Raton, FL, 1991, pp. 3–71.

Monteiro-Riviere N.A., Inman A.O., Rhyne B.N., and Riviere J.E. Cutaneous irritation of topically applied jet fuels in the pig. *Toxicologist* 2000: 54: 151.

National Research Council. Physical and Chemical Properties of Military Fuels. Permissible Exposure Levels for Selected Military Fuel Vapors. National Academy Press, 1996, pp. 13–17.

Panchagnula R., and Ritschel W.A. Development and evaluation of intracutaneous depot formulation of corticosteroids using DGME as a cosolvent: *in vitro*, *ex vivo*, and *in vivo* rat studies. *J. Pharm. Pharmacol.* 1991: 16: 609–614.

Pleil J.D., Smith L.B., and Zelnick S.D. Personal exposure to JP-8 jet fuel vapors and exhaust at air force bases. *Environ. Health Perspect.* 2000: 108: 183–192.

Potts R.O., and Francoeur M.L. The influence of stratum corneum morphology on water permeability. *J. Invest. Dermatol.* 1991: 96: 495–499.

Ritschel W.A., and Hussain A.S. *In vitro* skin penetration of griseofulvin in rat and human skin from an ointment dosage form. *Arzneim.-Forsch./Drug Res.* 1988: 38: 1630–1632.

Riviere J.E., Brooks J.D., Monteiro-Riviere N.A., Budsaba K., and Smith C.E. Dermal absorption and distribution of topically dosed jet fuels Jet-A, JP-8, and JP-8(100). *Toxicol. Appl. Pharmacol.* 1999: 160: 60–75.

Robinson P.J., and McDougal J.N. Correlation approaches for estimating skin permeability of hydrocarbon components of JP-8. *Toxicologists* 2000: 54: 150.

Sartorelli P., Aprea C., Cenni A., Novelli M.T., Orsi D., Palmi S., and Matteucci G. Prediction of percutaneous absorption from physicochemical data: a model based on data of *in vitro* experiments. *Ann. Occup. Hyg.* 1998: 45: 267–276.

Sing J. Skin permeability, biophysics, and irritation from JP-8. Proceedings of AFOSR JP-8 Jet Fuel Toxicology Workshop, Tucson, AZ, 1998.

Sloan K.B., Koch S.A.M., Siver K.G., and Flowers F.P. Use of solubility parameters of drug and vehicle to predict flux through skin. *J. Invest. Dermatol.* 1986: 87: 244–252.

Smith E., and Surber C. The absolute fundamentals of transdermal permeation. In: Gabard B., Elsner P., Suber C., and Treffel P. (Eds.), Dermatopharmacology of Topical Preparations. Springer, New York, NY, 2000, pp. 23–36.

Twist J.N., and Zatz J.L. Membrane–solvent–solute interaction in a model permeation system. *J. Pharm. Sci.* 1988: 77: 536–540.

Twist J.N., and Zatz J.L. A model for alcohol-enhanced permeation through polydimethylsiloxane membranes. *J. Pharm. Sci.* 1990: 79: 28–31.

Wenkers B.P., and Lippold B.C. Skin penetration of nonsteroidal anti-inflammatory drugs out of a lipophilic vehicle: influence of the viable epidermis. *J. Pharm. Sci.* 1999: 88: 1326–1331.

Yazdanian M., and Chen E. The effects of diethylene glycol monoethyl ether as a vehicle for topical delivery of ivermectin. *Vet. Res. Commun.* 1995: 19: 309–319.

Zeiger E., and Smith L. The first international conference on the environmental health and safety of jet fuel. *Environ. Health Perspect.* 1998: 106: 763–764.

ELSEVIER

Toxicology Letters 000 (2000) 000–000

Toxicology Letters

www.elsevier.com/locate/toxlet

Cytokine induction as a measure of cutaneous toxicity in primary and immortalized porcine keratinocytes exposed to jet fuels, and their relationship to normal human epidermal keratinocytes

D.G. Allen *, J.E. Riviere, N.A. Monteiro-Riviere

Department of Clinical Sciences, Center for Cutaneous Toxicology and Residue Pharmacology, North Carolina State University, 4700 Hillsborough Street, Raleigh, NC27606, USA

Received 16 October 2000; received in revised form 6 December 2000; accepted 7 December 2000

Abstract

The purpose of this study was to identify biomarkers of toxicity in primary porcine keratinocytes (PKC) and an immortalized porcine keratinocyte cell line (MSK3877) exposed to jet fuels Jet A, JP-8, and JP-8 + 100. Cells were exposed to 0.1% jet fuels and assayed for interleukin-8 (IL-8) and tumor necrosis factor alpha (TNF-α) mRNA using the TaqMan real time quantitative reverse transcriptase PCR assay. IL-8 and TNF-α protein release was measured using an ELISA. PKC exposed to jet fuels caused a slight upregulation of TNF-α mRNA at early time points, but no significant differences in TNF-α protein production were detected. IL-8 mRNA was increased at 4 h following exposure, and IL-8 protein was increased at 8 h. In MSK 3877 cells, jet fuels were shown to increase the production and expression of TNF-α mRNA and protein at 30 min and 1 h following exposure, respectively. IL-8 mRNA was only slightly induced compared to control. IL-8 protein release was suppressed by jet fuel exposure. These results were compared with those of a previous study in our laboratory to evaluate the utility of using porcine cells in lieu of normal human epidermal keratinocytes (NHEK). Similarities exist between PKC and NHEK with respect to both TNF-α and IL-8 production. The expression profile of TNF-α in MSK3877 cells mimics that of NHEK. In contrast, the profile of IL-8 expression opposes that of PKC and NHEK. These results suggest that porcine keratinocytes are susceptible to jet fuel toxicity. However, the responses of immortalized cells may vary from those of PKC and NHEK necessitating cautious interpretation of such data.

Keywords: Immortalized keratinocyte; Cytokine; Jet fuel; Toxicity

1. Introduction

Jet A is a kerosene-cut jet fuel used by commercial airliners that is composed of at least 228 aliphatic and aromatic hydrocarbon components.

* Corresponding author. Tel.: +1-919-5136398; fax: +1-919-5136358.

E-mail address: nancy_monteiro@ncsu.edu (D.G. Allen).

0378-4274/01/$ - see front matter

PII: S0378-4274(00)00316-7

The battlefield fuel for the U.S. Department of Defense as well as NATO forces is JP-8, which is a mixture of Jet A plus an icing inhibitor (diethylene glycol monoethyl ether, DIEGME), an anti-static compound (Stadis 450), and a corrosion inhibitor (DCI-4A). Recently an additional additive package has been included to JP-8 that increases its thermal stability 100°F (Baker et al., 1999). This fuel is known as JP-8 + 100 and is composed of JP-8 plus anti-oxidant, chelator, detergent, and dispersant components. The toxicity of these fuels has focused primarily on the nervous and pulmonary systems. However, the incorporation of these additives has created concern for the dermatotoxicologic potential of these compounds due to repeated occupational exposures to flight line personnel, engine maintenance technicians, and fuel handlers. These personnel may enter directly into the aircraft fuselage during maintenance operations or inspections. They are at risk to dermal exposure because they are subjected to the largest exposures (Carlton and Smith, 2000). These workers wear cotton coveralls to reduce the possibility of explosion due to the generation of static electricity. Exposures to the fuels results in saturation of the cotton cloth, resulting in an occluded environment for repeated, long-term exposure to the skin during the typical 8 h workday. To compound the problem, JP-8 was developed in order to have a higher flash point and lower vapor pressure than its predecessor, JP-4. An increased potential for systemic exposure exists because evaporative loss is reduced (which reduces inhalational exposures) facilitating dermal absorption (Ulrich, 1999). In addition, some aircraft fuel tanks are filled with a reticulated polyurethane foam to suppress explosions that may be caused by electrical arcing, lightning strikes, or static electricity. A significantly higher exposure to jet fuels was seen in operations involving foamed fuel tanks versus non-foamed (Carlton and Smith, 2000). Finally, a recent study has confirmed the potential for dermal toxicity as these fuels were shown to cross the epidermal barrier for potential access to the systemic circulation (Riviere et al., 1999).

The use of pig skin in dermatotoxicological research has been widely accepted due to its morphological and physiological similarities to human skin (Bartek et al., 1972; Meyer et al., 1986; Monteiro-Riviere, 1986; Monteiro-Riviere and Riviere, 1996; Simon and Maibach, 2000). Furthermore, the use of keratinocyte cell cultures have been gaining acceptance as an alternative to animal studies for such research (Roguet, 1998; Bernstein and Vaughan, 1999). Our lab has focused its research efforts on the use of both in vivo and in vitro pig models to study dermal pharmacology and toxicology. Therefore, the use of a porcine epidermal keratinocyte culture would be useful as a screening tool for toxic compounds to be used in more advanced studies. We have previously documented the response of normal human epidermal keratinocytes (NHEK) to jet fuel exposure (Allen et al., 2000). The purpose of this study was to evaluate the production and expression of the pro-inflammatory cytokines, TNF-α and interleukin-8 (IL-8), in primary porcine epidermal keratinocytes (PKC) and an immortalized porcine epidermal keratinocyte cell line (MSK3877) as biomarkers of dermal toxicity following exposure to the three jet fuels detailed above. In addition, as this study was performed on porcine keratinocytes, results are compared to those of the previous study using NHEK for the purpose of evaluating the utility of porcine keratinocytes as a test model system in lieu of NHEK.

2. Materials and methods

2.1. Cell culture

Female Yorkshire pigs were sedated with xylazine/ketamine and their dorsal skin clipped (Oyster electric clippers, size 40 blade). Full thickness skin (400 μm) was dermatomed and cut into 2 cm^2 pieces, which were subsequently floated, dermis side down, on 0.25% trypsin overnight at 4°C. The epidermis was peeled away from the underlying dermis and placed into DMEM supplemented with 10% fetal bovine serum (FBS). A single cell suspension was achieved by agitating the epidermal pieces with a pipet and filtering the resultant slurry through a 70 μm mesh screen. Primary keratinocytes were then plated onto collagen Type I (Collaborative Research Products) coated plastic vessels in serum-free, calcium-free keratinocyte

basal media (KBM, Clonetics) supplemented with human epidermal growth factor (0.1 ng/ml), insulin (5 μg/ml), bovine pituitary extract (0.4%), GA-1000 (gentamycin: 50 μg/ml; amphotericin-B: 50 ng/ml) to create keratinocyte growth media (KGM-2, Clonetics). For optimal keratinocyte growth and proliferation, 0.075 mM $CaCl_2$ was added to KGM-2.

Immortalized porcine keratinocytes (MSK3877) were cultured on collagen Type I (Collaborative Research Products) coated plastic vessels in modified keratinocyte serum-free media (KSFM, Gibco-BRL). Briefly, KSFM was supplemented with gentamycin (10 μg/ml, Gibco-BRL), penicillin (25 U/ml), streptomycin (25 μg/ml), glutamine (29.2 μg/ml, Biowittaker), fungizone (500 ng/ml, Gibco-BRL), human epidermal growth factor (0.15 ng/ml), and bovine pituitary extract (25 μg/ml, Gibco-BRL). This media was then diluted 4:1 with DMEM (Gibco-BRL) containing 10% FBS to obtain a working media solution. MSK3877 cells have been shown to be non-tumorigenic and to exhibit similar morphological and physiological characteristics of primary pig keratinocytes (Hengge et al., 1996).

Cryopreserved adult normal human epidermal keratinocytes (NHEK) were purchased from Clonetics, Corp. (San Diego, CA, USA) and maintained in serum-free, calcium-free keratinocyte basal media (KBM, Clonetics) supplemented with human epidermal growth factor (0.1 ng/ml), insulin (5 μg/ml), bovine pituitary extract (0.4%), GA-1000 (gentamycin: 50 μg /ml; amphotericin-B: 50 ng/ml) to create keratinocyte growth media (KGM-2, Clonetics). 0.06 mM$CaCl_2$ was added back to the cultures for optimal growth without initiating Ca^{2+}-induced differentiation of the cells.

2.2. Chemical treatment

All cells were plated onto 24-well plates (protein assays) or 12-well plates (mRNA assays) and were maintained in a humidified incubator at 37°C with a 95% O_2/5% CO_2 atmosphere. Upon reaching approximately 70–80% confluency, fresh KGM-2 (NHEK) or KSFM (MSK3877) was added and test chemicals were added to appropriate wells ($n = 3$) for 1–24 h. Jet fuels were dissolved in 100% ethanol (final concentration 1.0%) prior to their addition to the culture media at a final concentration of 0.1%. Based on previous experiments in our lab, the effects of ethanol only treatments are not significantly different than control ($P < 0.05$). The concentration of jet fuels was chosen based on a fixed volume applied to the surface area of the culture dish derived from previous experiments in our lab, as well as those performed on airway epithelial cells (Witten et al., personal communication). Control wells consisted of culture media only.

2.3. Cytotoxicity assay

Cells were plated onto 96-well plates and maintained as stated above. Chemicals were added as above to each well ($n = 12$) and incubated for 24 h. Following exposure, media was replaced with balanced salt solution containing *p*-nitrophenyl phosphate and incubated for 4 h at 37°C. A yellow color developed in those wells with sufficient membrane-associated acid phosphatase to liberate the *p*-nitrophenyl. Spectrophotometric measurements were made (405 nm) on a Multiskan RC plate reader (Labsystems, Helsinki, Finland). Controls consisted of media alone (negative) and 1.0N HCl (positive). To confirm that no evidence of apoptosis had occurred, treated and control cells were also examined by transmission electron microscopy.

2.4. Enzyme-linked immunosorbent assay (ELISA)

To determine secreted protein from porcine keratinocytes in response to jet fuel exposure, a sandwich ELISA assay was used for both IL-8 and TNF-α. PKC and MSK3877 were plated onto 24-well plates as detailed above ($n = 3$). Cells were dosed with either 0.1% Jet A, JP-8, or JP-8 + 100 and at each time interval following dosage (1, 4, 8, 24 h), the supernatant was removed and frozen at −80°C for later assay. Commercial kits for the detection of porcine and human TNF-α and IL-8 (Biosource) were performed as indicated in the manufacturer instructions. The plates were

read at 450 nm on a Multiskan RC plate reader (Labsystems, Helsinki, Finland). For both ELISA assays, a recombinant porcine IL-8 or TNF-α was diluted to create a standard reference curve. To ensure that neither the culture media nor the dosed chemicals adversely affected the efficiency of the ELISA, a sample from each treatment group was spiked with a known concentration of the recombinant proteins and measured for accuracy.

2.5. RNA extraction

Keratinocytes were plated onto 12-well plates and treated ($n = 3$) with test chemicals for various time intervals (30 min, 1, 2, 4 h). At each time point, the supernatant was removed and lysis buffer (Qiagen, Valencia, CA, USA) added directly to the wells. Cells were homogenized by loading the buffer lysate onto Qiashredder columns (Qiagen, Valencia, CA, USA). Total RNA was extracted using RNeasy spin columns as per manufacturer instructions (Qiagen), eluted with dH_2O, and quantified spectrophotometrically.

2.6. TaqMan quantitative RT-PCR

The TaqMan RT-PCR reaction uses the 5′ nuclease activity of the Taq DNA Polymerase (AmplTaq Gold, PE Biosystems) to cleave a fluorescently labeled gene-specific probe during PCR. The probe is labeled by a reporter dye on the 5′ end, and a quencher dye on the 3′ end. While the probe is intact, the close proximity of the reporter and quencher dyes causes suppression of the reporter fluorescence. However, during PCR, the probe anneals to the target sequence between the sites specific to the forward and reverse primers. As the Taq polymerase moves 5′-3′, it releases the reporter dye and separates it from the quencher dye allowing its fluorescence to be detected. Therefore, accumulation of PCR products can be monitored based on an increase in reporter fluorescence. Reporter fluorescence is normalized by generating a ratio of reporter emission intensity to that of a passive reference dye contained in the PCR buffer (Heid et al., 1996; Shiels and Sweeney, 1999). This technique has been shown to be far superior in sensitivity than other methods of RNA analysis (e.g. Rnase Protection Assay, Northern Analysis). Furthermore, because it is performed on a 96-well platform and does not require the use of a competitive fragment, it is much less labor intensive than conventional competitive RT-PCR methods and therefore more useful for high throughput experiments (Wang and Brown, 1999).

Primers and probes were designed for porcine GAPDH, TNF-α, and IL-8 using Primer Express Software (PE Biosystems, Foster City, CA) based on published mRNA sequences in GenBank (NCBI). Oligonucleotides were manufactured by Applied Biosystems using the sequences in Table 1. A single tube reverse transcriptase PCR (RT-PCR) and sequence detection were performed simultaneously using the ABI Prism 7700 Se-

Table 1
Oligonucleotide sequences for primers and probes used for TaqMan assay[a]

PigTNF-α	Forward = TGGCCCCTTGAGCATCA A
	Reverse
	= CGACGGGCTTATCTGAGGTTT
	Probe
	= 6FAM-TCTGGCCCAAGGACTCAGATC ATCGT-TAMRA
PigIL-8	Forward
	= TGGACCAGAGCCAGAGAGACTAG
	Reverse
	= AAACTGCCAAGAAGGCAACAG
	Probe
	= 6FAM-AGAAACAGCTCGTGTCAACAT GACTTCCAA-TAMRA
PigGAPDH	Forward
	= ATGGAAAGGCCATCACCATCT
	Reverse
	= CACAACATACGTAGCACCAGCAT
	Probe
	= VIC-CAGGAGCGAGATCCCGCCAACA -TAMRA

[a] 6FAM, 6-carboxyfluorescein; TAMRA, 6-carboxy-tetramethyrhodamine.

quence Detection System. Approximately 50 ng of total RNA was added to each reaction tube (50 μl final volume) of an optimized mixture of MultiScribe reverse transcriptase, AmplTaq Gold, $MgCl_2$, dNTP's, RNase inhibitor, and a passive reference dye (TaqMan One-Step RT-PCR, Applied Biosystems). Primer concentrations were optimized in preliminary reactions by varying their concentration from 50–900 nm. Negative controls consisted of no template and no enzyme samples. The reverse transcription step was performed for 30 min at 48°C followed by a 10 min incubation at 95°C to inactivate the RT enzyme, and activate the Taq polymerase. The PCR reaction consisted of 40 cycles of denaturation (15 s at 95°C) followed by annealing/extention (1 min at 60°C). Standard curves were generated using serially diluted (1:10) porcine spleen RNA (BD Pharmingen) to quantify mRNA concentrations using the Absolute Standard Curve method as per manufacturer instructions (Applied Biosystems). A ratio of cytokine mRNA to GAPDH mRNA was calculated to adjust for any variations in the RT-PCR reaction.

Quantitation of NHEK mRNA expression was performed by quantitative competitive RT-PCR (QCRT-PCR) as detailed in Allen et al., (2000). Briefly, 1 μg of total RNA extracted as above was reversed transcribed with SuperScript RT enzyme and Oligo $d(T)_{12-18}$ primers. The resultant cDNA strand was co-amplified with a competitive fragment of a slightly different size than the sample PCR product. Using a known amount of competitive fragment (serially diluted), the amount of mRNA in the sample could be estimated based on densitometric similarity to the appropriate competitive fragment dilution.

2.7. Statistics

Protein concentrations were expressed as pg cytokine per ml media as determined using Genesis Lite Version 3 for Windows software (Labsystems). Statistical differences in protein release and mRNA were determined using ANOVA (SAS 6.12 for Windows; SAS Institute, Cary, NC, USA) at the 0.05 level of significance.

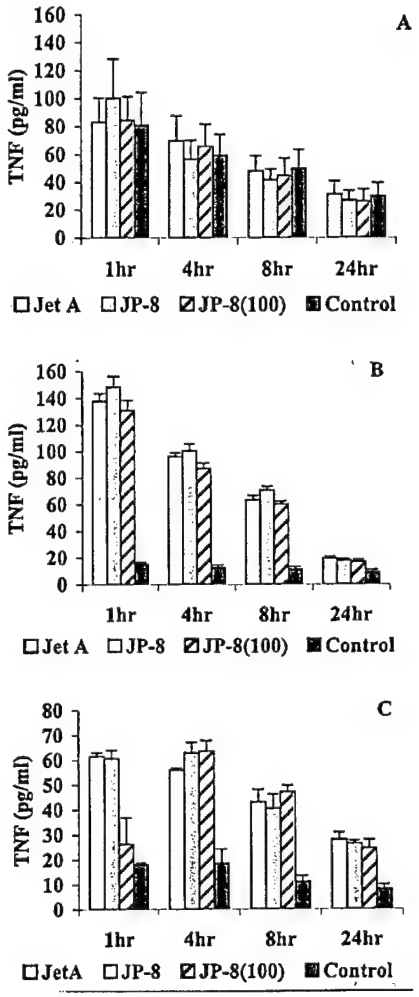

Fig. 1. TNF-α protein release by keratinocytes following exposure to Jet A, JP-8, and JP-8 + 100 jet fuels. Bars, standard error of the mean (A, PKC; B, SK3877 cells; C, NHEK).

3. Results

3.1. Cytokine release

TNF-α release from PKC was not significantly different from control at all time points due to a very high background level of release seen in untreated cells (Fig. 1A). TNF-α release from MSK3877 was maximal at 1 h for all three fuels (Fig. 1B). As shown in Fig. 1C, maximal TNF-α release from NHEK was seen at 1 h of exposure

to Jet A, and at 4 h after exposure to JP-8 and JP-8 + 100. For all cell types, after reaching a maximal release, TNF-α release decreased in a time-dependent manner over 24 h. In both NHEK and MSK3877, these levels remained significantly higher than control at all time points ($P < 0.05$).

IL-8 release from PKC increased at 8 h following jet fuel exposure (Fig. 2A). However, at 24 h control IL-8 levels approach those of treated cells. A constitutive level of IL-8 was seen in PKC at all time points. Fig. 2B shows that IL-8 release was suppressed at all time points by all three fuels in MSK3877 cells. A constitutive level of IL-8 release was seen in control MSK3877 cells that increased in a time-dependent manner, reaching a maximum comparable to control NHEK levels at 24 h. Fig. 2C shows that IL-8 release from NHEK increased at 8 h and reached maximum levels at 24 h. A constitutive level of IL-8 was also seen in NHEK at all time points, but treated cells had levels that were above those of control.

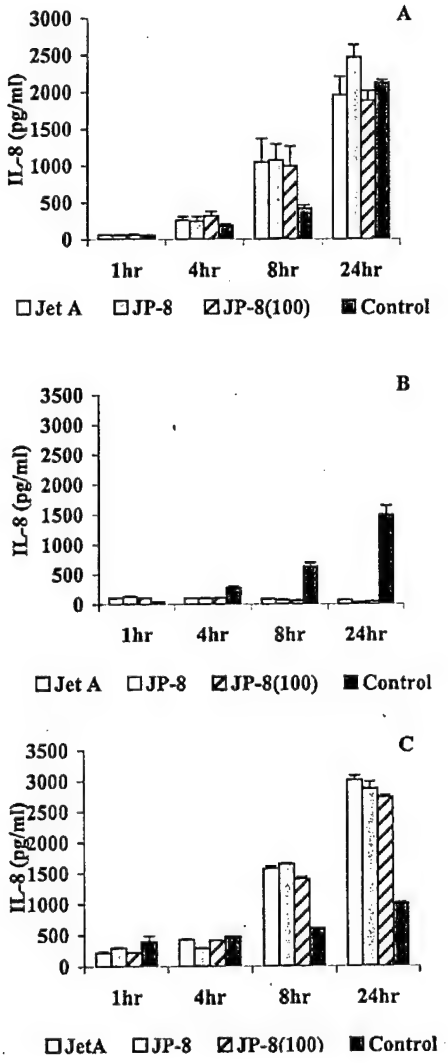

Fig. 2. IL-8 protein release by keratinocytes following exposure to Jet A, JP-8, and JP-8 + 100 jet fuels. Bars, standard error of the mean (A, PKC; B, MSK3877 cells; C, NHEK).

3.2. Cytokine mRNA

TNF-α mRNA in PKC increased slightly at 30 min in JP-8 treated cells, and at 2 h in Jet A treated cells, but these levels were not significantly different than control ($P > 0.05$). These levels returned to control by 4 h following exposure (Fig. 3A). JP-8 + 100 had no effect on PKC TNF-α mRNA. In MSK3877 cells, TNF-α mRNA was elevated slightly at 30 min during all three fuel treatments, but like PKC, these levels were not significantly different than control (Fig. 3B). These levels also returned to control levels within 4 h. Similarly, no significant differences in TNF-α mRNA between treated and control cells were determined in NHEK (Allen et al., 2000).IL-8 mRNA increased at 4 h in PKC exposed to all three fuel treatments ($P < 0.05$, Fig. 4A). IL-8 mRNA is slightly increased in MSK3877 cells at 30 min during JP-8 + 100 exposure, and at 1 h following Jet A exposure (Fig. 4B). JP-8 exposure did not affect IL-8 mRNA production in MSK3877 cells at any time. A time-dependent decrease in IL-8 mRNA can be seen for all treatments following maximal production, similar to the profile seen for TNF-α mRNA. All jet fuels caused a significant increase above control in NHEK IL-8 mRNA at 4 h (Allen et al., 2000).

3.3. Cytotoxicity assay

Jet fuel treatment did not cause a significant difference in toxicity as compared to control ($P >$ 0.05). No evidence of apoptosis (e.g. cell shrink-

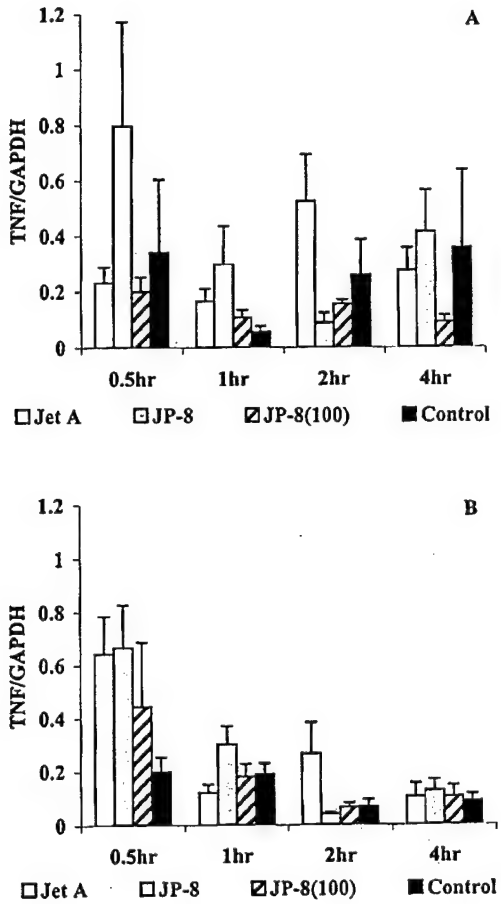

Fig. 3. TNF-α mRNA following exposure to Jet A, JP-8, and JP-8 + 100 jet fuels. Bars, standard error of the mean (A, PKC; B, MSK3877).

age, chromatin condensation, formation of cytoplasmic blebs) was seen by transmission electron microscopy.

4. Discussion

These results provide additional evidence that jet fuels Jet A, JP-8, and JP-8 + 100 have the capacity for affecting pro-inflammatory cytokine production in both human and porcine models. The induction of TNF-α release is very similar in both NHEK and MSK3877. TNF-α protein is released within 1 h in response to jet fuel treatment, and remains above control levels through 24 h. Therefore, it would appear that MSK3877 cells are a suitable model for a human in vitro system with respect to TNF-α production. PKC, in contrast, release a high level of constitutive TNF-α protein, which confounds detecting treatment effects. This could be due to the cellular stress induced by the tissue disruption during the culturing of primary cells. Alternatively, optimizing the culture conditions may decrease the level of background and thus improve the sensitivity of this assay system. In all three cell types, TNF-α protein release appeared to occur in the absence

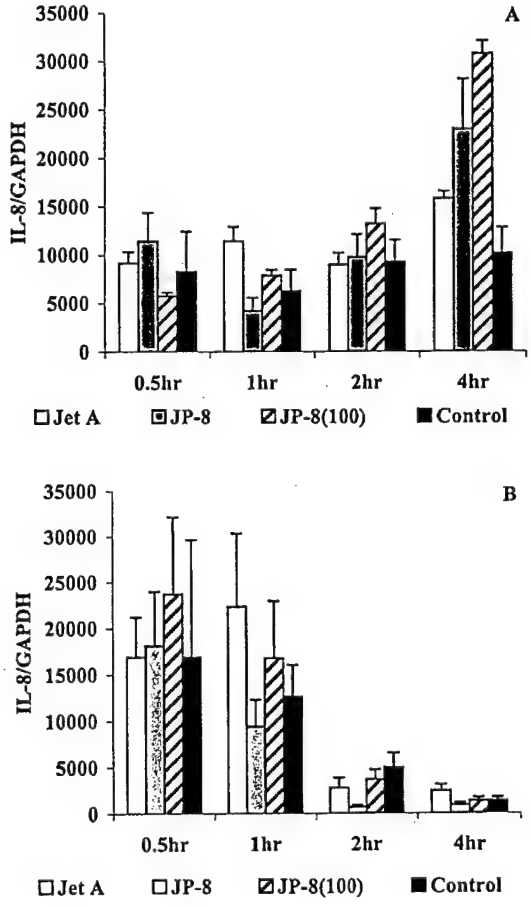

Fig. 4. IL-8 mRNA following exposure to Jet A, JP-8, and JP-8 + 100 jet fuels. Bars, standard error of the mean (A, PKC; B, MSK3877).

of significant upregulation of TNF-α mRNA, suggesting fuels release pre-packaged TNF-α.

These results also show that induction and release of IL-8 from MSK3877 cells is very different than both PKC and NHEK IL-8 mRNA is induced at 4 h and resultant protein release at 8 h in PKC and NHEK (although control levels in PKC approximate treated levels at 24 h). In contrast, the profile of IL-8 mRNA production is opposite to that of PKC and NHEK as peak levels of IL-8 mRNA were seen at 30 min. Furthermore, treated cells are only slightly different than control cells in their expression of IL-8 mRNA. The release of IL-8 from fuel treated MSK3877 is suppressed well below control levels. Therefore, the jet fuels appear to suppress the production of IL-8 in these cells. Despite the high background levels of IL-8 in PKC at 24 h, it is clear that IL-8 production causes a slight increase in its production at 8 h, indicating that no suppression occurs due to jet fuel exposure. Therefore, a species-specific etiology for the suppression seen in MSK3877 cell is not likely. This raises the question that the cytokine cascade is somehow affected in MSK3877 cells, possibly due to their transformation. In most examples of the keratinocyte cytokine cascade, IL-8 production and release is preceded by the release of TNF-α (Luger and Schwarz, 1990). Jet fuels clearly stimulated MSK3877 cells to produce TNF-α, but TNF release is not followed by IL-8 induction in treated cells. This could imply one of several possibilities: (1) jet fuels damage the IL-8 receptor in MSK3877 such that the TNF protein is unable to bind and induce IL-8 production; (2) jet fuels interfere with IL-8 protein synthesis; (3) the chromosomal abnormalities in MSK3877 cells result in an altered IL-8 receptor phenotype. It is not unusual for an immortalized cell line to behave biologically different than the normal or primary constituent of the same cell type. Virgill et al. (1998) noted that HaCaT cells have a different membrane fatty acid composition than normal keratinocytes, which makes them resistant to oxidative stress. Kiss et al. (1999) noted that HaCaT cells also fail to produce IL-8 mRNA or protein in response to treatment with certain neuropeptides. However, the authors did show that HaCaT cells produce a constitutive level of IL-8 (approximately 2000 pg/ml) which agrees with our data showing control MSK3877 cells releasing IL-8 throughout the exposure period. HaCaT cells, like MSK3877 cells, are a spontaneously immortalized cells line that is also non-tumorigenic. Marionnet et al. (1997) noted multiple differences between immortalized cell lines and NHEK with respect to the production of IL-1 and TNF-α. Their results showed that cells lines are different from NHEK and from each other, and that inappropriate expression or inhibition of cytokines may occur in cell lines following chemical or physical treatment. One final possibility for the IL-8 suppression may exist in recent studies that have shown jet fuels are immunotoxic. Jet fuels have been shown to induce IL-10, a potent immunosuppressant (Ulrich, 1999) as well as suppress natural killer cell activity and the generation of cytotoxic T-lymphocytes (Harris et al., 2000). IL-10 may act to suppress the generation of certain pro-inflammatory cytokines (i.e. IL-8) in MSK3877 cells.

Hengge et al. (1996) presents MSK3877 cells as physiologically similar to normal porcine epidermal keratinocytes with respect to proliferation and differentiation in response to calcium transients. However, they also describe the chromosomal abnormalities in MSK3877 to prove that they are indeed genetically altered cells. These cells were developed as a model for use in genetic manipulations for the purposes of dermal gene therapy, but have not been studied extensively with respect to their similarity to normal or primary cell cultures in the production of pro-inflammatory cytokines. Because our lab uses the pig in both in vivo and in vitro systems, we wanted to develop a cell culture system that could be used as a screening tool to justify more complex toxicology studies. These studies show that PKC may eventually provide a predictive screening tool for use in place of NHEK, but their use is precluded by further investigations on their culture conditions that may result in reducing the high level of IL-8 and TNF-α release. Because they have the capacity for many more passages than PKC, we obtained MSK3877 cells with hopes that they would mimic NHEK and PKC such that they alone would suffice in future long term, multiple

dose studies. However, they were found to react very differently to jet fuels than PKC and NHEK with respect to IL-8 production and release. Therefore, these studies also provide evidence that the use of immortalized cell lines for assays of biological toxicity must be entered into cautiously prior to replacing normal cell cultures.

Acknowledgements

This work represents partial fulfillment of the requirement for the degree of Doctor of Philosophy (D. Allen). Portions of this work were presented at the 2000 Annual Meeting of the National Society of Toxicology. This work was partially supported by the U.S. Air Force Office of Scientific Research FQ8671-98-000-462. MSK3877 cells were the generous gift of the laboratory of Dr Jonathan Vogel at the National Cancer Institute, Bethesda, MD. The authors wish to thank Dr Nigel Walker and Chris Miller (National Institute for Environmental and Health Sciences, Research Triangle Park, NC) for the use of the ABI 7700 Sequence Detector System and assistance in developing the TaqMan assays.

References

Allen, D.G., Riviere, J.E., Monteiro-Riviere, N.A., 2000. Identification of early biomarkers of inflammation in keratinocytes exposed to jet fuels Jet A, JP-8, and JP-8 + 100. J. Biochem. Molec. Toxicol. 14, 231–237.

Baker, W., McDougal, J., Miller, T., 1999 Repeated dose skin irritation study on jet fuels-a histopathology study. AFRL-HE-WR-TR-199-0022.

Bartek, M.J., LaBudde, J.A., Maibach, H.I., 1972. Skin permeability in vivo: comparison in rat, rabbit, pig, and man. J. Invest. Dermatol. 58, 114–123.

Bernstein, I.A., Vaughan, F.L., 1999. Cultured keratinocytes in in vitro dermatotoxicological investigation: a review. J. Toxicol. Env. Health B2, 1–30.

Carlton, G.N., Smith, L.B., 2000. Exposures to jet fuel and benzene during aircraft fuel tank repair in the U.S. Air force. Appl. Occup. Env. Hyg. 15, 485–491.

Harris, D.T., Sakiestewa, D., Robledo, R.F., Young, S.R., Witten, M., 2000. Effects of short-term JP-8 jet fuel exposure on cell-mediated immunity. Toxicol. Ind. Health 16, 78–84.

Heid, C.A., Stevens, J., Livak, K.J., Williams, P.M., 1996. Real time quantitative PCR. Genome Research 6, 986–994.

Hengge, U.R., Chan, E.F., Hampshire, V., Foster, R.A., Vogel, J.C., 1996. The derivation and characterization of pig keratinocyte cell lines that retain the ability to differentiate. J. Invest. Dermatol. 106, 287–293.

Kiss, M., Kemeny, L., Gyulai, R., Michel, G., Husz, S., Kovacs, R., Dobozy, A., Ruzicka, T., 1999. Effects of the neuropeptides substance P, calcitonin gene-related peptide and α-melanocyte-stimulating hormone on the IL-8/IL-8 receptor system in a cultured human keratinocyte cell line and dermal fibroblasts. Inflammation 23 (6), 557–567.

Luger, T.A., Schwarz, T., 1990. Evidence for an epidermal cytokine network. J. Invest. Dermatol. 95, 110S–104S.

Meyer, W., Gorgen, S., Schlesinger, C., 1986. Structural and histochemical aspects of epidermis development of fetal porcine skin. Am. J. Anat. 176, 207–219.

Marionnet, A.V., Chardonnet, Y., Viac, J., Schmitt, D., 1997. Differences in responses of interleukin-1 and tumor necrosis factor α production and secretion to cyclosporin-A and ultraviolet B-irradiation by normal and transformed keratinocyte cultures. Exp. Dermatol. 6, 22–28.

Monteiro-Riviere, N.A., 1986. Ultrastructural evaluation of the porcine integument. In: Tumbleson, M.E. (Ed.), Swine in Biomedical Research, vol. 1. Plenum Press, New York, p. 164.

Monteiro-Riviere, N.A., Riviere J.E. 1996. The pig as a model for cutaneous pharmacology and toxicology research. In: Advances in Swine Biomedical Research, Tumbleson and Schook (Eds.), Plenum Press, NY pp.425–458.

Riviere, J.E., Brooks, J.D., Monteiro-Riviere, N.A., Budsaba, K., Smith, C.E., 1999. Dermal absorption and distribution of topically dosed jet fuels Jet-A, JP-8, and JP-8 + 100. Toxicol. Appl. Pharmacol. 160, 60–75.

Roguet, R., 1998. Use of skin cell cultures for in vitro assessment of corrosion and cutaneous irritancy. Cell Biol. Toxicol. 15, 63–75.

Shiels, O.M., Sweeney, E.C., 1999. TSH receptor status of thyroid neoplasms — TaqMan RT-PCR analysis of archival material. J. Pathol. 188, 87–92.

Simon, G.A., Maibach, H.I., 2000. The pig as an experimental animal model of percutaneous permeation in man: qualitative and quantitative observations — an overview. Skin Pharmacol. Appl. Skin Physiol. 13, 229–234.

Ulrich, S.E., 1999. Dermal application of JP-8 jet fuel induces immune suppression. Toxicol. Sci. 52, 61–67.

Virgill, F., Santini, M.P., Canali, R., Polakowska, R.R., Haake, A., Perozzi, G., 1998. Bcl-2 overexpression in the HaCaT cell line is associated with a different membrane fatty acid composition and sensitivity to oxidative stress. Free Rad. Biol. Med. 24 (1), 93–101.

Wang, T., Brown, M.J., 1999. mRNA quantification by real time TaqMan polymerase chain reaction: validation and comparison with Rnase protection. Anal. Biochem. 269, 198–201.

THE USE OF ENZYME HISTOCHEMISTRY IN DETECTING CUTANEOUS TOXICITY OF THREE TOPICALLY APPLIED JET FUEL MIXTURES

Beth N. Rhyne, Jason R. Pirone, Jim E. Riviere and Nancy A. Monteiro-Riviere

Center for Cutaneous Toxicology and Residue Pharmacology
North Carolina State University
4700 Hillsborough Street
Raleigh, NC 27606

Running Title: Cutaneous Jet Fuel Enzyme Histochemistry

Address correspondence to: Nancy Monteiro-Riviere, Ph.D.
Professor of Investigative Dermatology and Toxicology
Center for Cutaneous Toxicology and Residue Toxicology
North Carolina State University
4700 Hillsborough Street
Raleigh, NC 27606
Telephone: (919) 513-6426
Fax: (919) 513-6358
E-mail: Nancy_Monteiro@NCSU.edu

ABSTRACT

The purpose of this study was to assess cutaneous enzyme activity in response to topical jet fuel exposure using enzyme histochemistry for alkaline phosphatase (ALP), acid phosphatase (ACP), and non-specific esterase (NSE) in the skin of pigs. Yorkshire pigs were exposed to Jet-A, JP-8, and JP-8 (100) for 5 Hr, 24 Hr, and 4 Days under occluded Hill Top chamber (25 μl), nonoccluded (25μl) conditions, and occluded fabric (335 μl) conditions. For ALP, the fabric Jet-A, JP-8, and JP-8 (100) were significantly more ($p<0.05$) intense than control sites in the stratum basale layer. ACP staining showed a general increase in staining from 24 hr to 4 Day in most layers of the Hill Top experiment, but no treatment effects. The nonoccluded fabric JP-8 and JP-8 (100) demonstrated significantly more ($p<0.05$) staining of NSE than control sites at 24 hr in both the stratum spinosum and stratum basale layers. In addition, NSE staining at 4 Day in the fabric dosed JP-8 and JP-8 (100) was significantly more ($p<0.05$) than the occluded fabric control of the stratum granulosum layer. The increased distribution and significant difference in staining of these enzymes in jet-fuel treated skin across many layers (particularly ALP) strongly supports the conclusion that enzyme histochemistry can effectively be used as an early biomarker for cellular injury.

The animal research conducted adhered to the Guide for the Care and Use of Laboratory Animals, prepared by the Committee on Care and Use of Laboratory Animals, Institute of Laboratory Animal Resource, National Research Council (NIH Publication No. 86-23, revised

1985).

INTRODUCTION

United States Air Force maintenance workers routinely have physical contact with jet fuels during fuel tank cleaning accompanied with various health complaints. Such jet fuel exposure has previously been shown to induce pulmonary and dermal irritation, immune suppression, and a variety of toxicological effects throughout the body (Pfaff *et al*, 1993; Ullrich, 1999; Dossing *et al,* 1985). However, comparatively little is known about early detection of jet fuel cytotoxicity in the skin.

Currently, the USAF uses three jet fuel formulations: Jet-A, JP-8, and JP8-100. Jet-A is a commercial jet fuel composed of over two hundred major hydrocarbon constituents; JP-8 is composed of the Jet-A fuel with three performance additives: a corrosion inhibitor (8Q21, also known as DC1-4A), an anti-static compound (Stadis450), and an icing inhibitor (diethylene glycol monomethyl ether); and JP-8(100) fuel contains a mixture of JP-8 and 100-additive package, which includes chelator, antioxidant, detergent, and heat dispersant components. Although the various additives have the advantageous qualities of easier storage and higher flash points, concern about their contribution to cutaneous jet fuel cytotoxicity has surfaced.

Abundant expression and production of certain hydrolytic enzymes, such as alkaline phosphatase (ALP), acid phosphatase (ACP), and non-specific esterase (NSE), readily found in the epidermis have historically been shown to be indicative of both irritation and cellular proliferation (Middleton, 1980; Volden *et al.*, 1983; Raekallio, 1965). Therefore, enzyme histochemistry of the jet fuel treated skin was performed to detect irritation by the presence and intensity of ALP, ACP, and NSE. ALP is a group of membrane bound (e.g. plasma membrane and endoplasmic reticulum) glycoproteins that catalyze the hydrolysis of inorganic and organic monophosphate esters in the alkaline pH range (optimal pH 9.0 to 9.6). It is widely distributed in human tissues, and associated with many physiological functions. ALP may play a role in active transport of soluble phosphates across membranes (Harris, 1990) and in calcification. ACP, which has an optimal activity from pH 4.5 to 5.5, catalyzes the hydrolysis of most phosphomonoesters. This enzyme is intracellularly localized within lysosomes, with some extralysosomal activity in the rough

endoplasmic reticulum and the cytoplasm. ACP may play a role in the process of transphosphorylation. The NSEs are a group of enzymes that primarily hydrolyze esters of long chain fatty acids at an optimum pH range of 5.0 to 8.0. They have been localized to the cytoplasm, endoplasmic reticulum, lysosomes, and mitochondria of the cell (Troyer, 1980).

A porcine *in vivo* experiment was conducted to compare three jet fuel mixtures (Jet-A, JP-8, and JP-8 (100)) at 5 Hr, 24 Hr, and 4 Day intervals under occluded (cotton fabric and Hill Top chambers) and nonoccluded conditions. The fabric occlusions were to mimic the saturation effects of the workers fuel-soaked cotton uniforms in direct contact with the skin, and the Hill Top occlusions were to represent a condition of occlusion lacking direct contact with the uniform. The increased presence and activity of enzymes is typically indicative of cellular damage, proliferation, and/or inflammation. ALP, ACP, and NSE are each considered to be released early in response to cellular injury. Therefore, this study was conducted to determine epidermal damage at different time intervals, and under differing occlusion statuses of Jet-A, JP-8, and JP-8 (100), using enzyme histochemistry as an early biomarker of cellular injury.

MATERIALS AND METHODS

The entire *in vivo* study was divided into three groups of experiments: Hill Top occluded and nonoccluded sites (5 hr and 24 hr), Hill Top occluded and nonoccluded sites (4 Day), and fabric occluded and nonoccluded sites (5 hr, 24 hr, and 4 Day).

Experiment One: The initial 5 hr and 24 hr Hill Top chamber experiment was conducted to assess the *in vivo* effects of 25 µl of jet fuel, a comparable dose to previous porcine skin *in vitro* absorption studies of our laboratory (Riviere *et al,* 1999). Four female weanling Yorkshire pigs were utilized. Each was sedated with an intramuscular injection of ketamine/xylazine/telazol, and the back hair was clipped 24 hours prior to dosing. The Hill Top occluded sites were randomized in the dorsal thoracic region: 5 hr control, 5 hr Jet-A, 5 hr JP-8, 5 hr JP-8 (100), 24 hr control, 24 hr Jet-A, 24 hr JP-8, and 24 hr JP-8 (100). The nonoccluded sites were randomized cranial and caudal to the occluded sites: 5 hr control, 5 hr Jet-A, 5 hr JP-8, 5 hr JP-8 (100), 24 hr control, 24 hr Jet-A, 24 hr JP-8, and 24 hr JP-8 (100).

Occluded sites were dosed with 25µl of the appropriate fuel (control, Jet-A, JP-8, or JP-8 (100)) and covered with a Hill Top chamber (Hill Top Cooperation, 3.14 cm^2 dose area) without the pad. Medipore™ (3M Healthcare, St. Paul, MN) tape adhered the chambers to the skin, and a cloth body stocking bordered with Elastikon® (Johnson & Johnson Medical, Arlington, TX) elastic tape was placed around the mid-thoracic area to further stabilize and protect the chambers from fecal contamination. The nonoccluded sites were dosed with 25µl of the appropriate fuel and left uncovered.

Five hours after dosing, a 4mm biopsy was taken from each 5 hr site. The biopsy wounds were treated with a triple antibiotic ointment (American Fare, Troy, Michigan) that contained an analgesic. The same protocol was followed for the 24 hr samples. Upon completion of the 24 hr sampling, each pig was euthanatized with 5 ml of Beuthanasia®-D Special (Schering-Plough Animal Health Corp., Kenilworth, NJ) solution.

Experiment Two: Additional pigs (n=4) were prepared as outlined above for a 4 Day exposure Hill Top experiment to determine the long term repetitive effects of 25 µl of the jet fuels. Four randomized sites (control, Jet-A, JP-8, and JP-8 (100)) in the mid-dorsal region of the pig were dosed with 25µl of the appropriate fuel and covered with a Hill Top chamber. Four nonoccluded sites were dosed with 25µl of the appropriate fuel and left uncovered cranial and caudal to the occluded sites.

Each site was re-dosed daily with 25µl of the appropriate jet fuel the following three days. Four days after the initial dose, a 4mm biopsy was taken from each site and each pig was euthanatized.

Experiment Three: A final set of experiments using cotton fabric to occlude the sites was performed to mimic complete fuel saturation of cotton clothing (for 5 hr, 24 hr, and 4 Day). Additional pigs (n=4) were prepared as outlined above for the 5 and 24 hr Hill Top experiment. To secure the fabric to the occlusion sites, a holding template was attached to the skin. This template was created from Stomahesive® (Convatec-Squibb, Princeton, NJ) with a dosing area of 5.0cm^2 and a 0.75cm border for attachment to the skin with Medipore™ tape. The cotton fabric was placed directly inside of the template and dosed with 335µl of the appropriate fuel (control, Jet-A, JP-8, or JP-8 (100)) on the cotton fabric, the volume required to achieve saturation. Again a cloth body stocking bordered with Elastikon® tape was placed around the mid-thoracic area to further stabilize and protect the chambers from fecal contamination. Nonoccluded

sites were dosed with 25µl of the appropriate fuel and left uncovered. The appropriate samples were taken at the conclusion of 5 and 24 hrs respectively as in the Hill Top experiment, and each pig was euthanatized.

For the 4 Day exposure fabric experiment, four additional pigs (n=4) were used to assess acute repetitive cotton saturation effects. Similar protocol to the 4 Day Hill Top was followed, except utilizing a Stomahesive® template identical to the previous fabric experiments. Occluded sites were dosed with 335µl of the appropriate fuel (control, Jet-A, JP-8, and JP-8 (100)) on the cotton fabric within each template to achieve saturation. Nonoccluded sites were dosed with 25µl of the appropriate fuel and left uncovered.

Dosing of 335 µl for the occluded sites and 25 µl for the nonoccluded sites was repeated daily for the next 3 days. On the fourth day of exposure, an 8mm biopsy was taken from the sites and the pigs were euthanatized.

Techniques: Tissue biopsies from the dosed sites were oriented in an aluminum foil boat, embedded in O.C.T. compound (Tissue Tek®, Torrance, CA), frozen in an isopentane well immersed in liquid nitrogen, and stored at -80°C. Enzyme histochemistry was performed on frozen samples that had been sectioned at 8µm in a cryostat (Cryocut 1800, Reich-Jung) and mounted on positively charged slides. Modified azo coupling methods were used in the location and histochemical staining of ALP, ACP, and NSE. The substituted napthol method for alkaline phosphatase (Litwin, 1985) located ALP, where reddish pink deposits indicated enzyme activity. The substituted napthol method for acid phosphatase (Litwin, 1985) was performed to determine ACP activity where bright pink deposits indicated activity. NSE was detected by a α-napthyl acetate method (Noble, 1982) using hexazotized pararosanilin as the coupler, where activity was indicated by dark red staining. Each enzyme reaction also included paired negative controls that lacked the specific substrate for comparison. The intensity of enzyme staining was scored in four layers of the epidermis (stratum basale-SB, stratum spinosum-SS, stratum granulosum-SG, and stratum corneum-SC) and the dermis (aprocrine gland and fibroblast) using the following scale: O=no staining; 1=slight staining; 2=moderate staining; and 3=intense staining. The mean staining intensities were generated and significant differences ($p<0.05$) of the SB, SS, and SG layers determined using ANOVA (Analysis of Variance) test with the General Linear Models Procedure in the SAS System.

RESULTS

Few significant differences were found within ALP, ACP, and NSE between the three jet fuels (Jet-A, JP-8, and JP-8 (100)). However, when comparing the time response (5hr, 24 hr, and 4 Day), a trend of increased staining intensity with increased time is apparent (see Table 1). The occluded sites, especially fabric occluded, tended to be more intense than the nonoccluded sites over time. Control (nondosed) sites tended to demonstrate less enzymatic activity than treatment sites. While the SC and aprocrine glands and fibroblasts of the dermis were scored for activity and mean intensities generated, staining was indifferent between the control and treatments for these layers in each enzyme.

ALP: The mean staining intensity in the fabric sites increased from 5 and 24 hr to 4 Day for all treatments except nonoccluded JP-8 (100), which stained moderately at each time point (see Figure 1). In addition, there was an increase in staining distribution in fabric sites from primarily the SB at 5 hr to include the SS and SG at 24 hr and 4 Day. Except in isolated sites at 4 Day, staining in fabric nonoccluded treatments was localized to the SB layer. In the fabric occluded control sites, mean staining of the SB layer was significantly less ($p<0.05$) than the occluded Jet-A, JP-8, and JP-8 (100) at 4 Day (see Figure 1 and Figure 7). In the Hill Top occluded sites, there was an increase in staining intensity of the SB layer with time, especially between 5 hr and 24 hr treatments (see Figure 2). In the 5 hr Hill Top sites, only occluded Jet-A induced staining in the SS layer. The 24 hr time point displayed staining of the SS layer in more Hill Top treatments, and by 4 Day, this staining was found in occluded Jet-A, occluded JP-8, occluded JP-8 (100), nonoccluded JP-8, and nonoccluded JP-8 (100) (see Figure 2).

ACP: ACP staining occurred in all epidermal cell layers, with no significant differences over time in fabric occluded or nonoccluded sites (see Figure 3). At 24 hr, fabric occluded JP-8 (100) was greater that other occluded treatments in all layers, and fabric nonoccluded JP-8 (100) was greater that other nonoccluded treatments in all layers. Although no significant treatment effects were present in the Hill Top sites, an intensity increase was observed in the SG, SS, and SB layers from 24 hr to 4 Day (see Figure 4).

NSE: Mean enzyme staining, found in all epidermal cell layers (see Figure 5), was more intense in the SG layer of the fabric treatments at each time point. The control was statistically less ($p<0.05$) than JP-8 and

JP-8 (100) for both the 24 hr nonoccluded fabric sites in the SS and SB layer (see Figure 5). By Day 4, staining intensity had increased in the SG, SS, and SB layers (see Table 1). The mean staining of the fabric occluded control was significantly less ($p<0.05$) than the fabric occluded JP-8 and JP-8 (100) on Day 4 in the SG layer (see Figure 5). In general, staining in the Hill Top occluded sites slightly peaked at 24 hr and slightly decreased by Day 4 (see Figure 6). No significant differences were noted between the jet fuel treatments.

DISCUSSION

Controversy has long surrounded the validity of considering the stratum corneum a viable layer of the skin. Since the nuclei of these cells have disintegrated, debate remains as to whether enzyme release of these cells is a response to irritating stimuli, or whether the staining present is merely residual. In addition, the staining observed in the dermis is often non-specific, thereby obscuring subtle responses. Therefore, as expected, our study found no differences in the SC and dermis staining between the treatments and the control. For these reasons, our analytical and statistical focus was on the remaining three layers: stratum basale (SB), stratum spinosum (SS), and stratum granulosum (SG). Additionally, all 4 Day sites required a repetitive daily application of the jet fuel for four days, whereas the 5 and 24 Hr experiments were singularly dosed, making statistical comparisons across time difficult. Also, as the methods used in the fabric experiments required a saturation of cotton (335µl), which was different from the fabric nonoccluded and Hill Top saturation (25µl), statistical comparisons can not accurately be made between the two. Therefore the statistical comparisons were between the Hill Top occluded and Hill Top nonoccluded data, within the fabric occluded data, and within the fabric nonoccluded data at each time interval (5 Hr, 24 Hr, and 4 Day).

ALP is a membrane-associated protein involved with cell-surface enzymatic cleavage. Other studies conducted in our laboratory have demonstrated that jet fuel exposure promotes inflammation, cell damage, and cell proliferation (Monteiro-Riviere *et al,* 2000 and Allen *et al*, 2000), which would be indicated by an increase in ALP activity. Such activity may serve a variety of biochemical transportation functions in any one of those responses. In addition, the occluded treatments would be expected to increase enzyme activity when compared to the nonoccluded treatments due to hydration of the SC,

thereby enhancing fuel absorption. Occlusion also prevented evaporative loss of the volatile fuel. As exposure time to the jet fuel increased, inflammation, damage, and proliferation also increased. The general observations of increased activity and the statistical difference found in our study for ALP supported both expectations.

ACP is an enzyme intracellularly localized within the lysosomes. Therefore, access of the substrate to the ACP is dependent upon permeability of the lysosome membrane, which increases at a more acidic pH. If differences between the control and treatments were found, either lysosomal membrane damage would be suspected to have leaked the ACP, or the treatments caused membrane permeability by lowering the cellular pH. However, since the histochemical process used for ACP detection requires an acidic pH medium, the non-damaged, otherwise impermeable membrane in the control samples may then become more permeable. This would result in both sites appearing to have the same ACP activity. In our study, the 4 Day Hill Top sites produced the greatest activity, but no statistical differences were found between controls and treatments, which supports this possibility.

NSEs are a wide classification of enzymes that includes phosphatases. Predominately they are cytosolic and indicative of inflammatory cells. Much like the alkaline and acid phosphatases, their increase in activity is expected in response to an increase in inflammation, cell damage, or cell proliferation. Jet fuel treated skin was expected to have an increase in these responses and NSE activity when compared to the control, as well as occluded when compared to the nonoccluded treatments. In addition, an increased exposure time should have increased the response and subsequent activity. These predictions were supported by the statistical differences in our study.

No statistical differences with any of the Hill Top occluded or nonoccluded treatments were found in this study. Likely, the small dose applied (25µl) was not enough to produce significant observable effects on enzyme production using these methods, even when applied repetitively for 4 Days.

The few correlations found between enzyme intensity and the different jet fuels could be explained by more closely examining the fuel. The differences between the three jet fuels themselves account for less than 0.02% of the overall fuel, so the differences in enzyme activity was likely equally minute. Enzyme histochemistry then was probably too insensitive for detecting such small differences

between *in vivo* responses to the three jet fuels. It should be noted, however, that JP-8 (100), which contains the most components of the three fuels, tended to consistently produce a high amount of enzyme activity. Therefore, the enzyme histochemical methods used do sufficiently detect a high production of these enzymes in injured skin. Previous studies have demonstrated an overall increase in ACP and NSE staining and a marked increase in ALP in response to a mild epidermal insult, such as paraquat on skin (Srikrishna *et al*, 1982). Epidermal damage due to the topical application of SLS and methyl nicotinate mixtures has been indicated by an increase in ACP activity of the SB layer (Baynes, *et al*). Monteiro-Riviere and Inman (2000) found an increase in epidermal ACP and NSE activity in response to the severe toxic exposure of topically applied sulfur mustard, but a marked decrease in ALP activity. The increased production and activity of ALP, ACP, and NSE in our study then suggest that topically applied Jet-A, JP-8, and JP-8 (100) results in mild cellular injury. In this study, ALP particularly showed a marked increase in intensity in response to exposure time. Therefore the clear increase in ALP activity, which indicates injury from jet fuel treatments, suggests that ALP is a more sensitive early biomarker than ACP and NSE.

In all, this study's most conclusive observation is the distribution of these enzymes across epidermal cell layers in jet fuel treated skin. Historically, in normal pig skin, ALP stained only in the SB and dermis, ACP stained the SG, SC, and dermis, and NSE stained the SB, SS, SG, SC, and dermis, with SS and SG being more intense (Meyer, 1976; Meyer *et al,* 1978). Our findings supported this distribution, with minimal staining also observed in the SG and SS layers for ALP, and additional staining in the SS and SB layers for ACP, indicating that the jet fuels induced cellular damage, and consequently enzyme production. Enzyme histochemistry of ALP, ACP, and NSE, therefore adequately detects early cellular damage, such as sustained from topical jet fuel exposure.

ACKNOWLEDGEMENTS

The authors would like to thank Al Inman for technical assistance. This work was presented at the 39th annual meeting of the Society of Toxicology, Philadelphia, PA and was supported by the United States Air Force Office of Scientific Research under grant FQ8671.

TABLE 1 . Summary of ALP, ACP, and NSE Intensity of Jet-Fuel Treated Pig at 5 Hr, 24 Hr, and 4 Day in SG, SS, and SB Layers of Epidermis

		OCCLUDED (HILL TOP)			NONOCCLUDED (HILLTOP)			OCCLUDED (FABRIC)			NONOCCLUDED (FABRIC)		
		5 Hr	24 Hr	4 Day	5 Hr	24 Hr	4 Day	5 Hr	24 Hr	4 Day	5 Hr	24 Hr	4 Day
ALP	Jet A								+SG	+SG			
		+SS	+SS	+SS		+SS			+SS	+SS			
		+SB	++SB	+++SB	+SB	++SB	+++SB	++SB	++SB	++++SB	++SB	+SB	++++SB
	JP-8								+SG				
			+SS	+SS			+SS	+SS	+SS	+SS			
		+SB	++SB	+++SB	+SB	+++SB	+++SB	++SB	++SB	++++SB	+++SB	++SB	+++SB
	JP-8 (100)								+SG				
				+SS			+SS		+SS	+SS			
		+SB	++SB	+++SB	+SB	++SB	++++SB	++SB	++SB	+++++SB	++SB	++SB	++SB
ACP	Jet A	+SG	++SG	+++SG	++SG	+SG	++SG	+++SG	+SG	++SG	++SG	++SG	+SG
		+SS	+SS	++SS	++SS	+SS	++SS	+SS	+SS	++SS	++SS	++SS	+SS
		+SB	+SB	++SB	++SB	+SB	++SB	+SB	+SB	++SB	++SB	++SB	+SB
	JP-8	++SG	+SG	+++SG	++SG	+SG	+++SG	++SG	+SG	+SG	++SG	++SG	+SG
		++SS	+SS	+++SS	++SS	+SS	+++SS	++SS	+SS	+SS	+SS	+SS	+SS
		++SB	+SB	+++SB	++SB	+SB	+++SB	++SB	+SB	+SB	++SB	++SB	+SB
	JP-8 (100)	+SG	++SG	+++SG	++SG	+SG	+++SG	++SG	++SG	+SG	++SG	+++SG	+SG
		+SS	+SS	+++SS	++SS	+SS	+++SS	+SS	++SS	+SS	+SS	++SS	+SS
		+SB	+SB	++++SB	++SB	+SB	+++SB	+SB	++SB	+SB	++SB	+++SB	+SB
NSE	Jet A	+SG	+++SG	++SG	+++SG	++SG	+++SG	++SG	++SG	++++SG	+++SG	++SG	++++SG
		+SG	+++SS	++SS	++SS	++SS	++SS	++SS	+SS	+++SS	+SS	+SS	+++SS
		+SB	+++SB	++SB	++SB	+SB	+SB	+SB	+SB	++SB	+SB	+SB	++SB
	JP-8	++SG	++SG	+SG	++SG	++SG	+++SG	+++SG	++SG	++++SG	++SG	++SG	++++SG
		++SS	++SS	+SS	+SS	++SS	++SS	+SS	+SS	+++SS	++SS	++SS	+++SS
		++SB	++SB	+SB	+SB	++SB	+SB	+SB	+SB	++SB	+SB	++SB	++SB
	JP-8 (100)	+SG	+++SG	++SG	++SG	++SG	++SG	++SG	++SG	++++SG	++SG	++SG	++SG
		+SS	+++SS	++SS	+SS	++SS	++SS	+SS	+SS	+++SS	+SS	++SS	+++SS
		+SB	+++SB	++SB	+SB	++SB	+SB	++SB	+SB	++SB	+SB	++SB	++SB

Note. + = slight intensity, ++ =moderate intensity, +++ = high intensity, > +++ =very high intensity

REFERENCES

1. Allen, D.G., Monterio-Riviere, N.A., and Riviere, J.E. 2000. Cytokine Release from Keratinocytes Exposed to Jet-A, JP-8, and JP-8 (100) Jet Fuels. *Toxicol. Sci.*, 54: 151.
2. Baynes, R.E., Monteiro-Riviere, N.A., Qiao, G.L., and Riviere, J.E. 1997.Cutaneous toxicity of the benzidine dye direct red 28 applied as mechanistically-defined chemical mixtures (MDCM) in perfused porcine skin. *Toxicol. Letters,* 93: 159-169.
3. Dossing, M., Loft, S., and Schroeder, E. 1985. Jet fuel and liver function. *Scandenavian J. Work Environ. Health.* 11:433-437.
4. Harris, H. 1990. The human alkaline phosphatases: what we know and what we don't know. *Clin. Chim. Acta.* 186:133-150.
5. Litwin, J.A. 1985. Light microscopic histochemistry on plastic sections. *Prog. Histochem. Cytochem.* 16:1-79.
6. Meyer, W. and Neurand, K. 1976. The distribution of enzymes in the skin of the domestic pig. *Lab. Anim.* 10:237-247.
7. Meyer, W., Schwartz, R., and Neurand, K. 1978. The skin of domestic mammals as a model for the human skin, with special reference to the domestic pig. *Curr. Probl. Dermatol.* 7:39-52.
8. Middleton, M.C. 1980. Evaluation of cellular injury in skin utilizing enzyme activities in suction blister fluid. *J. Invest. Derm.* 74:219-223.
9. Monteiro-Riviere, N.A. and Inman, A.O. 2000. Characterization of sulfur mustard-induced toxicity by enzyme histochemistry in porcine skin. *Toxicol. Methods.* 10:1-16.
10. Monteiro-Riviere, N.A., Inman, A.O., Rhyne, B.N., and Riviere, J.E., 2000. Cutaneous Irritation of Topically Applied Jet Fuels in the Pig. *Toxicol. Sci.,* 54: 151.
11. Noble, L.W. 1982. Histochemistry workshop. In Proceedings of the Ninth Annual Spring Seminar of the North Carolina Society of Histopathological Technologists, April 29-May 1.
12. Pfaff, J., Parliman, G., Parton, K., Lantz, R., Chenh, H., Hays, A., and Witten, M. 1993. Pathological changes after JP-8 jet fuel inhalation in Fischer 344 rats. *FASEB*, 7: A408.
13. Raekallio, J. 1965. Histochemical demonstration of enzymatic response to injury in experimental skin wounds. *Exp. Mol. Pathol.* 4:303-310.
14. Riviere, J.E., Brooks, J.D., Monteiro-Riviere, N.A., Budsaba, K. and Smith, C.E. 1999. Dermal absorption and distribution of topically dosed jet fuels Jet-A, JP-8, and JP-8 (100). *Toxicol. and Appl. Pharmacol.* 160:60-75.
15. Srikrishna, V., Riviere, J.E., and Monteiro-Riviere, N.A. 1992. Cutaneous toxicity and absorption of paraquat in porcine skin. *Toxicol. Appl. Pharmacol.* 115:89-97.
16. Troyer, H. 1980. Esterases and Lipases. In *Principles and Techniques of Histochemistry,* 233-247. Boston, PA: Little, Brown and Company.
17. Ullrich, S. 1999. Dermal application of JP-8 jet fuel induces immune suppression. *Toxicol. Sci.* 53:61-67.
18. Volden, G, Kavli, G., Haugen, H.F., and Skrede S. 1983. The pattern of lysosomal, cytosolic and plasma membrane enzymes in epidermis, dermis and suction blister fluid after ultraviolet radiation. *Br. J. Dermatol.* 109 (Supplement 25): 68-71.